2008-04-28

Contribution of Recharge Along Regional Flow Paths to Discharge at Ash Meadows, Nevada

Michelle Bushman
Brigham Young University - Provo

CONTRIBUTION OF RECHARGE ALONG REGIONAL FLOW PATHS TO DISCHARGE AT ASH MEADOWS, NEVADA

by
Michelle Bushman

A thesis submitted to the faculty of

Brigham Young University

In partial fulfillment of the requirements for the degree of

Master of Science

Department of Geological Sciences

Brigham Young University

August 2008

BRIGHAM YOUNG UNIVERSITY

GRADUATE COMMITTEE APPROVAL

of a thesis submitted by

Michelle Bushman

This thesis has been read by each member of the following graduate committee and by majority vote has been found to be satisfactory.

_____	_____
Date	Stephen T. Nelson, Chair
_____	_____
Date	John H. McBride
_____	_____
Date	Alan L. Mayo

BRIGHAM YOUNG UNIVERSITY

As chair of the candidate's graduate committee, I have read the thesis of Michelle Bushman in its final form and have found that (1) its format, citations, and bibliographic style are consistent and acceptable and fulfill university and department style requirements; (2) its illustrative materials including figures, tables, and charts are in place; and (3) the final manuscript is satisfactory to the graduate committee and is ready for submission to the university library.

_____ _____

Date Stephen T. Nelson
Chair, Graduate Committee

Accepted for the Department

_____

Michael Dorais
Graduate Coordinator

Accepted for the College

_____

Tom Sederberg
Associate Dean
College of Physical and Mathematical Sciences

ABSTRACT

CONTRIBUTION OF RECHARGE ALONG REGIONAL FLOW PATHS TO DISCHARGE AT ASH MEADOWS, NEVADA

Michelle Bushman

Department of Geological Sciences

Master of Science

Springs in the Ash Meadows, Nevada wetland area are discharging groundwater at a high volume that cannot be sustained by local, present-day precipitation and associated recharge. Previous groundwater flow models for this region have required groundwater to flow through complex geology for long distances (160km) through fractures that, in the current stress field, should be closed in many instances in the presumed flow direction.

This thesis examines several possible flow paths and evaluates each flow path using chemical and isotopic signatures in the water, as well as geologic and geophysical constraints, and determines that flow from beneath the Yucca Mountain area is the most viable source of groundwater for the springs at Ash Meadows. Isotopic signatures also indicate that recharge likely occurred during the last pluvial, a cooler, wetter period about 13,000 or more years ago, and that present-day water is discharging from storage.

Geophysical investigations show the relationship of a deep-seated crustal feature (the Gravity Fault) with shallow offset faults near the Ash Meadows springs. The damage zone of the Gravity Fault appears to provide a conduit for groundwater flow; the

north-south fractures should have the greatest aperture under the current stress field, and the buried tufa mounds (revealed with ground penetrating radar data) indicate localized upwelling from a deeper regional water source.

ACKNOWLEDGMENTS

This study was generously supported (financially and otherwise) by the BYU Department of Geological Sciences. Dr. John McBride at Brigham Young University processed the shallow seismic data collected at Ash Meadows, and re-processed the deep seismic, gravity, and aeromagnetic data. David Tingey, John South, Maxwell Okure, Rachel Henderson, Gregg Carling, and Eric Bushman assisted with the field work. Sharon McKelvey at the Ash Meadows National Wildlife Refuge was instrumental in helping us obtain the necessary permits for the seismic survey. Mary Fisher graciously allowed us to obtain water samples from her private property. Carol Frost and Liddy Brinck at the University of Wyoming and Chris Eastoe at the University of Arizona analyzed the water samples in their labs for strontium and sulfur isotopes, respectively. Dennis Eggett from the BYU Statistics Department helped with the statistical analyses. Don Sweetkind sent well logs from Ash Meadows to assist with the seismic interpretation. Rick Blakely sent the gravity and aeromagnetic data for our re-analysis. Tom Brocher sent the deep seismic data for comparison with our shallow seismic line. Brigham Young University gratefully acknowledges software grants from the Landmark (Halliburton) University Grant Program (GeoProbe™, SeisWorks3D™, and ProMAX2d™) and from Seismic Micro-Technology (The Kingdom Suite™). Lastly, my deepest gratitude goes to my patient and supportive thesis advisor, Dr. Stephen Nelson, and my committee members, Dr. John McBride and Dr. Alan Mayo.

TABLE OF CONTENTS

LIST OF FIGURES

LIST OF TABLES

Introduction

The purpose of this thesis is to evaluate possible up-gradient flow paths of groundwater to Ash Meadows, and to determine the relative contributions of water from each source.

Springs at Ash Meadows, Nevada, are considered a major discharge location for the Death Valley regional carbonate aquifer (Winograd and Thordarson, 1975). The Death Valley regional groundwater flow model is a conceptual model for interbasin flow in the Basin and Range province in the western United States (Fig. 1). Present-day climate conditions are extremely arid, and between the high rate of evapotranspiration (25.9×10^6 m^3/yr evapotranspiration over an area of 41.9×10^6 m^2) and the low rates of precipitation (0.05 to 0.12 m/yr, or 5.02×10^6 m^3/yr over an area of 41.9×10^6 m^2), the present-day recharge on the adjacent hills cannot sustain such high rates of discharge at Ash Meadows (21.2×10^6 m^3/yr) (Laczniak et al., 1999; Steinkamf and Werrell, 2001). The water budget for Ash Meadows requires some other source of water input, either from distant precipitation or local storage:

		INPUT =	OUTPUT	
Local Precipitation +	Interbasin/Storage =	Evapotranspiration +	Discharge	
(5.02×10^6 m^3/yr) +	(18.8×10^6 m^3/yr =	(25.9×10^6 m^3/yr) +	(21.2×10^6 m^3/yr)	(Eq. 1)

The Death Valley conceptual model for interbasin flow allows continuous recharge from high elevation mountains and plateaus located up to 160 km away, reaching Ash Meadows through a thick sequence of highly fractured Paleozoic carbonate

Figure 1 Overview of the interbasin flow model, with arrows perpendicular to potentiometric flow lines to show theoretical direction of interbasin flow. Deuterium (δD‰) isotope values are shown for Pahranagat Valley, Spring Mountains, Yucca Mountain and Ash Meadows.

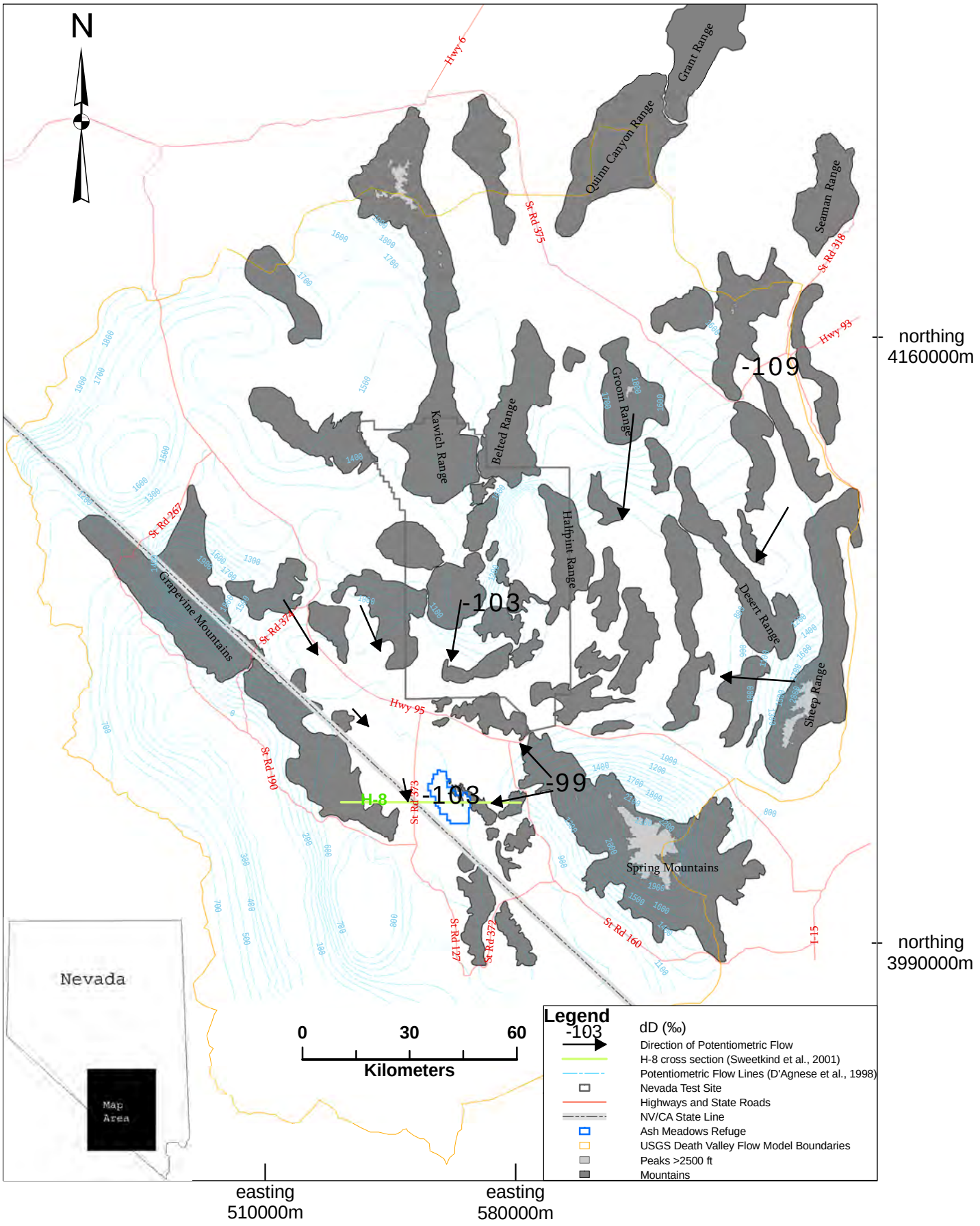

GIS data for base maps taken from U.S. Geological Survey 30 x 60 minute quadrangles: Beatty (1986), Cactus Flats (1988), Tonopah (1987), Warm Springs (1987), Death Valley Junction (1986), Goldfield (1985), Indian Springs (1988), Pahranagat (1985), Pahute Mesa (1979), Quinn Canyon Range (1988), Salina Valley (1985). 1:100,000-scale metric topographic map, Universal Transverse Mercator zone 11, 1927 North American Datum.

rocks (D'Agnese et al., 2002; Laczniak et al., 1999). According to Winograd and Pearson (1976) and Winograd and Thordarson (1975), present-day precipitation recharges fractured carbonate rocks at the Spring Mountains and the Sheep Range, then travels through secondary fractures and solution channels to the Gravity Fault. The Gravity Fault is presumed to act as a significant barrier to southwestward flow in the regional carbonate aquifer, causing upwelling from the aquifer to the Ash Meadows wetland area (Winograd and Thodarson, 1975). The intervening Basin and Range topography requires the groundwater of this aquifer to travel beneath several mountain ranges and through complex geology, including many other faults that have been largely overlooked. The flowpaths in the regional interbasin flow model are based on decreasing head in each valley, and rely on the continuous nature of the carbonate aquifer, with very few barriers to the flow of water (Thomas, 1996). Regional-scale groundwater flow is generally assumed to flow parallel to the gradient of the potentiometric surface (Ferrill et al., 1999; D'Agnese et al., 2002; Potter et al., 2002) (Fig. 1).

However, the simplifying assumption of a homogenous aquifer due to the large-scale cancellation of heterogeneities is not applicable to the fractured Paleozoic carbonate rocks that make up this regional aquifer (Winograd and Pearson, 1976). The Death Valley Region has undergone episodes of regional-scale compression, extension, and volcanism, that have disrupted the originally thick and continuous Paleozoic rocks (Thomas et al., 1996), making this aquifer very heterogeneous (Fig. 2). The regional aquifer has anisotropic transmissivity, because the fractures with the highest aperture are oriented north-south in the current stress field rather than universally parallel to the potentiometric gradient (Ferrill et al., 1999). The subsurface channels for groundwater

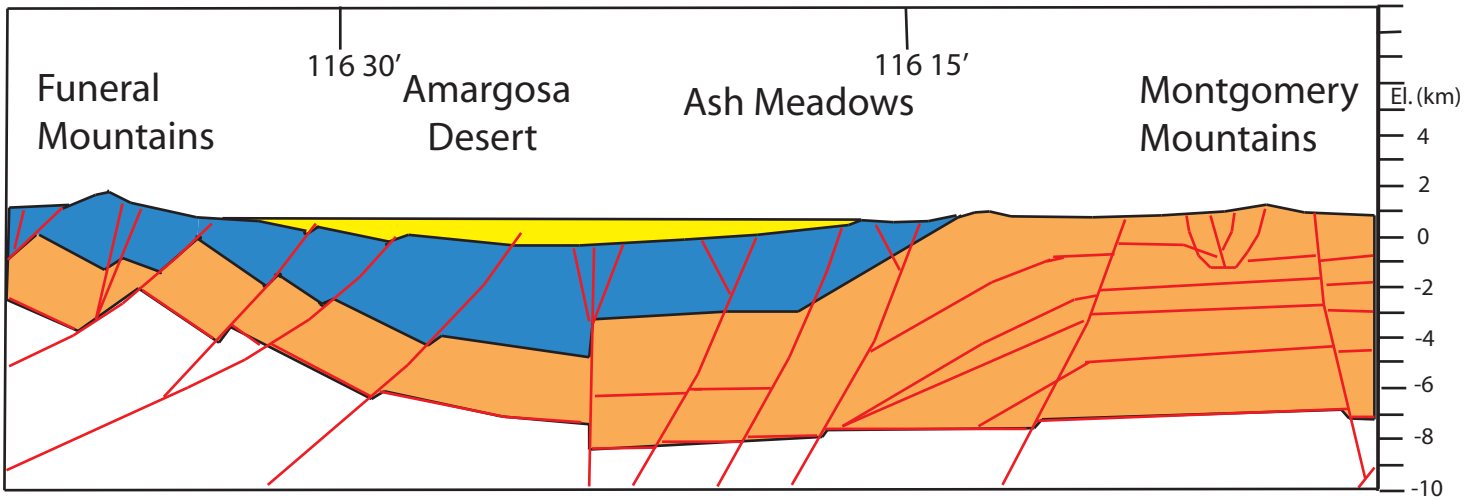

Figure 2. Part of H-8 cross-section near Ash Meadows, Nevada (see line of cross-section on Fig. 1 map). Generalized cross section adapted from Sweetkind et al. (2001) showing the complex faulting and heterogeneous nature of this aquifer. Discontinuous blue carbonate layers are underlain by orange aquitards. Yellow represents valley fill.

flow are probably structurally-controlled rather than dissolution karst features, and with groundwater continuously precipitating calcite, the high transmissivity can only be maintained as long as active extension keeps pace with calcite infilling (Riggs et al., 1994). Fault scarps are recorded throughout the Death Valley region during late Pleistocene and Holocene times, and recent seismicity indicates that local faults remain active today (Brogan et al., 1991; Blakely et al., 2000).

Distant interbasin flow for groundwater may require a lengthy time period between recharge and discharge, or very large, continuous fractures for rapid flow rates. Regional aquifer storage, on the other hand, may allow longer residence times with smaller fractures and slower flow rates. Estimates of groundwater residence times are in dispute. According to Winograd, et al. (1997), groundwater residence times in the regional carbonate aquifer are as short as 1000 years (from ^{14}C and $\delta^{18}O$ data at Devils Hole), and may be an order of magnitude *shorter* (as low as 400 years) based on hydrogeologic data such as high fracture transmissivity, effective porosity, and hydraulic gradients. Earlier ^{14}C data from the springs at Ash Meadows, however, are an order of magnitude *greater* in age (Winograd and Pearson, 1976). Winograd and Pearson (1976) also considered the possibility that the two distinct populations of waters present at Ash Meadows (with ~2.3 pmc and 11.1 pmc) reflect two major recharge intervals, from 19,000-28,000 years ago and from 8,000-13,000 years ago, respectively. Anderson et al. (2006) estimated Ash Meadows groundwater residence times of 13,000-25,000 years based on ^{14}C data from Rose et al. (1997).

An alternate hypothesis to interbasin flow is that a significant portion of the water discharging at Ash Meadows was recharged more locally during the last pluvial (about

12,000 years ago) and is currently being released from storage in the aquifer. During the late Pleistocene, glaciers formed in the higher mountains of the Great Basin, and the isotopic signature of groundwater recharge would have been lighter than it is today (Soltz and Naiman, 1978; Smith et al., 1998). Claassen (1985) concluded from geochemical data that groundwater in the west-central Amargosa Desert was recharged locally from snowmelt in approximately the same location as present-day stream channels during late Pleistocene to early Holocene time. Grove et al. (1969) also pointed to large volumes of water stored locally as an alternative to interbasin flow to account for the ability of warm springs to dampen the effects of seasonal and climate variations.

Purpose and Objectives

The purpose of this research is to investigate flow paths to test the validity of the Death Valley conceptual model of interbasin flow. The hypothesis of this research is that several of the potential flow paths within the conceptual model are foreclosed by the complex intervening geology.

The objectives of this thesis are to:

1. Compile historical groundwater data into a database that will be archived as part of this thesis (including Excel, PDF, and ArcMap files);
2. Collect water samples from the field where data is missing and analyze samples in the laboratory in order to better constrain possible flow paths to Ash Meadows;
3. Analyze the groundwater data to test flow paths using geochemical methods, including the chemical mass balance software program NETPATH (Plummer et al., 1991);

Figure 3. Seven flow path regions, with boundaries based on spring and well locations.

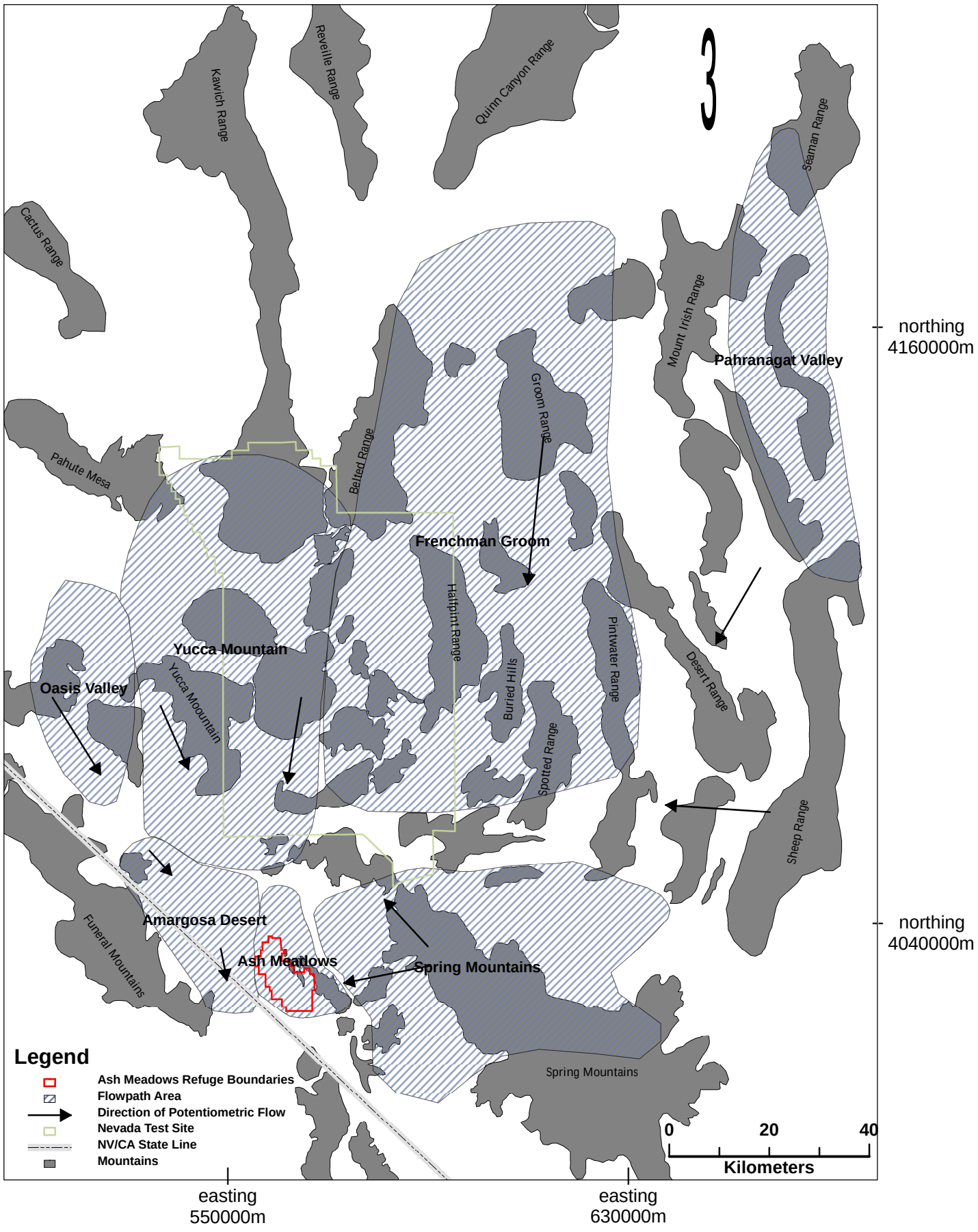

4. Collect seismic data at Ash Meadows across the lineament of springs to determine whether the Gravity Fault can be imaged closer to the surface and located relative to the springs.

Study Area

The study area includes seven potential geographic flow paths in southwestern Nevada: Ash Meadows, Amargosa Desert, Oasis Valley, Yucca Mountain, Frenchman/Groom, Spring Mountains and Pahranagat Valley (Fig. 3). The Funeral Mountains lie to the southwest, Oasis Valley to the northwest, Yucca Mountain and the Nevada Test Site to the north, Pahranagat Valley to the northeast, and the Spring Mountains to the east and southeast.

The Ash Meadows region is a wetland with several discharging springs (Fig. 4). Low-lying outcrops of fractured limestone form the eastern boundary of this small geographic region (Fig. 5). The Gravity Fault damage zone – inferred from a convergence of geophysical data and a roughly linear pattern of springs – abuts the western foot of the limestone outcrops, and most of the water samples of this region are located above (in elevation) and directly to the west of this poorly-defined subsurface feature. The Ash Meadows region also includes a large fracture collapse feature, Devils Hole, which is the home of the Pleistocene fish *Ciprinodon Diabolis*, and the site of a 500,000 year old continuous calcite record (Riggs et al., 1994; Soltz and Naiman, 1978; Winograd et al., 1992).

The Amargosa Desert region is distinctive because the aquifer is largely valley fill interbedded with Miocene lava flows (Sweetkind et al., 2001). The Amargosa River, an old perennial stream that is now an ephemeral stream, is located in the middle

Figure 4. Ash Meadows springs located near the Gravity Fault Damage Zone.

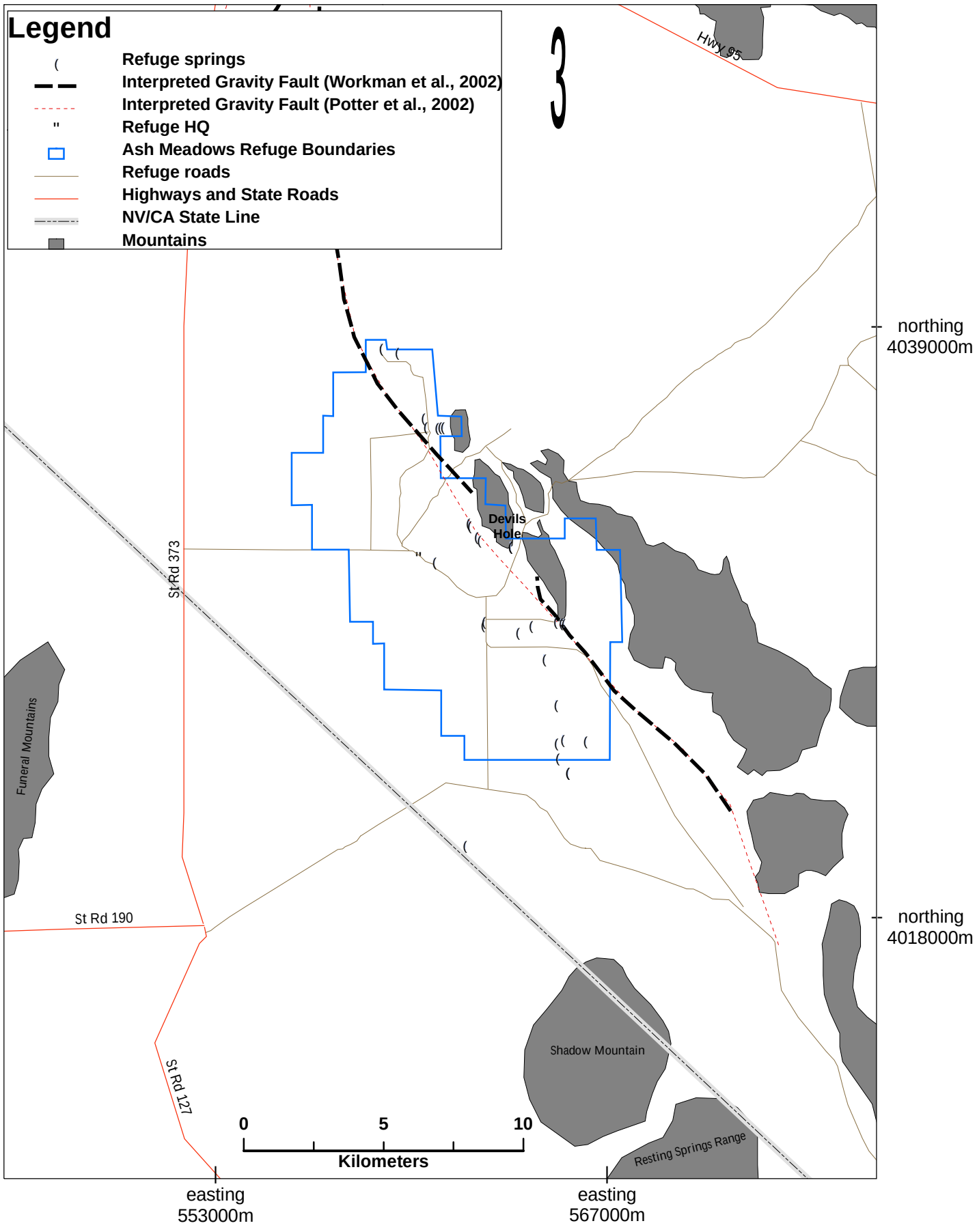

Figure 5 Map showing simplified surface geology and several major faults in the flow path regions

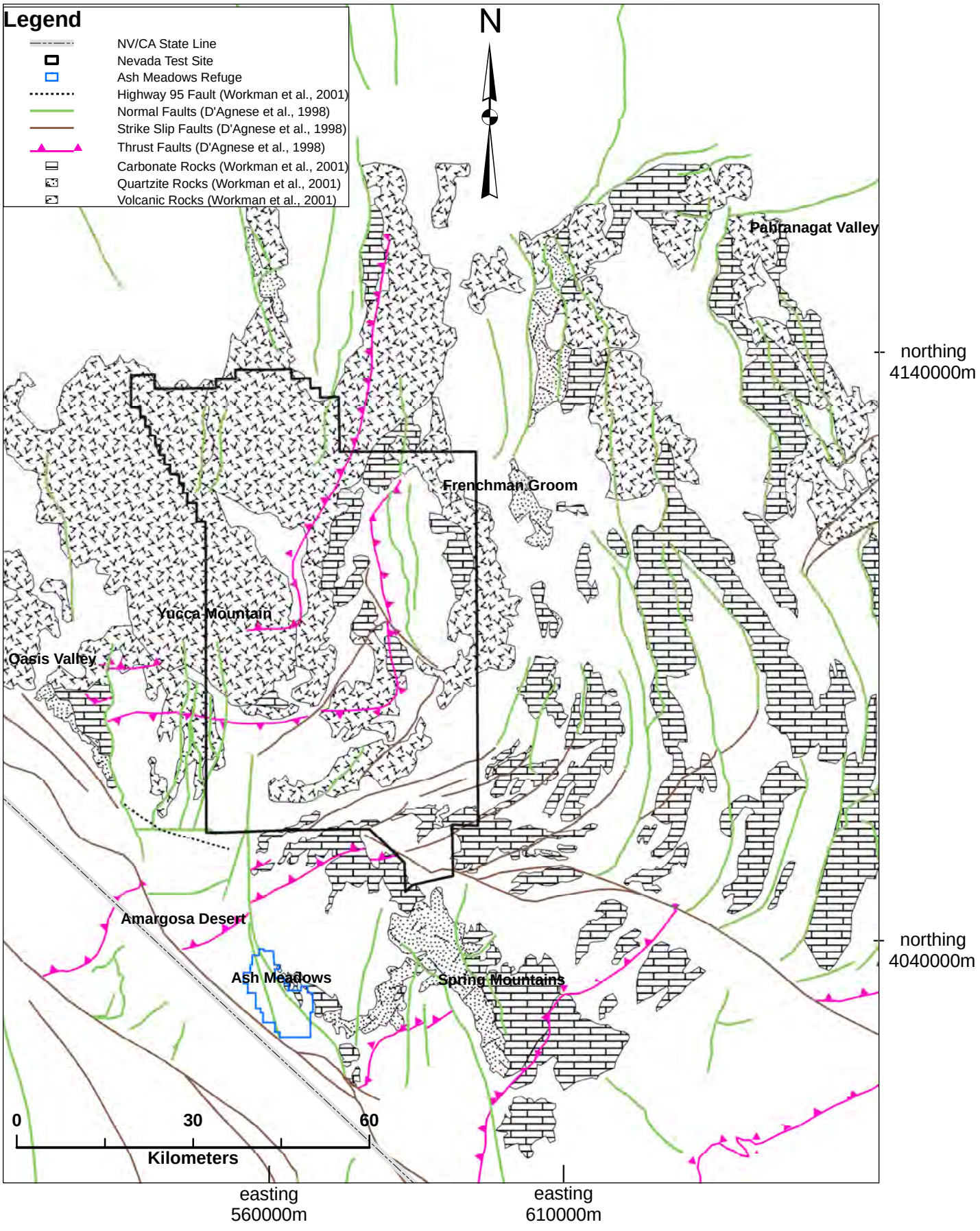

of this region, and when it is not running on the surface during winter rains, it still has groundwater in the subsurface. This groundwater flows east toward Ash Meadows and then south to Death Valley (Claassen, 1985).

The Oasis Valley region is a valley surrounded by hills and underlain by volcanic and plutonic rocks (Fig. 5). It has a thermal (groundwater-fed) perennial stream running alongside Highway 95 flowing south through Beatty and then east to the Amargosa River and Ash Meadows. The surrounding hills are dotted with several small springs.

The Yucca Mountain region is located within and near a large nested caldera complex (Workman et al., 2001a) (Fig.5), which distinctly affects the chemical and isotopic signature of the groundwater. Many of the water samples have been taken from deep monitoring wells, which were drilled to monitor groundwater in the vicinity of the Nevada Test Site, tracking past contamination and examining the suitability of the same area for a proposed nuclear waste repository.

The Frenchman Flat and Groom Mountain region is a general area between Yucca Mountain and the Sheep Mountains, lying north of the Spring Mountains and Las Vegas, but south of Pahranagat Valley. The geology consists of complex mixture of Paleozoic carbonates and Tertiary volcanic rocks, as well as Quaternary sedimentary deposits. There are relatively few water samples collected from this area due to the paucity of wells and springs. Presumably, if Pahranagat Valley water and Spring Mountain water flow all the way to Ash Meadows, they may encounter and mix with whatever water comes from the Frenchman Flat and Groom Mountain and surrounding area.

The Spring Mountains are generally considered a large contributor to the Ash Meadows discharge because they are the tallest mountains up-gradient of the Ash

Meadows Springs and have significant annual precipitation, particularly snow (Fig. 1). It also exposes a major outcrop of the regional carbonate aquifer (Fig. 5). Several of the springs discharging on the western side of the mountains are located adjacent to large outcrops of quartzite. Indian Springs, directly to the north of the Spring Mountain foothills, is also included in the Spring Mountains region. The springs on the eastern slope of the Spring Mountains are not included in this area, as they flow toward Las Vegas rather than to the west where Ash Meadows lies.

The Pahranagat Valley region has tall, narrow mountains that extend north-south for a large distance and is considered the northernmost and easternmost recharge area (Thomas, 1996). There are only a few springs in this area to represent the groundwater. The geology is also a complex mixture of Paleozoic carbonates and Tertiary volcanic rocks (Fig. 5). The primary appeal of Pahranagat Valley as a flow path contributing to interbasin flow in the Death Valley conceptual model is the low isotopic signature (δD -109‰), which reflects cool temperature recharge. The interbasin flow model mixes the isotopically enriched Pahranagat Valley waters with the recharge of depleted Spring Mountain waters, which have a high isotopic signature (δD -99‰). The Spring Mountains isotopic signature is too high (less negative) to become Ash Meadows water (δD -103‰) on its own (Fig. 1).

Previous Studies and Significance of Project

Due to the interest of the U.S. Government in the Nevada Test Site, Yucca Mountain, and Death Valley, as well as the interest of the States of Nevada and California in desert water resources for local farmers, wildlife habitats, and continued population growth in nearby cities such as Pahrump and Las Vegas, this area has been

relatively well-studied (e.g., Benson and McKinnley, 1985; Blakely et al., 2000; Classen, 1985; D'Agnese et al., 1988; Ferrill et al., 1999; Forester et al., 1999; Grove et al., 1969; Ingraham and Taylor, 1991; Larson, 1974; Malmberg and Eakin, 1962; Maxey and Jameson, 1948; Moore, 1961; Naff, 1973; Paces and Whelan, 2001; Perfect et al., 1995; Quade et al., 1998; Rose et al., 1997; Schoff and Moore, 1964; Thordarson et al., 1967; White, 1979; Winograd and Thordarson, 1975; Winograd et al., 1998; Thomas et al., 1996; Workman et al., 2001).

A large number of maps and official reports exist detailing the geology, hydrogeology, hydrochemistry, geophysical (seismic, gravity, and magnetic) features, and paleoclimatic data. The value of this project lies in the approach; most studies dealing specifically with the hydrogeology of the Ash Meadows area assume that the interbasin groundwater model is accurate, and very few seriously mention the possibility of water recharged closer to Ash Meadows (see Classen, 1985), that flow may include aquifer systems and water sources other than carbonate rocks, or that the flow paths to Ash Meadows are severely restricted by the intervening geology.

Geology

The Ash Meadows recharge area is located in the southwestern Great Basin, and determining that location, along with associated flow paths, is a key element of this thesis. The regional Basin and Range topography is largely underlain by Paleozoic carbonate rocks in horsts and unconsolidated Cenozoic sediments in the valleys (Fig. 2). Surface geology in the valleys includes alluvial fans, playas, eolian, lacustrine, and spring deposits (Workman et al., 2001a). Bedrock geology in the valleys includes lava flows and tuffs, intrusive rocks, thick sequences of sedimentary rocks (sandstone, limestone,

conglomerates, and mudstone), and a crystalline basement (Workman et al., 2001a) (Fig. 5).

The Ash Meadows wetland area is located in the Walker Lane Belt, which trends north-northwest along the Nevada-California border, and is dominated by a right-shear and extensional strain field (Workman et al., 2001b). The Gravity Fault is a west-dipping normal fault indirectly defined by geophysical surveys and the westward limit of bedrock hills in the Amargosa Desert. A series of small scarps and discontinuous lineaments, called the Ash Meadows fault zone, approximately overlies the southern trace of the Gravity Fault and has a late Pleistocene age for the most recent rupture (Workman et al., 2001b).

Hydrogeology

Four major hydrogeologic units in the Death Valley Region consist of local valley-fill aquifers, a lava-flow and tuff aquifer, an upper carbonate aquifer, and a lower carbonate aquifer (Winograd and Thordarson, 1975; Anderson, 2002). The carbonate aquifers have been structurally deformed by both compression and extension and are pervasively fractured (Thomas, 1996). High altitude winter precipitation in the Spring Mountains and Sheep Range (Fig. 1) is considered the main recharge source for the carbonate aquifer (Winograd and Thordarson, 1975; Coplen et al, 1994; Winograd et al, 1997). Groundwater mixing from different recharge sources is thought to occur prior to discharge at Ash Meadows (Winograd and Pearson, 1976; Smith et al, 1992; Thomas, 1996). The minerals that appear to control groundwater solute chemistry primarily include dolomite, calcite, gypsum, halite, quartz, feldspars, and volcanic glass (Thomas, 1996).

Research Methods

Seismic Acquisition

High resolution seismic reflection data was collected along a gravel road near Devils Hole at the Ash Meadows Wildlife Refuge (Fig. 6). The sound source was primarily a 100-lb accelerated weight drop attached to the back of a 4-wheel ATV, replaced in one section with a 10 pound sledge hammer.

Data Collection

A large number of water samples have been collected for many studies in southwestern Nevada and southeastern California, from Pahranagat Valley in the northeast corner of the Death Valley Regional Flow Model boundaries, to the Panamint Range in the southwest (Fig. 7). A database comprising historic solute chemical and isotopic data for over 4,500 water samples was compiled from over 50 published sources, with the data from each source organized to appear in the same order (see Database1.xls on accompanying CD).

Since this thesis dealt only with potential flowpaths to Ash Meadows, only sites that are up-gradient from Ash Meadows were further analyzed. The remaining 3,900 samples were grouped into seven geographic regions based on specific geologic characteristics: Ash Meadows, Amargosa Desert, Oasis Valley, Yucca Mountain, Frenchman Flat and Groom Mountain, Pahranagat Valley, and Spring Mountains. Most of the original samples do not contain a full suite of chemical and isotopic data, and many of the samples were collected on different dates by different people from the same

Figure 6. Map showing the locations of the Ash Meadows seismic line (DH-1) relative to the deep seismic line AV-1 (Brocher et al., 1993) and Felderhoff wells (Carr, 1995).

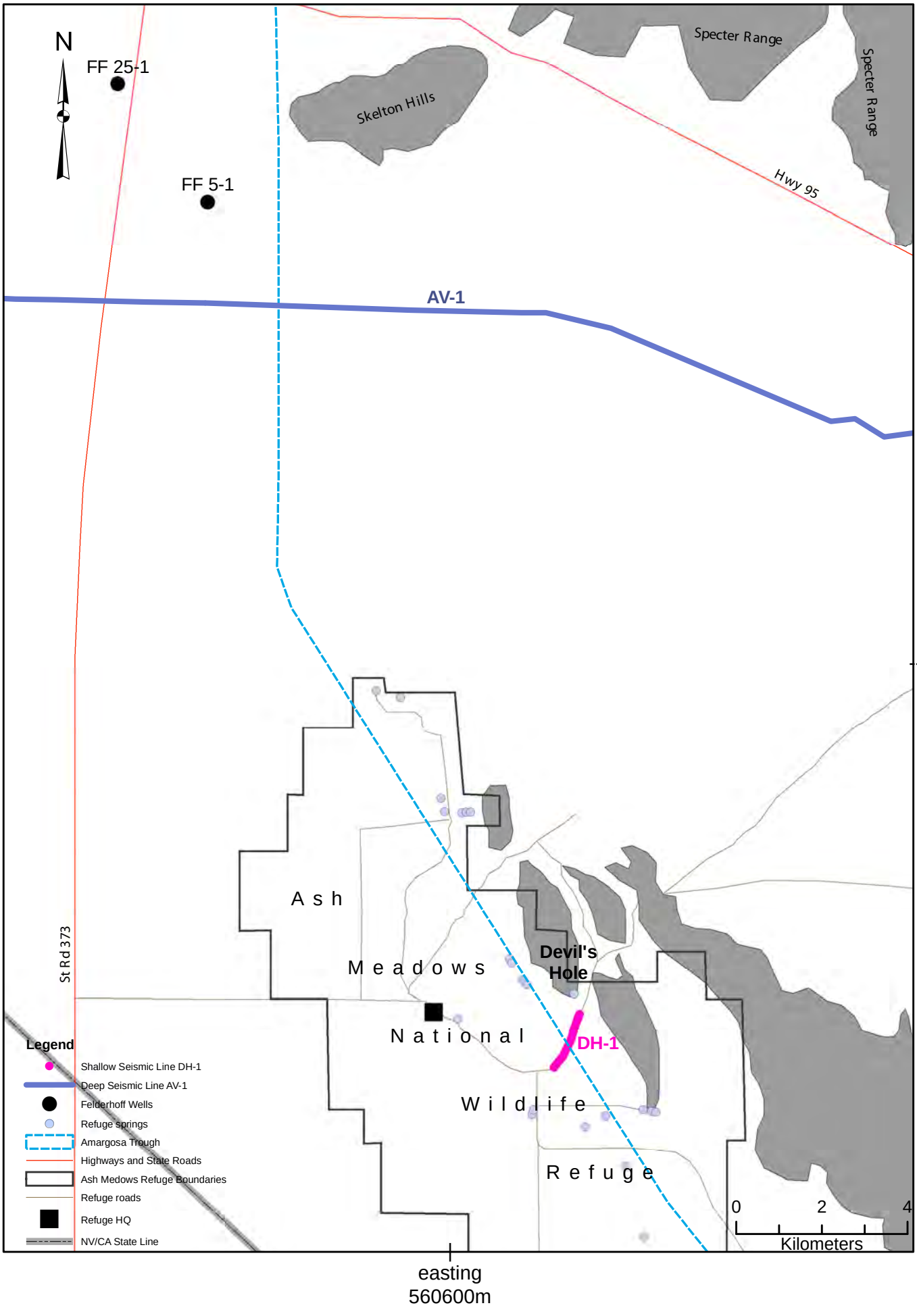

Figure 7. Map showing 4000+ water samples from springs and wells in southern Nevada and California.

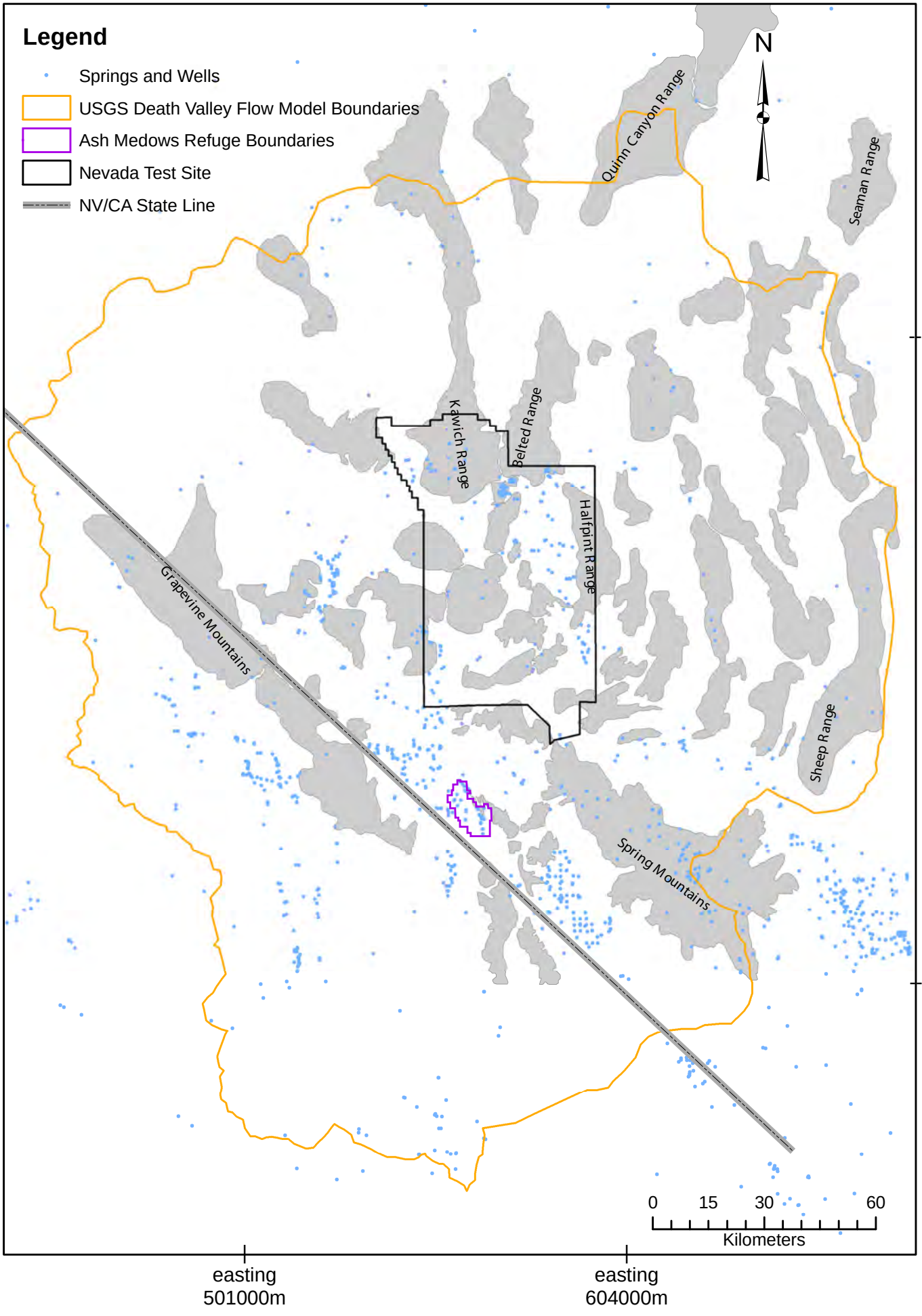

springs or wells and therefore contain some overlapping data. Samples from the same location (evidenced by either the same name or the same geographical coordinates) were merged together, and averages were used where chemical and/or isotopic data overlapped.

After grouping the samples into each of the seven regions, the samples were further culled for mass balance modeling in NETPATH by taking only those samples that have charge balance within an error of ±5%.

Regional waters around Ash Meadows tend to have temperatures around 27 ºC, which is substantially warmer than the mean annual surface temperature of about 18.5 ºC (Paces and Whelan, 2001). Cold waters with short flowpaths would be less likely to represent regional flow, so all samples below 20 ºC were eliminated, including many samples without temperature data. This left a total of 247 samples (Appendix A). However, some of these remaining samples did not have complete isotopic data, so each region's average isotopic data from the samples that were eliminated for low temperature (or lack of temperature) were added back into the relevant thesis samples for isotopic analysis where needed.

New Water Sample Collection

One objective of this project was to determine where critical gaps in information existed along potential flow paths to Ash Meadows and to collect samples to fill those gaps. Several new water samples were collected in the field from accessible springs and analyzed for $\delta^{34}S$ and $\delta^{87}Sr$ at the University of Arizona and the University of Wyoming, respectively (Appendix B).

Solute Chemistry

Hydrochemical data were evaluated in the context of available subsurface geologic information, including fault locations; orientations of fractures with aperture; hydrostratigraphy and water-rock chemical interactions; heterogeneity of the aquifer; and an analysis of where the water has been stored since the last pluvial.

The computer programs WATEQ4F (Ball and Nordstrom, 1991) and NETPATH (Plummer et al., 1991) were used to constrain chemical equilibrium and mixing along potential flow paths. Stiff diagrams were constructed from the mean solute chemistries of each geographic cluster (see explanation below) using GEOSTIFF software (Boghici and Boghici, 2001) and were plotted in ArcView in order to illustrate the flow path evolution (Fig. 8).

Cluster Analysis

Although a significant number of samples met the temperature and charge balance criteria, the solute chemistry for each region was still highly variable (e.g. the values for HCO_3^- ranged from 74 mg/L to 723 mg/L for the Yucca Mountain region). This extreme variability produced mean values for each region with a very high standard deviation (e.g., for HCO_3^- in the whole Yucca Mountain region, the mean value is 160 mg/L with a standard deviation of ±102). It was necessary to further separate and simplify the water chemistries with a statistical cluster analysis in order for the mean values to produce models representative of endmember waters.

With the remaining 247 waters from each of the seven regional flow paths, a statistical cluster analysis was performed to determine which samples were most like each other within each flow path, based on major solute chemistry (see Güler and Thyne,

Figure 8. Map of NETPATH model areas based on the cluster analysis, grouping together samples that are most like each other within a flow path region. Stiff diagrams are based on the mean value of all the samples within each cluster.

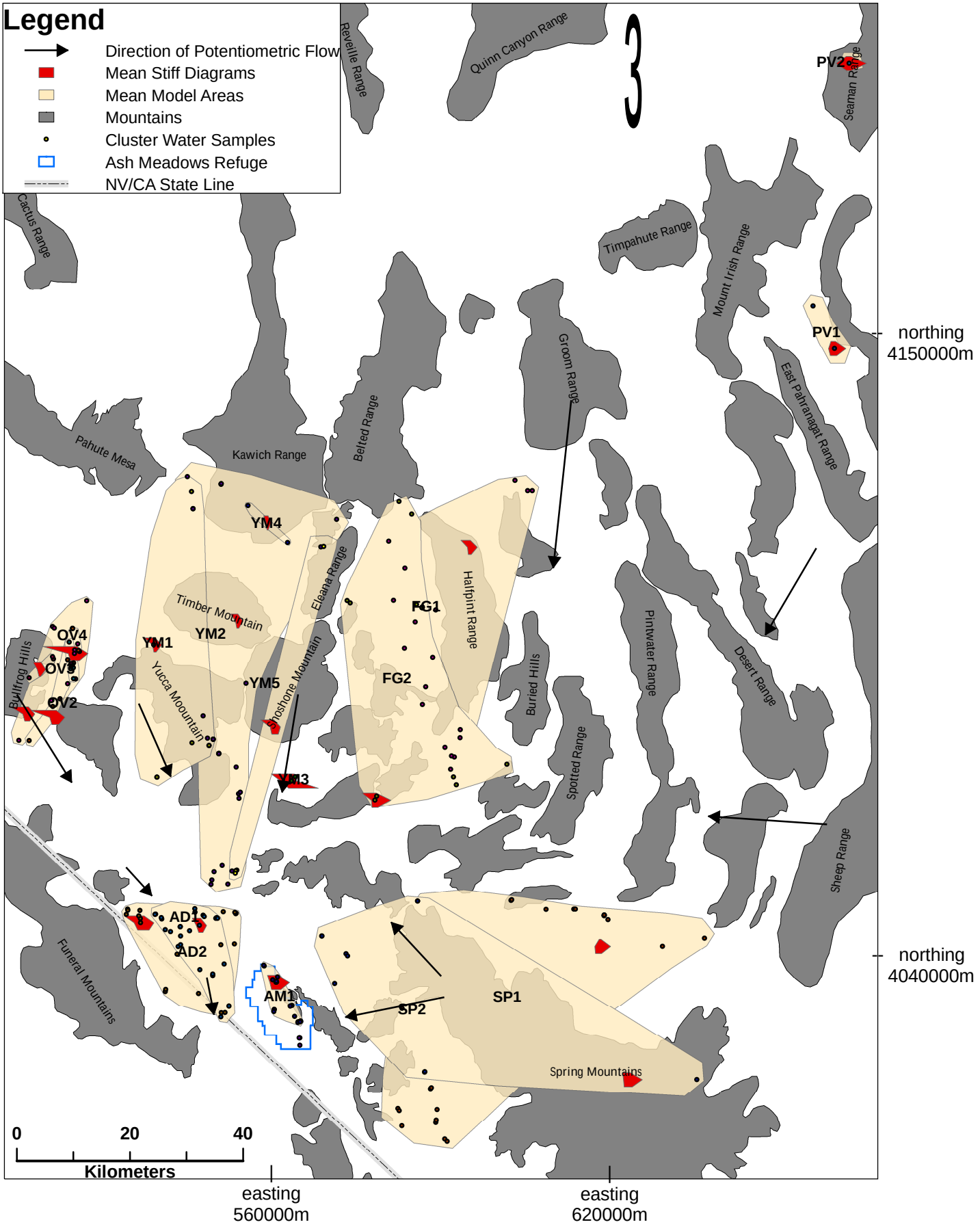

2006) (HCO_3^-, SO_4^-, Cl^-, Ca^+, Na^+, K^+, Mg^+). Each flow path was then separated into 2 to 5 clusters based on a visual inspection of the resulting cluster trees (Appendix C). The higher the average Euclidean distance between clusters (based on the y-axis values), the less alike the water sample chemistries are, and the more distinctive the clusters become. The Euclidean distance between samples in any chosen cluster was less than 1.0. "Clusters" with only one sample were generally eliminated. The average for each distinctive cluster within the region was modeled in NETPATH (Appendix D).

Saturation Index: WATEQ4F and Normalization

In order to better constrain the NETPATH models, the water chemistries for the mean samples were examined with WATEQ4F to obtain saturation indices and to determine whether each averaged up-gradient water was oversaturated (inclined to precipitate) or under-saturated (inclined to dissolve) with respect to certain minerals, particularly calcite and dolomite. Some samples had sufficient chemical data to determine saturation indices for gypsum, illite, potassium feldspar (k-spar), potassium mica (k-mica), and kaolinite (Appendix F) as well.

The mean cluster solute chemistry was also normalized relative to Ash Meadows to see how ions and minerals (particularly quartz) in up-gradient waters compared to waters discharging at Ash Meadows. Each ion from an up-gradient water cluster was divided by its corresponding ion from the Ash Meadows cluster (Appendix E). This facilitates the identification of relative enrichment and depletion patterns in the respective clusters.

All up-gradient waters were under-saturated with respect to gypsum and halite, and over-saturated with respect to quartz (except Spring Mountain waters), so any

NETPATH model results that required gypsum or halite precipitation or quartz dissolution (except Spring Mountain waters) were rejected. Similarly, all up-gradient waters were oversaturated with respect to illite, kaolinite, and k-mica, so any model results that required additional dissolution of those minerals were rejected. The majority of waters were over-saturated with respect to calcite, so when those model results required calcite dissolution in order to evolve into Ash Meadows waters, they were rejected. Similar methods were used with the other samples depending on the chemical data that were available for saturation index analyses.

WATEQ4F analysis explicitly considers CO_2 gas, so CO_2 was permitted to enter or leave the aquifer system. Although regional waters are unlikely to dissolve additional CO_2 gas from the surface, it is possible for upwelling CO_2 to be added to the system via faults and the thermal decomposition of carbonates (Mayo et al, 1991) or other sources.

The addition of CO_2 also increases the acidity of water, which allows additional calcite dissolution, so it is possible that waters that were saturated with respect to calcite and required both the addition of CO_2 as well as the addition of calcite, should not be rejected.

NETPATH

The temperature, pH, and solute chemistry data (mg/L) were entered into the NETPATH database program, and later the stable isotopic data (‰) were added. Gaps in isotopic data were filled in using mean isotope values from samples that had previously been eliminated due to low water temperature and anion-cation charge imbalance. In NETPATH, the option for charge balance approximation was ignored because the mean value outputs from the cluster analysis were already charge balanced (within ±5%).

Redox was ignored because no redox sensitive species were used. Dissolved inorganic carbon (bicarbonate) was entered as "field alkalinity," and sulfur isotopes were assumed to represent sulfate rather than hydrogen sulfide.

NETPATH allows the user to determine which constraints (ions/isotopes) and phases (minerals/gases) allow for the up-gradient water to chemically evolve into the down-gradient water, if at all possible. In this sense, NETPATH can only exclude candidate up-gradient candidate waters. Flow path geology, including surface and likely subsurface lithologies, were considered along each flow path for potential water-rock interactions. In order to cover all possible paths the water could take, the surrounding surface (Workman et al., 2001a) and subsurface (Sweetkind et al., 2001) geology for each sample was listed, between the mean water sample and Ash Meadows (Appendix G).

Each rock type was then tabulated into a likely mineralogy and associated ionic chemistry of waters. All of the potential flow paths to Ash Meadows contain calcite, dolomite, quartz, and clay minerals (illite, koalinite, and k-mica). The surface geology in part of the Spring Mountain and Frenchman/Groom Mountain areas contained playa/salt pan deposits, so halite and gypsum were included in those models. The Oasis Valley, Yucca Mountain, Frenchman Groom, and Pahranagat Valley areas all contained lava flows and tuffs, so diopside and plagioclase were included in those models. Biotite was included in the Frenchman Groom, Yucca Mountain, and Oasis Valley models. K-spar was included in the Yucca Mountain, Frenchman Groom, and Oasis Valley models. Other minerals that could have been used (e.g., hornblende, orthoclase, olivine, fluorite, or augite) were ignored, either because they were not available in NETPATH or because

they were deemed unimportant for modeling purposes. Based on this information, model parameters were set up in a spreadsheet and entered into NETPATH (Appendix H).

NETPATH was permitted to include/exclude any of the chosen minerals, if necessary, to achieve a model result. The minerals with known saturation indices were constrained in NETPATH to only precipitate or dissolve consistent with thermodynamic tendencies. Several model results were rejected because NETPATH stated that it could only achieve model results by ignoring the precipitation/dissolution constraints. In the case of CO_2 dissolution where calcite constraints were ignored, the models were re-evaluated to determine whether they should be rejected.

The chemical evolution of up-gradient waters into Ash Meadows waters was initially evaluated without isotopic constraints. All mixing models included calcite and dolomite with the isotopes δD and $\delta^{18}O$ to constrain mixing fractions.

Stable and Radiogenic Isotopes

The stable isotopes of hydrogen (D/H), oxygen ($^{18}O/^{16}O$), carbon ($^{13}C/^{12}C$), sulfur ($^{34}S/^{32}S$), and the radiogenic isotope strontium ($^{87}Sr/^{86}Sr$), were evaluated for both historic data and samples collected in this study. The relationship between δD_{VSMOW} and $\delta^{18}O_{VSMOW}$ values between Ash Meadows and potential up-gradient sources was evaluated by plotting them against each other and comparing the slopes of these waters against the location of the global Meteoric Water Line (Fig. 9) (Friedman, 1953; Craig, 1961; and Gat, 1980). This was useful for understanding the climate at the time the groundwater was recharged, and assessing the degree of any evaporation that may have occurred prior to recharge.

Mass Balance Models

Overview of Results

A number of up-gradient water sources and associated flow paths were ruled out on the basis of mass balance models combined with further consideration of saturation indices. The best model results came from Yucca Mountain, Frenchman Groom, and Oasis Valley waters (Table 1).

Table 1 Overview of NETPATH models, with number of water samples in each cluster and number of models NETPATH produced.

Region	cluster	# of samples	# NETPATH models
Amargosa Desert	AD1	76	1 (ignored constraints)
Amargosa Desert	AD2	41	4 (ignored constraints)
Ash Meadows	AM1	115	final water
Frenchman Groom	FG1	132	13
Frenchman Groom	FG2	217	1
Oasis Valley	OV1	5	6
Oasis Valley	OV2	43	12
Oasis Valley	OV3	79	4
Oasis Valley	OV4	26	11
Pahranagat Valley	PV1	6	0
Pahranagat Valley	PV2	2	0
Spring Mountains	SP1	58	1 (ignored constraints)
Spring Mountains	SP2	92	1 (ignored constraints)
Yucca Mountain	YM1	61	0
Yucca Mountain	YM2	313	0
Yucca Mountain	YM3	26	36
Yucca Mountain	YM4	11	1
Yucca Mountain	YM5	17	24

Spring Mountain and Pahranagat Valley water samples generally did not produce good model results. The more models NETPATH produced for a given cluster, the more likely that the corresponding flow path represents up-gradient waters, because of the increased possibilities for water-rock interactions along the flow path. The northern Ash Meadows

cluster (AM1) was used as the final water for all mass balance models, due to the apparent siliciclastic aquifer source of southern Ash Meadows (AM2) waters (Fig.10).

Flow Paths to Ash Meadows

Amargosa Desert Region

The cluster analysis produced two geographically overlapping clusters of similar water samples (Fig. 8). Cluster AD1 represents a narrower area in the middle of the Amargosa Desert, and the water chemistry of these samples may be affected by proximity to the Amargosa River subflow, though deep regional underflow may be hydrologically unconnected to the Amargosa River. Cluster AD2 represents a wider area, and the samples are predominantly located on the outer boundaries of the Amargosa Desert region (Fig. 8).

Both AD1 and AD2 clusters produced poor model results in NETPATH. Cluster AD1 was undersaturated with respect to calcite and dolomite, and saturated with respect to illite, k-mica, kaolinite, and quartz. By allowing AD1 to interact with various combinations of calcite, dolomite, illite, k-mica, kaolinite, quartz, and CO_2 gas, NETPATH produced 1 model that allowed AD1 to chemically evolve into Ash Meadows water. However, this model ignored the illite constraint, requiring illite to dissolve into the water rather than precipitate in order to turn into Ash Meadows water. The AD1 model also required CO_2 to enter the groundwater along the flowpath. Since the $\delta^{13}C$ isotopic signature (-6.05‰) is much closer to marine limestone (0‰) than to soil CO_2 (-20‰)(Clark and Fritz, 1997), it is likely that the primary contribution of CO_2 comes from decarbonation reactions, or the thermal breakdown of buried carbonate rocks that results

in the release of CO_2 gas which then travels upward through fractures (Mayo and Miller, 1997). Large fractures are present throughout this region (Fig. 2), permitting the upwelling of CO_2 gas.

Cluster AD2 was undersaturated with respect to dolomite, but saturated with respect to calcite, illite, k-mica, kaolinite, and quartz. AD2 was unable to chemically evolve into Ash Meadows water without igoring either illite or kaolinite constraints, but produced 4 model results. CO_2 gas left the groundwater aquifer system in all 4 model results. Since the δ13C isotopic signature for Amargosa Desert waters (-6.05‰) is so much closer to marine limestone (0‰) than to soil CO_2 (-20‰), it is likely that the primary contribution of CO_2 also comes from decarbonation reactions. Normalization of the solute chemistry (Appendix E) shows that AD2 waters have high chloride content relative to Ash Meadows water, requiring halite precipitation for AD2 to evolve into AM1, which cannot occur at such a low saturation. This eliminates the AD2 cluster from the flow path consideration.

Geologically, the Gravity Fault zone separates Ash Meadows water from all Amargosa Desert waters, such that they may not be able to interact much with the water discharging in the wetland springs. This may be especially true if the fault core of the Gravity Fault acts as an impermeable barrier for east-west flow.

Oasis Valley Region

The cluster analysis produced 4 geographically-overlapping clusters (Fig. 8). All four clusters are undersaturated with respect to dolomite. Cluster OV1 is undersaturated in calcite and saturated in quartz. Clusters OV2, OV3, and OV4 are saturated with respect to calcite, illite, kaolinte, k-mica, and quartz. All four clusters produced good model

results in NETPATH. Cluster OV1 produced 6 good model results, with 3 models requiring CO_2 gas to enter the system and 1 model requiring CO_2 gas to exit the system. Cluster OV2 produced 12 good models, with 7 models requiring CO_2 input. Cluster OV3 produced 4 good models, with all 4 models requiring CO_2 input. Cluster OV4 produced 11 good models, with 6 models requiring CO_2 input.

Normalization of the solute chemistry (Appendix E) shows that OV2 and OV4 waters have high chloride content relative to Ash Meadows water, requiring halite precipitation for OV2 and OV4 to evolve into AM1, which cannot occur at such a low saturation. This eliminates the OV2 and OV4 clusters from the flow path consideration.

Yucca Mountain Region

The cluster analysis produced 5 clusters, YM1-YM5 (Fig. 8). Clusters YM1 and YM2 did not produce any model results, but YM3, YM4, and YM5 produced good model results in NETPATH. All 5 clusters were undersaturated with respect to dolomite, and saturated with respect to illite, k-mica, kaolinite, and quartz. Cluster YM4 was undersaturated with calcite.

Cluster YM3 produced 36 good models, and 29 of them required large amounts (~6 mmols/L) of CO_2 gas input. Cluster YM4 produced 1 good model, and that model required CO_2 gas input. Cluster YM5 produced 24 good models, and 20 models required CO_2 gas input. The high number of models here indicates that these are likely candidates for upgradient waters, since Yucca Mountain water may chemically evolve into Ash Meadows water in a number of ways.

Normalization of the solute chemistry (Appendix E) shows that YM3 waters have high chloride content relative to Ash Meadows water, requiring halite precipitation for

YM3 to evolve into AM1, which cannot occur at such a low saturation. This eliminates the YM3 cluster from the flow path consideration.

Geologically, it makes sense for Yucca Mountain water to contribute to the discharge at Ash Meadows, because the Gravity Fault appears to be a widely fractured zone that could allow water to travel south from Yucca Mountain directly to Ash Meadows. The high relative fracture aperture of the north-south fractures (oriented perpendicular to the least principal horizontal stress direction) may permit significantly more water to flow from Yucca Mountain to Ash Meadows than any waters traveling through east-west fractures, which should be closed in the modern stress field (Miner et al., 2007; Ferrill, 1999). However, the groundwater from the Yucca Mountain Region may also encounter a barrier at the northward-dipping Highway 95 Fault (Fig. 5).

Frenchman Groom Region

The cluster analysis produced 2 clusters, FG1 and FG2 (Fig. 8). Both clusters are saturated with respect to calcite, illite, k-mica, kaolinite, and quartz, and undersaturated with respect to gypsum. With respect to dolomite, FG1 is saturated and FG2 is undersaturated. For cluster FG1, NETPATH produced 13 good model results, and 9 of them required CO_2 input. For cluster FG2, NETPATH produced 1 good model result, and that model required CO_2 input. The $\delta^{13}C$ isotopic signature for FG1 waters is -7.24‰, indicating a CO_2 source from a decarbonation reaction rather than the surface.

Spring Mountains Region

The cluster analysis produced two geographically overlapping clusters, SM1 and SM2 (Fig. 8). The charge balanced samples over 20 ºC were located around the base of

the Spring Mountains to the north and northwest as the springs in the interior of this range tend to have temperatures colder than this. The SP1 cluster includes all samples to the north near Indian Springs as well as some samples to the west. The SP2 cluster includes a smaller number of samples, primarily in the northwestern corner of the Spring Mountains Region. In addition to the two high-temperature clusters, four lower-temperature springs discharging from quartzite rocks up on the Spring Mountains (Grapevine, Horseshutem, Diebert, and Kwichup springs) were modeled separately. With respect to calcite, both clusters and all the springs except Kwichup spring were oversaturated. Clusters SP1 and SP2 are saturated with respect to calcite, k-mica, and kaolinite, and undersaturated with respect gypsum and quartz. NETPATH was unable to produce any good model results. All model results for SP1 and SP2 ignored the precipitation/dissolution constraints for k-mica and kaolinite in order to chemically evolve the water to Ash Meadows water.

Pahranagat Valley Region

The cluster analysis of the only 3 samples in this area above 20 ºC produced two discrete clusters, PV1, located far north in the Seaman Range, and PV2, located at the southern end of Pahranagat Valley (Fig. 8). Both clusters were saturated with respect to calcite and quartz. With respect to dolomite, PV1 was undersaturated and PV2 was saturated. NETPATH was unable to produce any model results for either cluster.

Isotopes

Mixing Models

Based on the results from the mass balance models, several mixing models were also run in NETPATH. Using $\delta^{18}O$ and δD as isotopic constraints, Yucca Mountain waters contributed over 99% to Ash Meadows water. Amargosa Desert contributed less than 1% isotopically, and Oasis Valley and Frenchman/Groom Mountain waters did not contribute at all. Table 2 shows the results from the successful mixing models. From these isotope model results, it appears that Yucca Mountain water makes a rather significant contribution to Ash Meadows water, perhaps to the exclusion of other regional waters.

Table 2 Mixing Model Results

Model #	Mixing Wells					constraints	
	1	2	3	4	5		
55	ADII	YMII	YMIII	FGII	FGIV	$\delta^{18}O$	δD
results	0.00941	0.82336	0.16723	0	0		
56	ADII	YMII	YMIII	OVII		$\delta^{18}O$	δD
results	0.00941	0.82336	0.16723	0			
60	ADII	YMII	YMIII			C, Ca	
results	0	0.44321	0.55679	preciptated calcite			

Climate Signature

Depleted oxygen and hydrogen isotopes are characteristic of colder and wetter or high altitude recharge areas, whereas arid recharge results in evaporative enrichment (Clark and Fritz, 1997). According to Smith and Street-Perrott (1983), the late-Pleistocene climate in the Great Basin was characterized by several cool, wet periods with greater precipitation than today. Classen (1985) indicated that the primary source

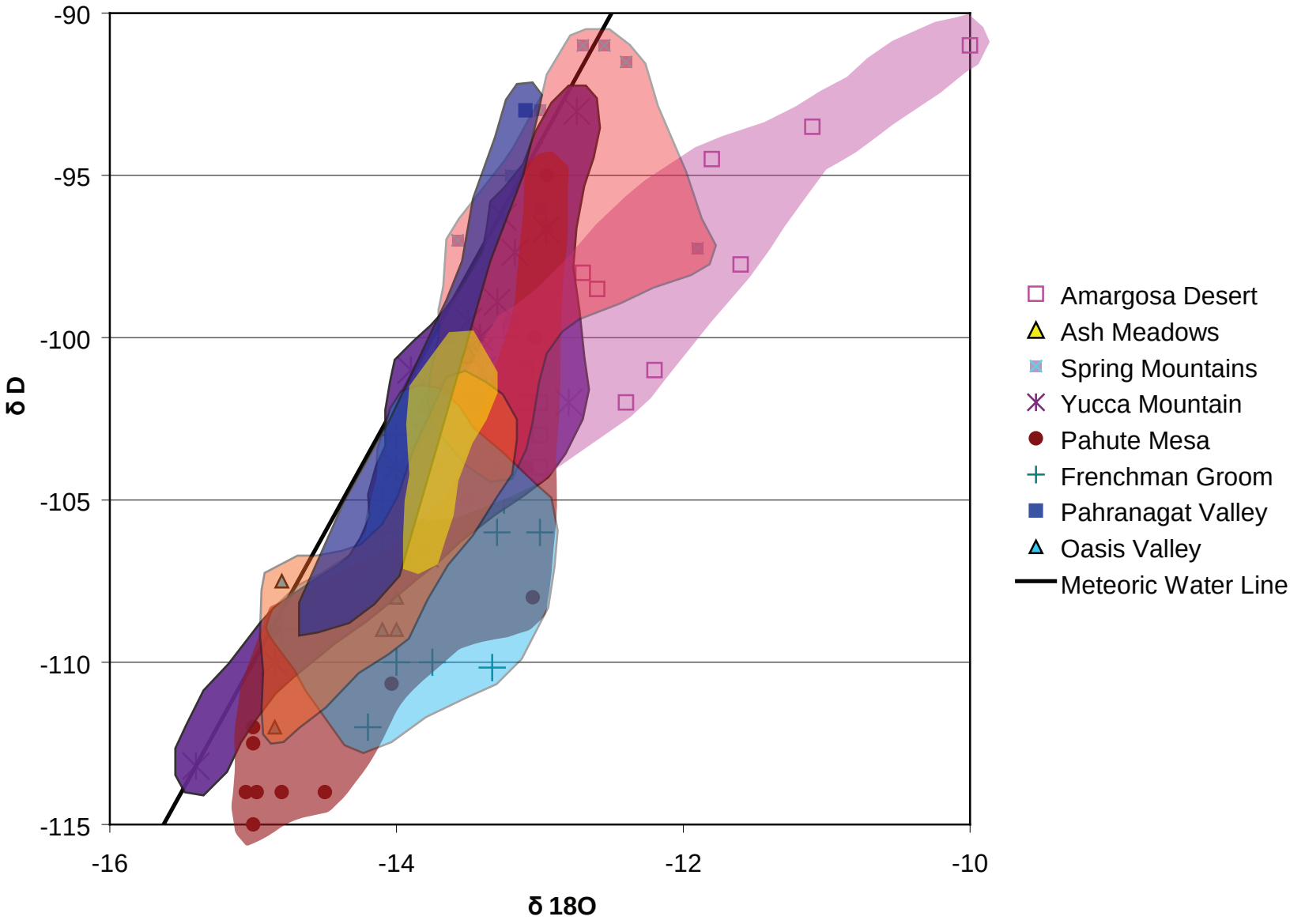

Figure 9. Water samples from each cluster relative to the Meteoric Water Line (Craig, 1961). Isotopic values for hydrogen and oxygen are in per mil.

of recharge for the Amargosa Desert aquifer was local precipitation and snowmelt during late Wisconsin time.

The isotopic signature of the Ash Meadows and Yucca Mountain (δD -103 ‰) groundwater is isotopically lighter than modern recharge in the arid Great Basin, including winter recharge in the Spring Mountains (δD -99 ‰) (Smith et al, 1992; Thomas, 1996) (Figs. 1 and 9). Previous studies have shown that a mixture of modern Pahranagat Valley (δD -109 ‰) and Spring Mountain recharge could result in Ash Meadows water (Thomas, 1996). However, as previously stated, neither up-gradient water is able to chemically evolve into Ash Meadows water. Thomas (1996) modeled flow from Pahranagat Valley and the Spring Mountains to Ash Meadows, with different results. In his model, he included similar Pahranagat Valley waters (corresponding to cluster PV1 in this study), but used very different Spring Mountain waters (sites 27-35, Thomas, 1996). In this study, those same Spring Mountain waters were eliminated from regional flow due to low temperature (below 20 ºC). The average solute chemistry of the waters Thomas chose from the Spring Mountains was higher in calcium, and lower in magnesium, sodium, potassium, chloride, and sulfate (Table 3). The average chemistries for the Spring Mountain clusters from this study (SP1 and SP2) are much closer to the sites Thomas chose at the foot of the Spring Mountains (sites 21-23, Thomas, 1996). That is because most of the most of the regional Spring Mountain waters (≤20 ºC) selected for this study were located at the foot of the Spring Mountains. Eliminating waters below 20 ºC for this study reduced the subjectivity of which waters to select for the mass balance models.

Table 3 Comparison of solute chemistries for Spring Mountain averages between Thomas (1996) and this study.

	Ca	Mg	Na	K	HCO_3	Cl	SO_4
Thomas, Spring Mountain samples							
Central Spring Mountains (sites 27-35)	60.44	15.67	1.82	0.52	253.22	1.67	11.03
Spring Mountain foothills (sites 21-23)	45.00	21.20	35.73	4.77	269.33	13.23	46.67
Bushman, Spring Mountain clusters							
SP1 AVG	40.75	22.56	9.61	1.80	226.28	5.81	20.70
SP2 AVG	42.88	22.25	50.70	7.41	294.39	14.90	54.93

Additionally, although Thomas used δD values strictly from Pahranagat Valley, for the mass balance models he used a composite solute chemistry from the entire White River System, which includes waters from the Sheep Range and other sites that are geologically restricted from westward flow (Thomas, 1996). The isotopic signature at Ash Meadows discharge may be depleted due to late Pleistocene cool temperature recharge rather than a mixture of present day recharge from Pahranagat Valley and Spring Mountains.

Radiogenic and Sulfur Isotopes

Flow paths can be further delineated by comparing the signature of radiogenic (U-series and $^{87}Sr/^{86}Sr$ ratios) and sulfur ($\delta^{34}S$) isotopes in waters with the isotopic composition in the proposed aquifers along the flow paths. Miner et al. (2007) showed the probable influence of both volcanic and carbonate aquifers on northern Ash Meadows waters (Fig. 10). Expected isotopic compositions of $^{234}U/^{238}U$ activity versus $\delta^{87}Sr$ from waters known to interact with carbonate, volcanic, and siliciclastic rocks were plotted as data fields, and northern Ash Meadows water plots on the border of overlap between

volcanic and carbonate aquifer data fields. The northern Ash Meadows waters are distinguishable from the southern Ash Meadows waters, which plot near the siliciclastic aquifer data field. The northern Ash Meadows waters appear to have interacted with carbonate and volcanic aquifers, while the southern Ash Meadows waters have interacted more strongly with a siliciclastic aquifer.

Comparison of $\delta^{34}S$ in Ash Meadows waters with waters derived from a volcanic aquifer and a carbonate aquifer shows a strong correlation between Ash Meadows water and volcanic aquifer waters (Fig. 11). The carbonate aquifers tend toward unusually low $\delta^{34}S$ values (0-8‰) (possibly due to sedimentary pyrite oxidation) than both Ash Meadows water (15-18‰) and volcanic aquifer waters (5-20‰), indicating a strong likelihood that Ash Meadows water interacted more with volcanic rocks than with carbonate rocks in order to pick up the higher $\delta^{34}S$ isotopic signature. Additionally, $^{87}Sr/^{86}Sr$ ratios tend to be lower in carbonate aquifers (0.7080-0.7140) than in volcanically-derived waters (0.7080-0.7169) (Fig. 11). Although there is considerable overlap, the Ash Meadows waters plot on the higher end of that overlapping range (0.7120-0.7139), probably indicating a stronger correlation with volcanic rocks than with carbonate rocks. U-series data alone are not as useful, as there is extensive overlap with carbonate and volcanic aquifers, and Ash Meadows waters plot well within the overlapping region.

In summary, the radiogenic and sulfur isotopes offer additional insight into the potential flow paths of waters that ultimately discharge at Ash Meadows. While the southern Ash Meadows (cluster AM2) waters derive from interaction with a siliciclastic aquifer, the northern Ash Meadows waters (cluster AM1) have clearly interacted with

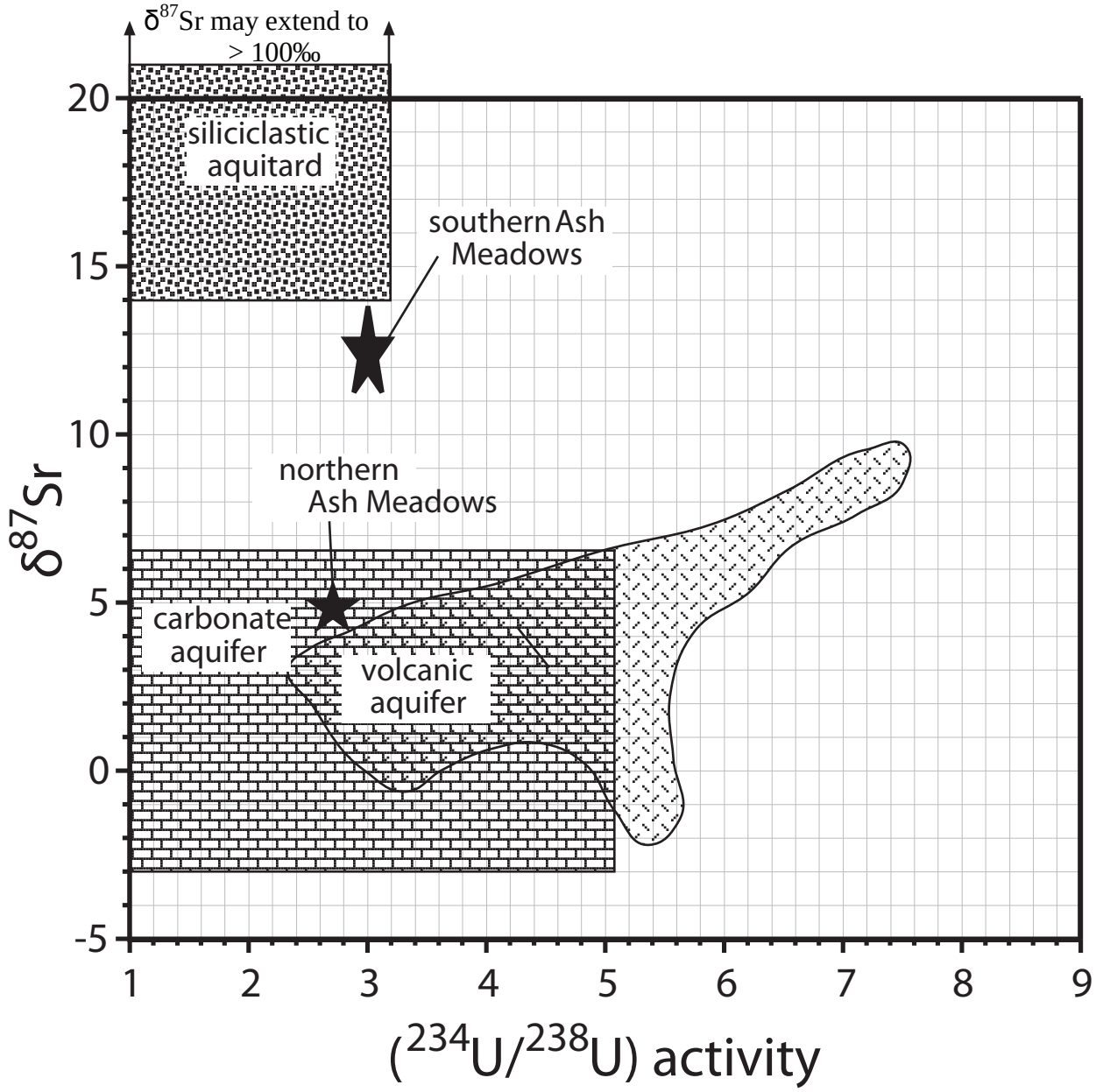

Figure 10 Ash Meadows waters plotted in relation to U-series and strontium isotopic compositions for water-rock interactions with carbonate, volcanic and siliciclastic aquifers, taken from Miner et al. (2007).

Figure 11 Comparison of sulfur, strontium and uranium isotopic data for carbonate aquifers, volcanic waters, and Ash Meadows waters.

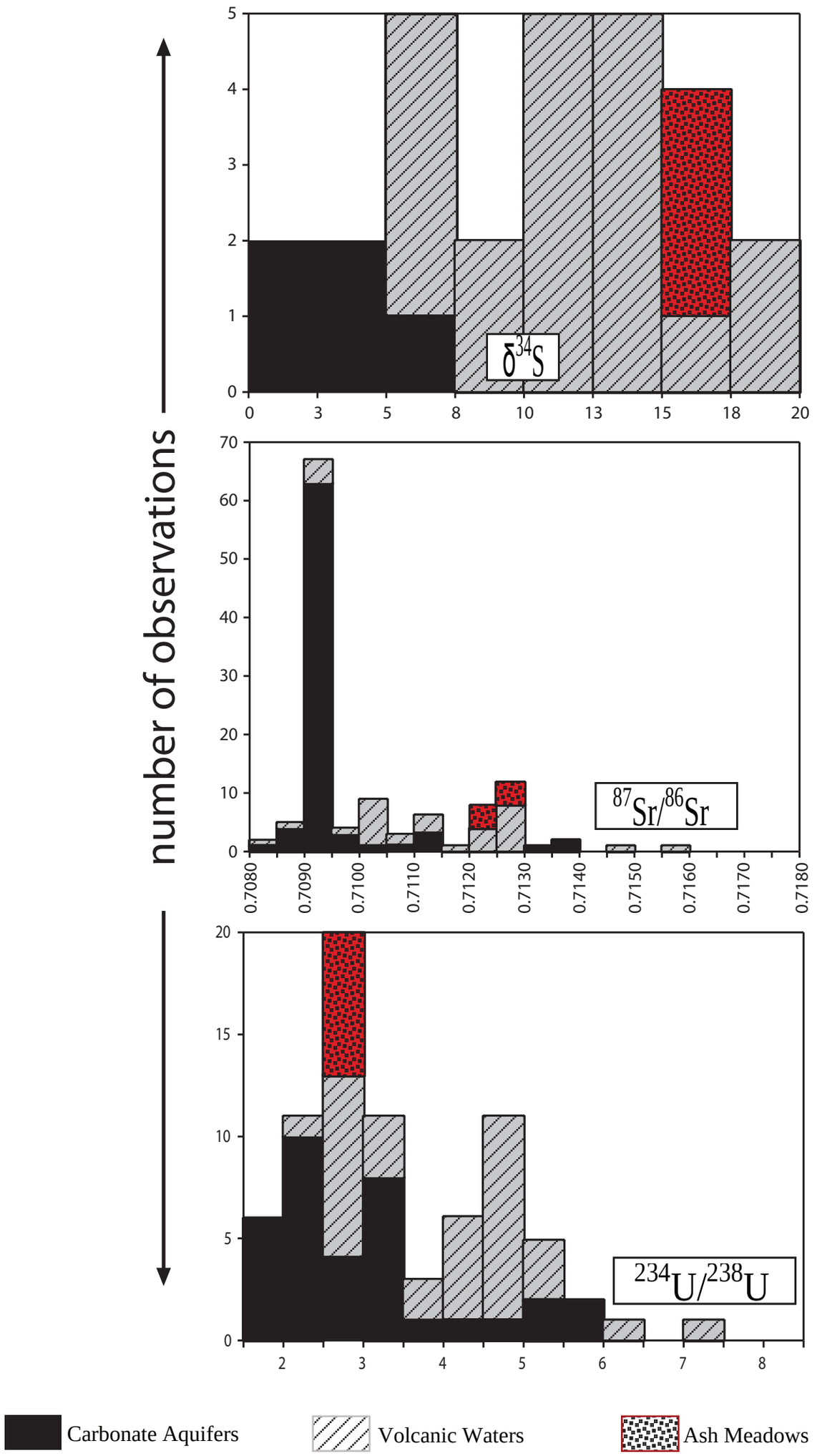

both carbonate and volcanic aquifers. While the strontium and U-series data have an overlapping signature for both carbonate and volcanic aquifers, the $\delta^{34}S$ isotopic signature in Ash Meadows waters clearly plots in the range of volcanic water-rock interaction. While there are volcanic rocks throughout several of the potential flow paths, the westward flow path from the Spring Mountains does not include a significant volcanic aquifer influence; therefore this flow path may reasonably be eliminated.

Geophysical Investigations

The volume of water and the direction of flow in an aquifer can only be inferred indirectly using the chemistry and isotopic data from wells and springs, but interpretation of the water data may be constrained in part by other geophysical methods, such as boreholes, deep and shallow seismic data, and gravity and aeromagnetic data.

The first gravity data in the vicinity of Ash Meadows were collected during the 1960s (Healey, 1968). Winograd and Thordarson (1975) proposed the existence of the Ash Meadows "gravity" fault as a possible structural control on the regional aquifer, because the 16-km long lineament of springs roughly coincided with a gravity anomaly. Subsequent geophysical data support the existence of this fault, including a deep seismic line (Brocher, 1993), borehole data from two wildcat wells (Carr, 1995) (Fig. 7), and gravity and aeromagnetic data (Blakely, 2000) (Figs. 15, 16). These data have led to the interpretation of a 160-km long asymmetrical structural trough known as the Kawich-Greenwater Rift (Carr, 1995) or the Amargosa Trough (Blakely, 2000), which is bordered on the east by a 2-km wide west-dipping zone of listric faults (Brocher, 1993) (Fig. 14). This rift zone shows up as a gravity low, and runs roughly north-south from Yucca Mountain through the Amargosa Desert to the Funeral Mountains (Fig. 16). The rifting is

likely related to the caldera complexes and volcanic centers in the Yucca Mountain area. (Carr, 1995). The south-eastern boundary of this structural trough coincides with the Ash Meadows springs.

Available potential field data (Blakely, comm. 2004) for a large area including Ash Meadows were re-analyzed (see explanation below) (Figs. 15, 16), and a shallow, high-resolution seismic survey was conducted in order to locate the near-surface expression of the faults or other deformation features more precisely in relation to the lineament of springs, and to determine whether the fault or faults inferred from the geophysical data could be imaged closer to the surface where the springs discharge.

Shallow Seismic Data

A high-resolution, shallow-penetration seismic P-wave reflection profile was acquired along a gravel road south of Devils Hole (Figs. 7, 12 and 13) in order to determine if faults could be detected in the shallow subsurface in the area of the springs and in the vicinity. The seismic acquisition parameters are given in Table 4. The processing consisted of 3D geometry assignment, adaptive deconvolution (operator length = 80 ms, lag = 15 ms), automatic gain control (200-ms window), air blast attenuation, bandpass trapezoidal frequency filter (60-90-240-400 Hz), muting of first breaks, automatic gain control (100-ms window), stacking velocity analysis, refraction statics (upper layer, 900 m/s; lower half space, 1600 m/s; elevation datum = 725 m), common mid-point (CMP) sorting, normal move-out correction (two stacks were generated at stacking velocities of 1000 m/s and 1400 m/s), CMP stacking, adaptive deconvolution (operator length = 80 ms, lag = 20 ms), 3-trace weighted mix (1,3,1), depth conversion (using bulk 1600 m/s).

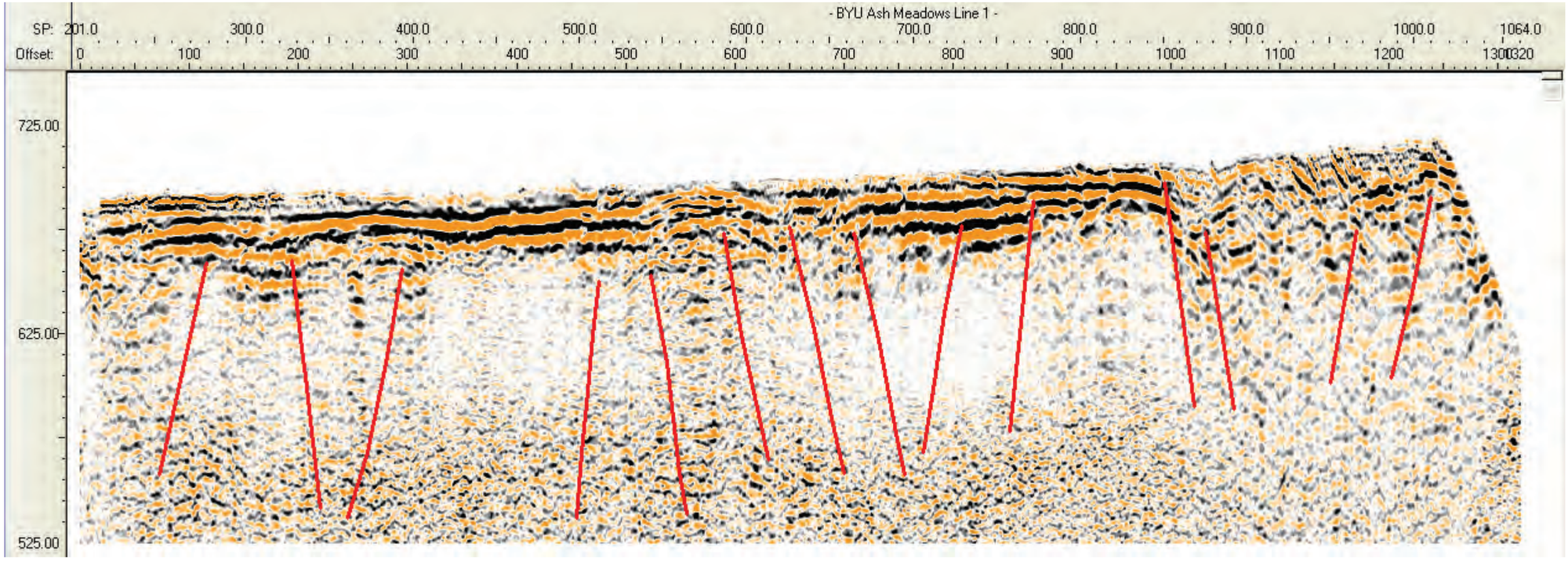

Figure 12. Profile with refraction statics, replacement velocity = 1600 m/s; stacking velocity = 1000 m/s; depth converted using 1600 m/s. Units are in meters. Elevation datum = 725 m.

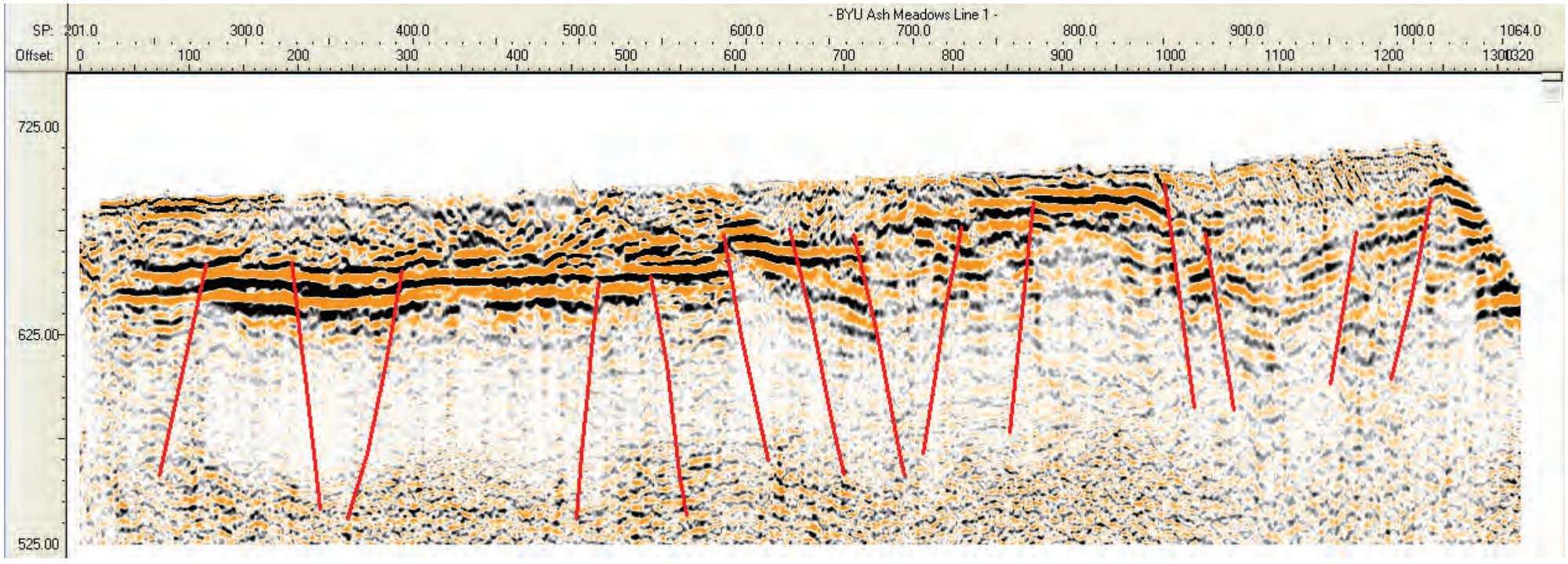

Figure 13 Profile with refraction statics, replacement velocity = 1600 m/s; stacking velocity = 1400 m/s; depth converted using 1600 m/s. Units are in meters. Elevation datum = 725 m.

Two stacks, with differing stacking velocities were prepared because of difficulty in NMO stacking of reflected events that arrived very close to, and therefore interfered with, one another. The stack with the lesser stacking velocity (1000 m/s, Fig. 12) shows reflections higher in the section, whereas that with higher velocity (1400 m/s, Fig. 13) shows reflections somewhat deeper. The sections are shown unmigrated due to the lack of steep reflectors and to avoid artifacts of possible over-migration. This also allows diffractions to be observed, which are indicators of strong disruption (e.g., beneath CMP 575 and CMP 840). The depth conversion is based on the replacement velocity, which probably represents a minimum value. Due to the uncertainty for this velocity and for that of the static correction velocities, the depths should be considered somewhat qualitative.

The interpretation of the sections for faulting is based primarily on the higher velocity stack. Faults are interpreted based on lateral change in reflection character and orientation and on offsets. The interpretation of the seismic data suggests a zone of discrete shallow faults with offsets up to almost 10 m intersecting the trend of the springs. The seismic profile also shows a major damage zone just east of the springs nearer Devils Hole.

Deep Seismic Data

The USGS conducted a deep seismic survey (line AV-1) 25 km to the north of Ash Meadows (Brocher et. al, 1993) (Fig. 14). These data reveal complex, deep crustal-scale features, as well as a 2 km-wide zone of westward-dipping listric faults.

Figure 14. Migrated stacked data for Brocher's (1993) deep seismic line AV-1, interpreted with deep faults (red lines) that may correlate with the shallow damage zone at Ash Meadows, line DH-1

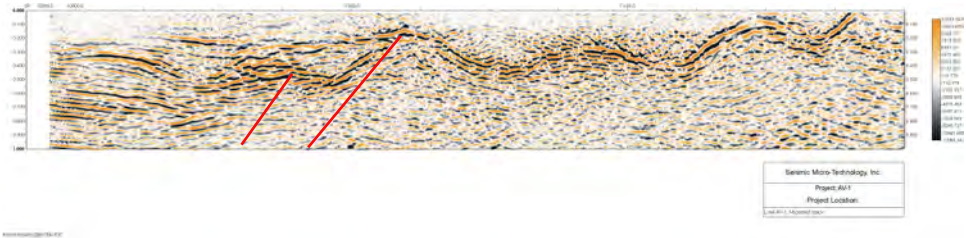

Re-analysis of Gravity and Aeromagnetic Data

Available aeromagnetic and gravity data were re-analyzed with first and second vertical derivative, Butterworth, and downward continuation filters (Telford et al., 1990). The USGS magnetic intensity data (created from the original USGS database (gxf) file) were first subjected to a 1-D 2nd vertical derivative, followed by a Butterworth filter, low-pass, cut-off wavelength of 250 ground units (m), filter order = 3. These data were then downward continued for 10 ground units (m) (Fig. 15). The USGS gravity data (from the original USGS database (gxf) file) were processed as a downward continuation of 100 ground units (m) (Fig. 16).

The re-analyzed potential field data suggest that the gravity gradient is the strongest along the western edge of the hills that trend through the northern part of the Ash Meadows National Wildlife Refuge. These analyses indicate that the seismically detected fault and damage zone (DH-1) lies just south of where the gravity gradient is strongest, but in a zone where the potential field signature is complex (Fig. 16). The potential field signature becomes more complex both to the north, where the deep seismic line AV-1 crosses the gravity anomaly, and to the south, where the shallow seismic line DH-1 crosses the gravity anomaly. Furthermore, the re-analyzed aeromagnetic and gravity data support earlier conclusions by previous workers (Winograd and Thodarson, 1975; Brocher, 1993; Carr, 1995; Blakely, 2000) of a major geophysical boundary and thus suggest that the Gravity fault, where coincident with the lineament of springs at Ash Meadows, represents a crustal-scale feature. The deep-seated nature of the Gravity fault has been previously supported by the USGS deep seismic profile (AV-1) located 25 km

Figure 15. Re-analyzed magnetic intensity data from Blakely et al. (2000) with deep seismic line AV-1 (Brocher et al., 1993) and shallow seismic line DH-1.

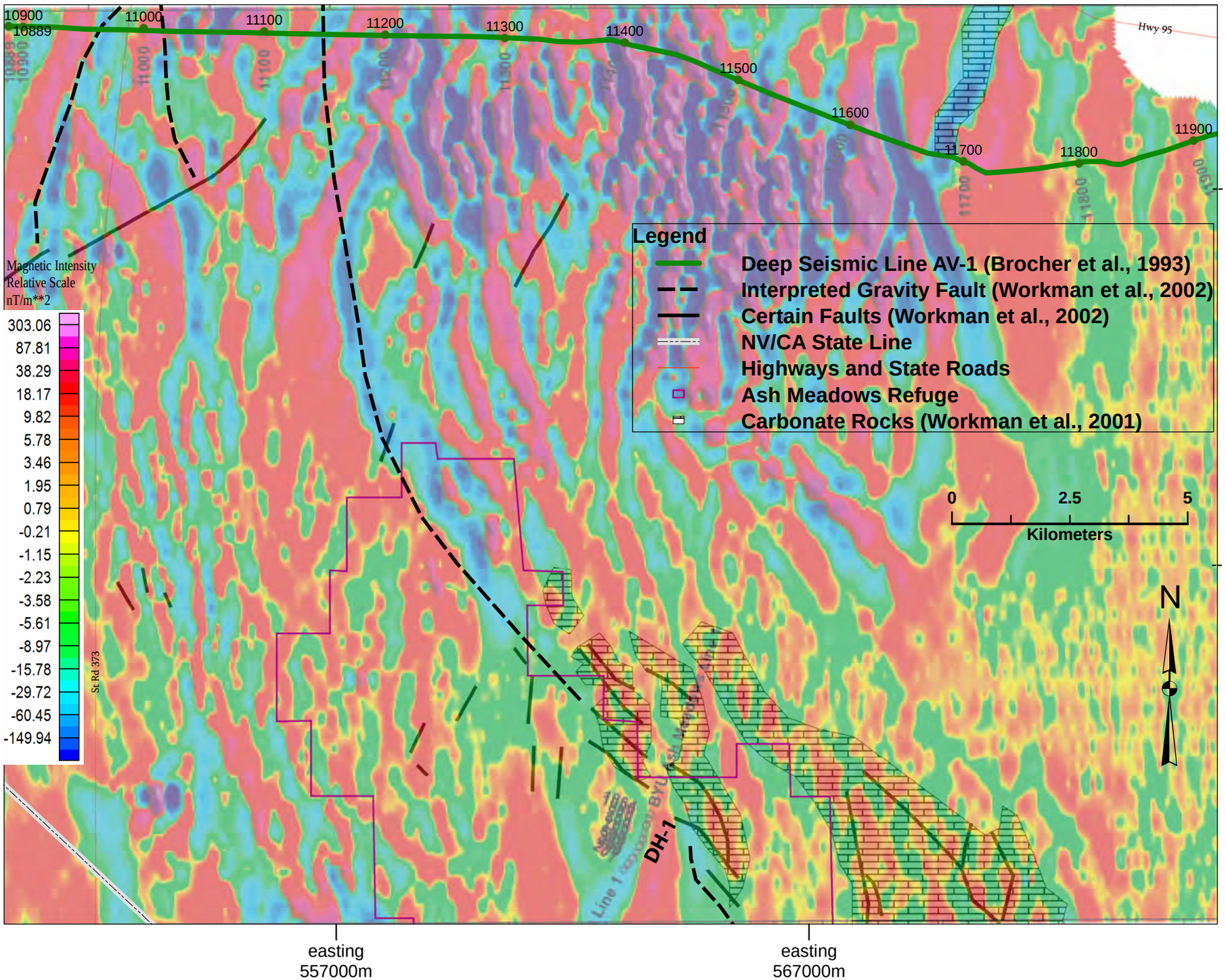

Figure 16. Re-analyzed Bouguer gravity data from Blakely et al. (2000) with deep seismic line AV-1 (Brocher et al., 1993) and shallow seismic line DH-1.

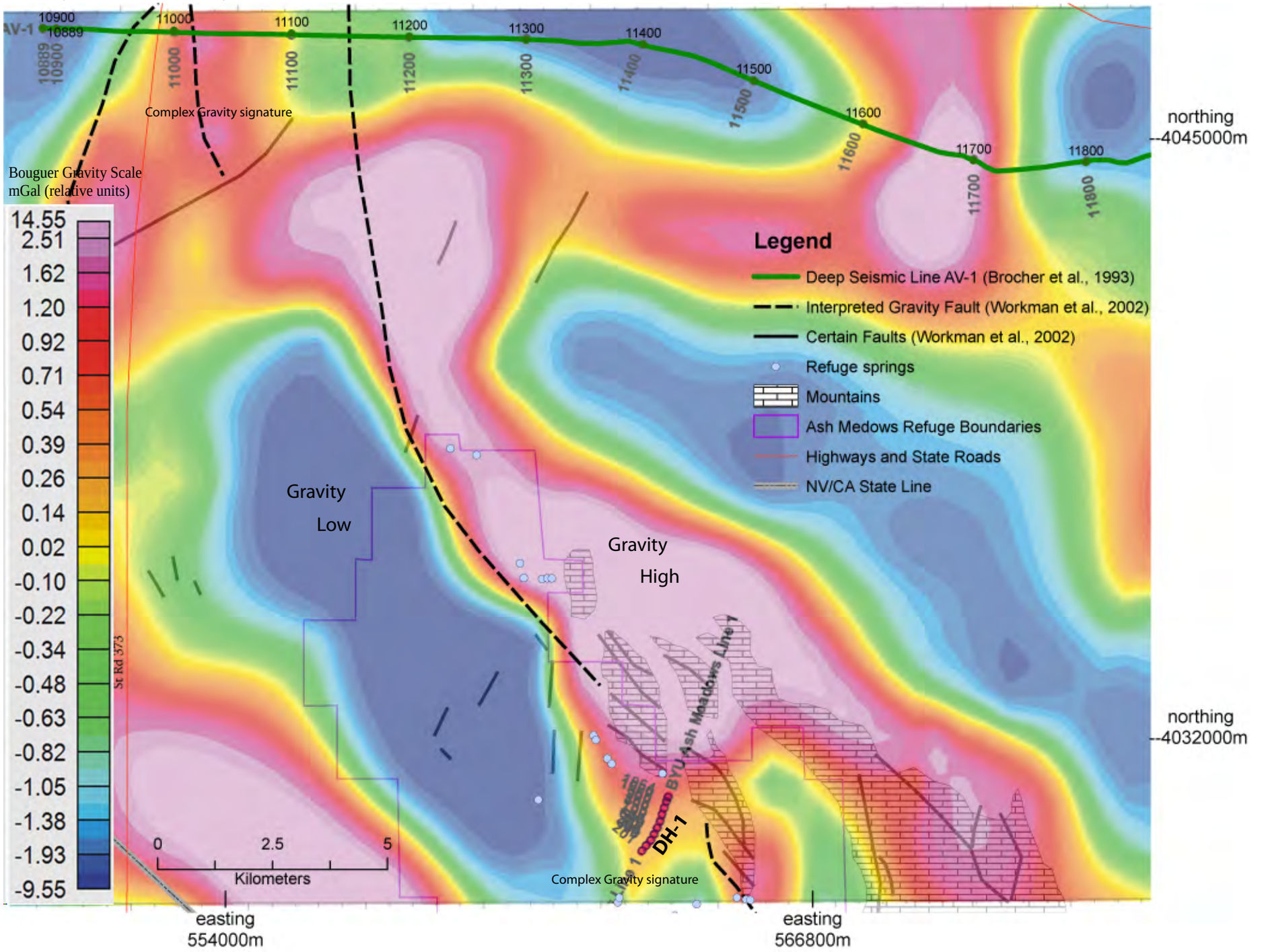

north of Ash Meadows.

By combining the re-analyzed potential field data with the deep (AV-1) and shallow (DH-1) seismic data, one may tentatively relate the deeper system of listric faults to the north with the shallow system of discrete shallow faults at Ash Meadows. Both sets of seismic data occur where the potential field data are more complex. Both sets of seismic data indicate that the Gravity fault may be a more complex system of faults than previously considered, with a wide damage zone that may allow groundwater to flow from the north and northwest through fractures. Further shallow seismic work should be conducted at Ash Meadows to the north of line DH-1, at a location where the gravity gradient is steeper.

Based on the integration of geophysical methods and the north-south fracture apertures in the current stress field, it is inferred that the Gravity fault acts as barrier to the flow of groundwater from the east, and as a conduit for the flow of water from the north. Further geophysical surveying is needed to map the detailed shallow subsurface structure of the Gravity fault and related deformation zone.

Table 4 Details for Collection of Geophysical Data

Shallow High-Resolution Common Mid-point (CMP) Seismic Reflection Survey Details	Re-Analysis of Gravity data	Re-Analysis of Aeromagnetic data
Source: 100-lb accelerated weight dropper Sample rate: 0.25 ms Receiver system: 72 28-Hz geophones spread over 710 ft. (48 active for each recording) Length of CMP Profile: 4315 ft Record length: 1500 ms	Bouguer gravity Downward continuation: 100 ground units (m) Scale: relative units, mGal	2nd vertical derivative of magnetic intensity Butterworth filter Low-pass cut-off wavelength: 250 ground units (m) Filter order: 3 Downward continuation: 10 ground units (m) Scale: relative units, nT/m**2

Conclusions

The results of this study, based on geochemical modeling, isotopic signatures and geophysical investigations, indicate that it is both possible and very likely that the waters discharging at Ash Meadows derive from the Yucca Mountain flow path rather than Spring Mountains or Pahranagat Valley. Geophysical investigations show that the springs are most likely fault controlled. Geochemical and isotopic modeling shows that the water discharging at Ash Meadows is most closely related to the water from Yucca Mountain to the north. The geochemical modeling also shows that representative waters from the Spring Mountains and Pahranagat Valley are unlikely to chemically evolve into Ash Meadows waters. Moreover, the complex interbedded structure and current stress fields of the fractured carbonate aquifer do not allow continuous flow from east to west, particularly considering the continuous precipitation of calcite filling in those fractures (Riggs et al., 1994).

The Yucca Mountain Region is the preferred flow path sustaining high discharge at the Ash Meadows springs. The mass balance models showed good results for all four of the Yucca Mountain water clusters. The isotopic signature of Yucca Mountain waters and Ash Meadows waters is identical, δD -103‰; therefore Yucca Mountain water is not required to mix with other distant waters such as Pahranagat Valley that cannot chemically evolve into Ash Meadows water, even mixing with down-gradient waters. The isotopes in the Yucca Mountain and Ash Meadows regions are indicative of a cooler, wetter climate, and recharge to this aquifer likely occurred during the last pluvial around 13,000 or more years ago.

The fractures in the current stress field are open in a generally north-south orientation, allowing water to flow from Yucca Mountain south to Ash Meadows, and would restrict east-west flow. The damage zone of the Gravity Fault appears to provide a conduit for flow, both from the northern Yucca Mountain Region to the southern Ash Meadows Region, as well as from the deep regional flow up to the surface. The deep seismic data and aeromagnetic-gravity data suggest the presence of a deep-seated crustal feature that affects the surface in the form of small-offset shallow faults that are coincident with high-temperature discharge at the Ash Meadows wetland.

Implications of a Yucca Mountain flow path to Ash Meadows spring discharge include a slower rate of groundwater flow (since the water does not have to travel as far to Ash Meadows during the ^{14}C decay process) as well as less dilution of contaminant transport from mixing with other distant groundwater systems before reaching the Ash Meadows National Wildlife Refuge.

References

Anderson, K.W., 2002, Contribution of local recharge to high flux springs in Death Valley National Park, California-Nevada, Master's thesis, Brigham Young University, 122p.

Ball, J.W. and Nordstrom, D.K., 1991, User's manual for WATEQ4F, with revised thermodynamic data base and test cases for calculating speciation of major, trace, and redox elements in natural waters, U.S. Geological Survey Open-File Report 91-183, (available at http://wwwbrr.cr.usgs.gov/projects/GWC_chemtherm/software.htm)

Batu, V., 1998, Aquifer hydraulics: A comprehensive guide to hydrogeologic data analysis: John Wiley and Sons, p. 28.

Benson, L.V. and Klieforth, H., 1989, Stable isotopes in precipitation and groundwater in the Yucca Mountain region, southern Nevada: Paleoclimatic implications, *in* Peterson, D.H., ed., Aspects of climate variability in the Pacific and the western Americas: American Geophysical Union, Geophysical Monograph, 55, p. 41-59.

Benson, L.V., and McKinley, P.W., 1985, Chemical composition of groundwater in the Yucca Mountain Area, Nevada, 1971-84: U.S. Geological Survey Open-File Report 85-484, 10.

Blakely, R.J., Langenheim, V.E., and Ponce, D.A., 2000, Summary of geophysical investigations of the Death Valley Regional Water-flow Modeling Project, Nevada and California: U.S. Geological Survey Open File Report 00-189, 25 p.

Boghici, E.M. and Boghici, R., 2001, Geostiff: A program that produces Stiff diagrams as GIS ArcInfo TM polygon converages: Texas Water Development Board Open File Report 01-001, available at http://www.twdb.state.tx.us/publications/reports/GroundWaterReports/Open-File/Open-File_01-001.htm

Brocher, T.M., Carr, M.D., Fox, K.F. Jr., Hart, P.E., 1993, Seismic reflection profiling across Tertiary extensional structures in the eastern Amargosa Desert, southern Nevada, Basin and Range province: Geological Society of America Bulletin, v. 105, p. 30-46.

Burchfiel, B.C., Fleck, R.J., Secor, D.T., Vincelette, R.R., Davis, G.A., 1974, Geology of the Spring Mountains, Nevada, Bulletin of the Geological Society of America, 85, p. 1013-1022.

Carpenter, E., 1915, Groundwater in southeastern Nevada, U.S. Geological Survey Water Supply Paper 365, pp.1-86.

Carr, W.J., Grow, J.A., Keller, S.M., 1995, Lithologic and geophysical logs of drill holes Felderhoff Federal 5-1 and 25-1, Amargosa Desert, Nye County, Nevada: U.S. Geological Survey Open-File Report USGS-OFR-95-155, 14 p.

Claassen, H.C., 1973, Water quality and physical characteristics of Nevada Test Site Water-Supply wells: U.S. Geological Survey Open-File Report USGS-474-158, 145 p.

Claassen, H.C., and White, A.F., 1979, Application if geochemical kinetic data to groundwater systems—A tuffaceous-rock system in southern Nevada, *in* Jenne, E.A., ed., Chemical modeling in aqueous systems: American Chemical Society Symposium Series 93, p 771-793.

Claassen, H.C., 1985, Sources and mechanisms of recharge for groundwater in the West-Central Amargosa Desert, Nevada—A geochemical interpretation: U.S. Geological Survey Professional Paper 712-F, 31 p.

Coplen, T.B., 1988, Normalization of oxygen and hydrogen isotope data: Chemical Geology, v. 72, pp. 293-297.

Coplen, T.B., 1993, Uses of environmental isotopes, *in* Alley, W.B., ed., Regional groundwater quality. Van Nostrand Reinhold, New York.

Coplen, T.B., Winograd, I.J., Landwehr, J.M., and Riggs, A.C., 1994, 500,000-year stable carbon isotopic record from Devils Hole, Nevada: Science, v.263, pp.361-365.

Craig, H., 1961, Isotopic variations in natural waters, Science, 133, p. 1702-1703.

Craig, R.W., and Robinson, J.H., 1984, Geohydrology of rocks penetrated by test well UE-25p#1, Yucca Mountain area, Nye County, Nevada: U.S. Geological Survey Water-Resources Investigations Report 84-4248, 57 p.

D'Agnese, F.A., C.C. Faunt, and A.K. Turner, 1998, An estimated potentiometric surface of the Death Valley Region, Nevada and California, developed using geographic information system and automated interpolation techniques: U.S. Geological Survey Water-Resources Investigations Report 97-4052

D'Agnese, F.A., O'Brien, G.M., Faunt, C.C., Belcher, W.R., and San Juan, C., 2002, Three-dimensional numerical model of predevelopment conditions in the Death Valley Regional Ground-Water Flow System, Nevada and California: U.S. Geological Survey Water-Resources Investigations Report 02-4102, 114 p.

Denney, C.S., and Drewes, H., 1965, Geology of the Ash Meadows quadrangle, Nevada-California: U.S. Geological Survey Bulletin 1181-L, p. L1-L56.

Dettinger, M.D., Harril, J.R., Schmidt, D.L., Hess, J.W., 1995, Distribution of carbonate-rock aquifers and the potential for their development, southern Nevada and adjacent parts of California, Arizona, and Utah, U.S. Geological Survey Water-Resources Investigative Report 91-4146, 100 p.

Duvernell, D.D. and B. J. Turner , 1998, Evolutionary genetics of Death Valley pupfish populations: Mitochondrial DNA sequence variation and population structure. Molecular Ecology, v. 7, pp. 279-288.

Emrich, K., Ehhalt, D.H., and Vogel, J.C., 1970, Carbon isotope fractionation during the precipitation of calcium carbonate, Earth Planet. Sci. Lett., 8 (5), pp. 363-371.

Epstein, S., and Mayeda, T., 1953, Variation of ^{18}O content of waters from natural sources: Geochimica et Cosmochimica Acta, v. 4, pp. 213-224.

Ervin, E.M., Luckey, R.R., and Burkhardt, D.J., 1993, Summary of revised potentiometric-surface map for Yucca Mountain and vicinity, Nevada. Proceedings, Fourth International Conference of High Level Radioactive Waste Management, Las Vegas, NV, April 26-30, 1993, American Nuclear Society, La Grange Park, IL, p. 1554-1558.

Faunt, C.C., 1997, Effect of faulting on ground-water movement in the Death Valley Region, Nevada and California: U.S. Geological Survey Water-Resources Investigations Report 95-4132.

Felsenthal, M., and Ferrell, H.H., Fluid flow in carbonate reservoirs, *in* Oil and Gas Production from Carbonate Rocks, chap. 3, pp. 83-142, edited by G.V. Chilingar, R.W. Mannon, and H.H. Rieke, III, Elsevier, New York, 1972.

Fenwick, J.K., 1994, Hydrologists field manual, National Institute of Water and Atmosphereic Research Ltd, New Zealand, NIWA Science and Technology Series no. 5, Chap. 4.5, pp. 4-11 to 4-23.

Ferrill, D.A., Winterle, J., Wittmeyer, G., Sims, D., Colton, S., Armstrong, A., Morris, A.P., 1999, Stressed rock strains groundwater at Yucca Mountain, Nevada: GSA Today, v. 9, n. 5, pp. 1-8.

Forester, R.M., Bradbury, J.P., Carter, C., Elvidge-Tuma, A.B., Hemphill, M.L., Lundstrom, S.C., Mahan, S.A., Marshall, B.D., Neymark, L.A., Paces, J.B., Sharpe, S.E., Whelan, J.F., and Wingand, P.E., 1999, The climatic and hydrologic history of southern Nevada during the late Quaternary, U.S. Geological Survey Open-File Report, 98-635, 63 p.

Friedman, I., and O'Neil, J.R., 1977, Compilation of stable isotope fractionation factors of geochemical interest: Data of Geochemistry, 6th ed., U.S. Geological Survey Professional Paper 440-KK, 110 pp.

Friedman, I., and Smith, G.I., Deuterium content of snow cores from Sierra Nevada area, Science, 169, pp. 467-470.

Friedman, I., and Smith, G.I., 1972, Deuterium content of snow as an index to winter climate in the Sierra Nevada area, Science, 176, pp. 790-793.

Friedman, I., and Smith, G.I., Gleason, J.D., and Veronda, G., 1984, Fossil origin of deep groundwaters in southeastern California confirmed by deuterium analysis, Geological Society of America, Abstract with programs, 97th annual meeting, Reno, Nevada, 512.

Friedman, I., 1953, Deuterium content of natural water and other substances, Geochimica et Cosmochimica Acta, 4, pp.89-103.

Friedman, I., Redfield, A.C., Schoen, B., Harris, J., 1964, The variation of the deuterium content of natural waters in the hydrologic cycle, Rev. Geophysics, 2, pp. 177-224.

Friedman, I., Benson, C., Gleason, J., 1991, Isotopic changes during snow metamorphism, *in* Stable Isotope Geochemistry, A Tribute to Samuel Epstein, The Geochemical Society Special Publication no. 3, eds. Taylor, H.P., Jr., O'Neil, J.R., and Kaplan, I.R., pp. 211-221.

Friedman, I. and O'Neil, J.R., 1977, Compilation of stable isotope fractionation factors of geochemical interest, U.S. Geological Survey Professional Paper 440-KK, 211pp.

Friedman, I., Smith, G.I., Gleason, J.D., Warden, A., and Harris, J.M., 1992, Stable isotope composition of waters in southeastern California—1. Modern precipitation: Journal of Geophysical Research, v. 97, n. D5, pp. 5795-5812.

Gat, J.R., 1980, The isotopes of hydrogen and oxygen in precipitation, *in* Handbook of Environmental Isotope Geochemistry, edited by P. Fritz nd J. Fontes, vol. 1, pp. 21-44, Elsevier, New York.

Gehre, M., Hoefling, R. and Kowski, P., 1996 (1966?), Sample preparation device for quantitative hydrogen isotope analysis using chromium metal: Analytical Chemisty, v. 68, pp. 4414-1417

Gleason, J.D., Veronda, G., Smith, G.I., Friedmand, I., Martin, P., 1992, Deuterium concentrations of water from wells and perennial springs, southeastern California, U.S.Geological Society Open-File Report 91-470, and U.S. Geological Society Hydrologic Atlas map with table and text (in press).

Grove, D.B., Rubin, M., Hanshaw, B.B., and Beetem, W.A., 1969, Carbon-14 dates of groundwater from a Paleozoic carbonate aquifer, south-central Nevada: U.S. Geological Survey Professional Paper 650-C, pp. C215-C218.

Güler, C. and Thyne, G.D., 2006, Statistical clustering of major solutes: Use as a tracer for evaluating interbasin groundwater flow into Indian Wells Valley, California: Environmental & Engineering Geoscience, Vol. 12, No. 1, pp. 53–65.

Hanshaw, G.T., Peterson, F.J. and Winograd, I.J., 1979,Deuterium and oxygen-18 content of Holocene through Wisconsin precipitation, Geological Society of America Abstract Programs, 10, 816.

Helgesen, H.C., 1968, Evaluation of irreversible reactions in geochemical processes involving minerals and aqueous solutions, I, Thermodynamic relations, Geochimica et Cosmochimica Acta, 32, p. 853-857.

Hershey, R.L., 1989, Hydrogeology and hydrogeochemistry of the Spring Mountains, Clark County, Nevada. Master's Thesis, University of Nevada, Las Vegas, 236 pp.

Hershey, R.L., Lyles, B.F., Hess, J.W., 1991, Stable isotopic evidence of warm season recharge to the Spring Mountains, southern Nevada, Geological Society of America, abstracts with programs, 23 (5), A381.

Hodge, V.F., Johannesson, K.H., and Stetzenbach, K.J., 1996, Rhenium, molybdenum, and unranium in groundwater from the southern Great Basin, USA: Evidence for conservative behavior: Geochimica et Cosmochimica Acta, v. 60, n. 17, pp. 3197-3214.

Hughes, J.L., 1966, Some aspects of the hydrogeology of the Spring Mountains and Pahrump Valley, Nevada, and environs, as determined by spring evaluation. Master's Thesis, University of Nevada, Reno, 116 pp.

Ingraham, N.L. and Taylor, B.E., 1991, Light stable isotope systematics of large-scale hydrologic regimes in California and Nevada: Water Resources Research, v. 27, n. 1, pp. 77-90.

Kerrisk, J.F., 1983, Reaction path calculations of groundwater chemistry and mineral formations at Rainier Mesa, Nevada, Los Alamos National Laboratory Report LA-9912-MS.

Laczniak, R.J., DeMeo, G.A., Reiner, S.R., Smith, J.L., and Nylund, W.E., 1999, Estimates of ground-water discharge as determined from measurements of evapotranspiration, Ash Meadows Area, Nye County, Nevada, U.S. Geological Survey Water-Resources Investigations Report 99-4079.

Larson, J.D., 1974a, Water-resources data collected in the Devils Hole area, Nevada 1972-1973, Water Resources Investigative Report 61-73, 14 pp., U.S. Geological Survey, Carson City, Nevada.

Larson, J.D., 1974b, Water-resources data collected in the Devils Hole area, Nevada 1973-1974, open-file report, 6 pp., U.S. Geological Survey, Carson City, Nevada.

Larson, J.D., 1975, Water-resources data collected in the Devils Hole area, Nevada 1974-1975, open-file report, 12 pp., U.S. Geological Survey, Carson City, Nevada.

Malmberg, G.T., and Eakin, T.E., 1962, Groundwater appraisal of Sacrobatus Flat and Oasis Valley, Nye and Esmerelda counties, Nevada, Serial Report 10, Nevada Department of Conservation and National Resources Groundwater-Resource Reconnaissance, Carson City, Nevada.

Maxey, G.B., and Jameson, C.H., 1948, Geology and water resources of Las Vegas, Pahrump and Indian Springs Valleys, Clark and Nye counties, Nevada, Nevada Water Resources Bulletin, 5, pp. 1-121.

Mazor, E., 1997, Chemical and isotopic groundwater hydrology. Dekker, New York.

McCrea, J.M., 1950, On the isotopic chemistry of carbonates and a paloetemperature scale: Journal of Physical Chemistry, v. 18, pp. 849-857.

Mehringer, P.J., Jr., 1965, Late Pleistocene vegetation in the Mohave Desert of southern Nevada, J. Arizona Acad. Sci., 3 (3), pp. 172-188.

Merlivat, L. and Jouzel, J., 1979, Global climate interpretation of deuterium-oxygen 18 relationship for precipitation, Journal of Geophysical Research 84, p. 5029-5033.

Mifflin, M.D., 1968, Delineation of groundwater flow systems in Nevada, Desert Research Institute, Technical Report Series H-W, Hydrol. Water Resour. Publ., 4, pp. 1-110.

Miller, G.A., 1977, Appraisal of the water resources of Death Valley, California-Nevada: U.S. Geological Survey open-file report 77-728, 68 p.

Miner, R.E., Nelson, S.T., Tingey, D.G., and Murrell, M.T., 2007, Using fossil spring deposits in the Death Valley region, USA to evaluate paleoflowpaths: Journal of Quaternary Science, vol. 22, No. 4, pp. 373-386.

Moore, J.E., 1961, Records of wells, test holes, and springs in the Nevada Test Site and surrounding area: U.S. Geological Survey Open-File Report TEI-781, 22 p.

Naff, R.L., 1973, Hydrogeology of the southern part of the Amargosa Desert in Nevada, M.S. Thesis, 207 pp., University of Nevada, Reno.

Nelson, S.T., 2000, A simple, practical methodology for routine VSMOW/SLAP normalization of water sample analyzed by continuous flow methods: Rapid Communications in Mass Spectrometry, v. 14, pp. 1044-1046.

Oliver, T. and Root, T. 1997, Hydrochemical Database for the Yucca Mountain Area, Nye County, Nevada. U.S. Geological Survey. Memo to the Technical Project Officer, pp. 1-9 with figures and Excel database file. Denver, Colorado: U.S. Geological Survey. MOL.19980302.0367.

Olsson, I.U., 1968, Modern aspects of radiocarbon dating, Earth Sci. Rev., 4, pp. 203-218.

Paces, J.B., Whelan, J.F., Forester, R.M., Bradbury, J.P., Marshall, B.D., and Mahan, S.A., 1997, Summary of discharge deposits in the Amargosa Valley: U.S. Geological Survey Milestone Report SPC 333M4, 23p.

Paces, J.B., Whelan, J.F., 2001, Water-table fluctuations in the Amargosa Desert, Nye County, Nevada: Proceedings of the Ninth International HLW Management Conference.

Parsons, R.W., 1966, Permeability of idealized fractured rock, Soc. Petrol. Eng. J., 6 (2), pp.126-136.

Pearson, F.J., Jr., 1965, $^{13}C/^{12}C$ ratios to correct radiocarbon ages of materials initially diluted by limestone, paper presented at the Sixth International Conference on Radiocarbon and Tritium Dating, International Atomic Energy Agency, Pullman, Washington.

Perfect, D.L., Faunt, C.C., Steinkampf, W.C., and Turner, A.K., 1995, Hydrochemical database for the Death Valley region, California and Nevada: U.S. Geological Survey Open-File Report 94-305.

Piper, A.M., 1945, A graphic procedure in the geochemical interpretation of water analysis: Transactions, American Geophysical Union, Pert 6, pp. 914-923.

Plummer, L.N., Jones, B.F., and TRuesdell, A.H., 1976, WATEQ, a computer program for calculating chemical equilibrium of natural waters, U.S. Geological Survey Water Resources Investigation Report 76-13, 61 p.

Plummer, L.N., Prestemon, E.C., and Parkhurst, D.L., 1991, An interactive code (NETPATH) for modeling net geochemical reactions along a flow path: U.S. Geological Survey Water-Resources Investigation Report 91-4078.

Potter, C.J., Sweetkind, D.S., Dickerson, R.P., Killgore, M.L., 2002.Hydrostructural maps of the Death Valley Regional flow system, Nevada and California. US Geological Survey Miscellaneous Field Studies map MF-2372, scale 1:350,000.

Quade, J., Forester, R.M., Pratt, W.L., and Carter C., 1998, Black mats, spring-fed streams, and late-glacial-age recharge in the southern Great Basin: Quaternary Research, v. 49, pp. 129-148.

Riggs, A.C., Carr, W.J., Kolesar, P.T., and Hoffman, R.J., 1994, Tectonic speleogenesis of Devils Hole, Nevada, and implications for hydrology and the development of long, continuous paleoenvironmental records: Quaternary Research, v. 42, pp. 241-254.

Rightmire, C.T., and Hanshaw, B.B., 1978, Relationship between carbon isotope composition of soil CO_2 and dissolved carbonate species in groundwater, Water Resources Research, 9, p. 958-967.

Root, T.L., 2000, Using ground water chemistry to delineate ground water flow paths near Franklin Lake Playa, Inyo County, California: University of Wisconsin-Madison, Master of Science Thesis, 122 p.

Rose, T.P., Kenneally, J.M., Smith, D.K., Davisson, M.L., Hudson, G.B., and Rego, J.H, 1997, Chemical and isotopic data for groundwater in southern Nevada, UCRL-ID-128000, Lawrence Livermore National Laboratory

Savard, C.C., 1998 (1996?), Estimated ground-water recharge from streamflow in Fortymile Wash near Yucca Mountain, Nevada: U.S. Geological Survey Water-Resources Investigations Report 97-4273, 30 p.

Schoff, S.L., and Moore, J.E., 1964, Chemistry and movement of groundwater, Nevada Test Site: U.S. Geological Survey Open-File Report TEI-838, 75 p.

Skibitzke, H.E., and Robinson, G.M., 1963, Dispersion in groundwater flowing through heterogeneous materials, U.S. Geological Survey Professional Paper 386-B, pp.1-3.

Smith, G.I., Friedman, I., Klieforth, H., Hardcastle, K., 1979, Areal distribution of deuterium in eastern California precipitation, 1968-1969, Journal of Appl. Meterol., 18, pp. 172-188.

Smith, G.I., Friedman, I., Gleason, J.D., and Warden, A., 1992, Stable isotope composition of waters in southeastern California—2. Groundwaters and their relation to modern precipitation: Journal of Geophysical Research, v. 97, n. D5, pp. 5813-5823.

Smith, G.I., and Street-Perrott, F.A., 1983, Pluvial lakes of the western United States, Late Quaternary Environments of the United States, edited by H.E. Wright and S.C. Porter, University of Minnesota Press, Minneapolis, pp. 190-212.

Soltz, D.L., and Naiman, R.J., 1978, The natural history of native fishes in the Death Valley system: Los Angeles, Death Valley Natural History Ass'n, 76p.

Stead, F.W., 1963, Tritium distribution in groundwater around large underground fusion explosions, Science, 142 (3596), pp.1163-1165.

Stewart, M.K., 1975, Stable isotope fractionation due to evaporation and isotopic exchange of falling raindrops: applications to atmospheric processes and evaporation of lakes, Journal of Geophysical Research, 80, pp.1133-1146.

Stiff, H.A., 1951, The interpretation of chemical water analysis by means of patterns: Journal of Petroleum Technology, v. 3, n. 10, pp. 15-17.

Sweetkind, D.S., Dickerson, R.P., Blakely, R.J., and Denning, P.D., 2001, Interpretive geologic cross sections for the Death Valley Regional Flow System and surrounding areas, Nevada and California: U.S. Geological Survey Miscellaneous Field Studies MF-2370.

Telford, W. M., Geldart, L. P., and Sheriff, R. E., 1990, Applied Geophysics, Cambridge University Press, 2nd Edition, 790 pp.

Thordarson, W., Young, R.A., and Winograd, I.J., 1967, Records of wells and test holes in the Nevada Test Site and vicinity, open-fie report Tel-872, 26 pp., U.S. Geological Survey, Carson City, Nevada.

Thomas, J.M., 1996, Geochemical and isotopic interpretation of groundwater flow, geochemical processes, and age dating of groundwater in the carbonate-rock aquifers of the southern Basin and Range, University of Nevada, Reno Ph. D. dissertation, 135p.

Thomas, J.M., Lyles B.F., Carpenter, L.A., 1991, Chemical and isotopic data for water from wells, springs, and streams in carbonate rock terrane of southern and eastern Nevada and southeastern California, 1985-88, U.S. Geological Survey Open-File Report 89-422, pp. 1-24.

Thomas, J.M., Welch, A.H., Dettinger, M.D., 1996, Geochemistry and isotope hydrology of representative aquifers in the Great Basin region of Nevada, Utah and adjacent states, U.S. Geological Survey Professional Paper 1409-C, C76.

Thomas, J.M., Benedict, F.C, Jr., Rose, T.P., Hershey, R.L., Paces, J.B., Peterman, Z.E., Farnham, I.M., Johannesson, K.H., Singh, A.K., Stetzenbach, K.J., Hudson, G.B., Kenneally, J.M., Eaton, G.F., and Smith, D.K., 2002, Geochemical and isotopic

interpretations of groundwater flow in the Oasis Valley Flow System, southern Nevada, U.S. Department of Energy, Pub. No. 45190, 113p.

U.S.G.S., 1979, Water resources data for Nevada—water year 1978: 383 p.

Walker, G.E., and Eakin, T.E., 1963, Groundwater resources of the Amargosa Desert, Nevada-California, State of Nevada Department of Conservation and Natural Resources, Division of Water Resources, Water Resources Reconnaissance Series Report 14, 45 p.

Warren, J.E., and Price, H.S., 1961, Flow in heterogeneous porous media, Soc. Petrol. Eng. J., 1 (3), pp. 153-169.

White, A.F., 1979, Geochemistry of groundwater associated with tuffaceous rock, Oasis Valley, Nevada: U.S. Geological Survey Professional Paper 712-E, p. E1-E25.

White, A.F., and Chuma, N.J., 1987, Carbon and isotopic mass balance models of Oasis Valley-Fortymile Canyon groundwater basin, southern Nevada: Water Resources Research, v. 23, n. 4, pp. 571-582.

White, A.F., Claassen, H.C., and Benson, L.V., 1980, The effect of dissolution of volcanic glass on the water chemistry in a tuffaceous aquifer, Rainier Mesa, Nevada, U.S. Geological Survey Water Supply Paper, 1535-Q.

Winograd, I.J., and Friedman, I., 1972, Deuterium as a tracer of regional groundwater flow, Southern Great Basin, Nevada and California, Geological Society of America Bulletin, 83 (12), pp.3691-3708.

Winograd, I.J., and Thordarson, W., 1968, Structural control of ground-water movement in the miogeosynclinal rocks of south-central Nevada, *in* Nevada Test Site, Geological Society of America Mem. 110, pp. 35-48, edited by E.B. Eckel, Geological Society of America, Boulder, Colorado.

Winograd, I.J., 1962, Interbasin movement of groundwater at the Nevada Test Site, Nevada: Art. 104 in U.S. Geological Survey Professional Paper 450-C, pp. C108-C111.

Winograd, I.J., and Thordarson, W. 1975, Hydrogeologic and hydrochemical framework, South-central Great Basin, Nevada-California, with special reference to the Nevada Test Site: U.S. Geological Survey Professional Paper 712-C, 123 p.

Winograd, I.J., and Pearson, Jr., F.J., 1976, Major carbon 14 anomaly in a regional carbonate aquifer: Possible evidence for megascale channeling, south central Great Basin: Water Resources Research, v. 12, n. 6, pp.1125-1143.

Winograd, I.J., Coplen, T.B., Landwehr, J.M., Riggs, A.C., Ludwig, K.R., Szabo, B.J., Kolesar, P.T., and Revesz, K.M., 1992, Continuous 500,000-year climate record from vein calcite in Devils Hole, Nevada: Science, v. 258, pp. 255-260.

Winograd, I.J., Landwehr, J.M., Ludwig, K.R., Coplen, T.B., and Riggs, A.C., 1997, Duration and structure of the past four interglaciations: Quaternary Research, v. 48, n. QR971918, pp. 141-154.

Winograd, I.J., Riggs, A.C., Coplen, T.B., 1998, The relative contributions of summer and cool-season precipitation to groundwater recharge, Spring Mountians, Nevada, USA: Hydrogeology Journal, v. 6, pp. 77-93.

Wolery, T.J., 1979, Calculation of chemical equilibrium between aqueous solution and minerals: The EQ3/EQ6 software package, Report UCRL 52658, Lawrence Livermore Laboratory, Livermore, California.

Workman, J.B., Menges, C.M., Page, W.R., Taylor, E.M., Ekren, E.B., Rowley, P.D., Dixon, G.L., Thompson, R.A., and Write, L.A., 2001a, Geologic map of the Death Valley ground-water model area, Nevada and California: U.S. Geological Survey Miscellaneous Field Studies map MF-2381-A, scale 1:250,000.

Workman, J.B., Menges, C.M., Page, W.R., Ekren, E.B., Rowley, P.D., and Dixon, G.L., 2001b, Tectonic map of the Death Valley groundwater model area, Nevada and California: U.S. Geological Survey Miscellaneous Field Studies MF-2381-B, scale 1:100,000.

Yang, G., Haas, H.H., Weeks, E.P., and Thorstenson, D.C., 1985, Analysis of gaseous-phase stable and radioactive isotopes in the unsaturated zone, Yucca Mountain, Nevada, in Proceedings of Conference on Characterization and Monitoring of the vadose zone, National Water Well Association, Denver, Colorado, pp. 488-506

Appendix A

Averaged and Merged Water Samples
Solute and Isotopic Sources

Abbreviations for Flow Path Regions

AM = Ash Meadows
AD = Amargosa Desert
OV = Oasis Valley
YM = Yucca Mountain
FG = Frenchman Groom
SP = Spring Mountains
PV = Pahranagat Valley

Appendix A

Averaged and merged samples used for cluster analysis, including isotopes and solute chemistry.

unique identifier	site	northing	easting	#avg/mrg	Sources
AD-1	Cooks East Well	554006.4	4047633	2	15, 21
AD-2	COOK'S WELL 16S/50E-7bcd	553932.37	4047540.36	5	5, 15, 16, 21, 23
AD-3	AMARGOSA WELL #27	551718.15	4047896.53	1	18
AD-4	16S/50E-7bcd	553756.86	4047785.77	1	14
AD-5	16S/48E-24aaa	544076.92	4045234.88	2	14
AD-6	S16 E48 24 4	544126.5	4045266	2	14, 15
AD-7	230 S16 E48 25AA JACOB'S #1	544159.88	4043602.22	2	5, 15, 18, 21, 23
AD-8	16S/49E-19daa JACOB'S #2	545771.19	4044535.02	2	5, 15, 18, 21, 23
AD-9	16S/48E-36dcc	543529.57	4040394.5	4	5, 17, 25, 23
AD-10	16S/49E-08acc	546723.08	4047806.32	3	5, 15, 23
AD-11	AMARGOSA WELL #23	540838.37	4046636.29	1	18
AD-12	16S/48E-10cba KIRKER (FOX WELL)	539765.71	4047463.22	6	5, 15, 16, 21, 23
AD-13	NICHOLS' WELL NENENE 15-16S-48E	540762.78	4046851.63	6	5, 15, 16, 21, 23
AD-14	16S/48E-8ba	536979.18	4048128.66	1	14
AD-16	S16 E49 16 1	547506.3	4045500	3	15, 16, 18, 21
AD-17	18S/49E-11bbb	551306.79	4029283.04	2	14, 15
AD-18	FL-1 SWSE SEC31 T25N,R6E FL1-1	556699.17	4012123.34	2	14
AD-19	Finley's Well, 16S/48E-07bba	534791.2	4048366	2	14, 15
AD-20	AMARGOSA WELL #25	539641.58	4047431.83	1	14
AD-21	Mathew's Well, Amargosa Valley	553717.0776	4042208.294	2	16, 18, 21, 22
AD-23	16S/49E-35baa	551305.7	4042040	5	14, 15
AD-24	ROSE 16S/48E-7cbc NWNWSW 7-16S-48E	534546.43	4047440.67	2	5, 23
AD-25	AMARGOSA WELL #47, 16S/48E-7cbc	534841.68	4048181.37	2	14, 15
AD-26	16S/48E-23da	542390.67	4044363.65	2	14, 15
AD-27	17S/49E-8ddb	547574.65	4037611.9	3	5, 15, 18, 21, 23
AD-28	17S/49E-15bc	549869.88	4036577.23	1	14
AD-29	16S/49E-09cda K. CAREY	548167.49	4047290.46	6	5, 15, 17, 21, 23, 25
AD-30	16S/48E-23bdb LATHROP	541468.97	4044728.92	2	5, 17, 23, 25
AD-31	16S/48E-17abb LATHROP	537035.12	4046680.71	3	14, 15
AD-32	18S/49E-2cbc	551377.12	4030022.96	2	5, 18, 21, 23
AD-33	16S/49E-15aaa	550407.8	4046718	2	12, 18
AD-34	16S/49E-15aaa	550556.23	4046841.96	1	14
AD-35	SCHOOLHOUSE NWNWNW 14-16S-49E	550705.91	4046750.41	1	14
AD-36	TENNACO WELL #2	552049.16	4030088.6	2	6, 15, 21, 23
AD-37	AMARGOSA DESERT 25N/5-14c1	552722.5	4017644.49	1	25
AD-38	SESWSW 36-17S-49E	553163.98	4031050.57	1	6, 23
AD-39	SULLIVAN NESESW 8-16S-48E	536784.58	4047141.83	1	14
AD-40	16S/48E-8cda	537063.16	4045941.33	1	14
AD-41	16S/48E-36a	543721.8	4041720	2	14, 15
AD-42	BETTY SMITH WELL, 16S/48-36aaa	544167.93	4042030.81	4	5, 15, 18, 21, 23, 25
AD-43	S16 E49 09DCC 1 AMARGOSA ELEM SCHOOL	548342.85	4047044.94	2	14, 15
AD-44	16S/49E-08abb K. FINICAL	546694.72	4048453.24	4	14, 15, 16
AD-45	17S/49E-15bbd	549843.4	4036854.39	3	5, 15, 18, 21
AD-46	WELL, 17S/49-11ba	551873.38	4038622.68	5	14, 15

unique identifier	site	northing	easting	#avg/mrg	Sources
AD-47	WELL NW27-27N-4E 11MI NW OF DEATH V JUNC	541447.05	4033759.58	1	14
AD-48	WELL NW 27-27N-4E (27N/4-27bbb) INYO CO?	541519.96	4034129.68	2	14
AD-50	DEATH VALLEY JUNCTION CA WELL	552822.82	4017552.66	3	14, 15
AD-51	230 N24 E05 01BA 1 WELL-13	554634.01	4011124.15	5	14, 15
AD-52	17S/49E-29acc, IMV#1	547348.8	4033420.15	2	14, 15
AD-54	WELL 5 N24 E06 07A FRANKLIN LK	556386.71	4010272.59	4	14, 15
AD-55	230 N25 E06 18A WELL-15	556858.91	4018225.2	5	14, 15, 16
AD-56	ASH TREE SPRING 17S/49E-35ddd	552739.72	4031202.03	8	5, 7, 15, 18, 21, 23, 25
AM-1	Five Springs Group, Ash Meadows	561052.1786	4035416.515	4	8, 15, 16
AM-2	NWNW 23-17S-50E	561101.96	4035416.87	1	14
AM-3	WELL 7 17S/50-23BB2	561176.41	4035448.21	1	14
AM-4	SWNESW 14-17S-50E	561344.28	4036342.99	1	14
AM-5	SPRING 17S/50-23BBC	560977.73	4035385.18	1	14
AM-6	WELL 17S/50-36DD	563895.17	4031308.06	1	14
AM-7	IND. RK. SPRING 18S/51-07DBA1	565311.72	4028391.36	1	14
AM-8	230 S17 E50 23BBCA1, Five Springs Well	561125.76	4035571.1	9	14, 15
AM-9	DEVILS HOLE SWSWSE 36-17S-50E NYE CO	563572.36	4031182.43	41	6, 7, 15, 21, 23, 25
AM-10	KING POOL 18S/51-07DBB	565261.67	4028421.8	3	14
AM-11	POINT OF ROCK SPR (SMALL) NWSE 7-18S-51E	565385.51	4028515.17	4	6, 23
AM-12	Point of Rocks (King)	565410.4	4028515	5	14, 15
AM-14	Big Spring (Ash Meadows), 18S/51E-19acb	565283.027	4025587.13	2	8
AM-15	NWNWNW 7-18S-51E	564332.92	4029370.06	1	14
AM-17	230 S18 E50 03ADB 1 CRYSTAL POOL	560737.49	4030607.42	4	6, 18, 21, 23
AM-21	230 S18 E50 03ADBA1	560762.61	4030576.78	3	14
AM-23	WELL 4 18S/51-07CAA	564987.66	4028419.74	1	14
AM-24	KING SPRING	565410.42	4028515.36	7	6, 21, 23
AM-26	Well #2	565636.5	4028271	3	15
AM-27	Crystal Pool Spring, 18S/50E-03adba1, Ash Meado	560690.2817	4030237.331	11	8, 15, 16
AM-28	Fairbanks Spring, 17S/50E-9ad	558966.5972	4038298.482	4	8, 9, 16
AM-29	230 S18 E51 19ACB 1 BIG SPRING	565158.44	4025586.19	20	6, 15, 16, 18, 21, 23
AM-30	POOL SW 7-18S-51E NYE CO	564938.77	4028296.12	1	14
AM-31	230 S17 E50 09AD 1	558891.32	4038390.41	4	21
AM-33	WELL 1 18S/51-07DAA	565610.4	4028424.43	1	14
AM-34	LONGSTREET SPRING NENWNE 22-17S-50E NYE	560476.71	4035843.85	8	8, 15, 16, 23
AM-35	WELL 2 18S/51-07DAC	565487.25	4028238.62	1	14
AM-36	RABBIT SPRING NWSENW 18-18S-51E NYE CO	564747.32	4027247.03	3	6, 23
AM-37	JACK RABBIT SPRING 18S/51-18DBD	564623.91	4027092.04	1	14
AM-38	WELL 17S/51-31DDD	565589.84	4031135.87	1	14
AM-39	18S/51E-07dac	565635.8	4028363	4	14, 15
AM-40	BOLE SPRING NENWNE 30-18S-51E (18S/51-30aba)	565268.09	4024262.05	1	14
AM-41	WELL 8 17S/50-10CDD	559818.1	4037503.19	1	14
FG-2	S14 E52 03DD TEST WELL F	578870.02	4068348.73	10	18, 23, 21
FG-3	UE-15j N892,694 E705,826	592295.48	4117392.99	1	14
FG-4	UE15j-A5 N892,333 E704,891	592025.32	4117297.57	3	14

unique identifier	site	northing	easting	#avg/mrg	Sources
FG-5	S10 E53 21CABC5 U3cn-5 HTH	586934.34	4101710.49	40	6, 16, 18, 21, 23
FG-6	TEST WELL E, AREA 3 NTS, 13 FLAT	589358.97	4101335.13	2	14
FG-7	TUNNEL N894000 E696000	589307.97	4117792.21	1	14
FG-8	U-3cn #5 HTH	586909.6381	4101710.239	1	8
FG-9	U-2bs PS #1db 13 FLAT	583876.06	4108706.26	21	14
FG-11	WELL 73-66 ROCK VALLEY NYE CO	578553.92	4067667.86	3	14
FG-12	ER-6-1 Well, NTS, Area 6	589640.3958	4093417.638	2	8, 16
FG-13	TEST WELL 3 FRENCHMAN LAKE	601938.92	4074016.96	1	14
FG-14	WELL C-1 N790011 E692132 13 FLAT	588232.97	4086098.9	18	4, 17, 18, 23
FG-15	E53 09AADA1 WATER WELL C	588207.9	4086129.46	44	4, 8, 16, 17, 21, 23
FG-16	U3-cn PS #2 Well, NTS, Area 3	586982.4633	4101834.264	110	16, 21, 23
FG-17	U-3cn PS #2	586957.7657	4101834.009	1	8
FG-18	WELL 2 N880000 E668720 13 FLAT	581016.62	4113486.03	11	4, 17, 23
FG-19	WELL UE15d N895709 E682084 13 FLAT	585062.4	4118302.94	7	4, 6, 17, 23
FG-23	WATERTOWN No. 2 N909062 E752226	606408.98	4122429.62	7	14
FG-25	WELL A N833000 E684000 13 FLAT	585700.04	4099201.57	20	4, 17, 23
FG-26	UE5c N760,133 E700,997 FRENCHMAN FLAT	590978.01	4077005.63	3	6, 8, 16, 23
FG-27	UE-1a Well, NTS, Area 1	578400.3194	4100394.306	2	8, 16
FG-30	UE-5n Well, NTS, Area 5	592631.5941	4075297.621	2	16
FG-32	WELL RNM-2S N755,119.74 E704,809.90	592134.09	4075477.14	4	14
FG-33	WELL 5B N747359 E704263 FRENCHMAN FLAT	591986.26	4073102.55	16	4, 12, 17, 23
FG-35	Water Well 4, NTS, Area 6	586961.756	4084575.706	2	8, 16
FG-38	Watertown #1 Well, Emigrant Valley	605620.1615	4122450.481	7	6, 12, 16, 17, 23
FG-39	23 Test Well D, 10S/53E-16-1	581858.1393	4103015.817	2	8, 16
FG-42	S13 E53 25ABBA1 WW-5C FRENCHMAN FLAT	592471.8	4071751.81	21	4, 12, 17, 21, 23
FG-43	WELL 5A N738361 E707514 FRENCHMAN FLAT	592982.61	4070370.54	13	4, 12, 17, 23
FG-44	UE-5PW-1	593659.663	4078698.878	2	8, 16
FG-45	UE-5PW-2	593668.4936	4080147.445	2	8, 16
FG-46	Watertown #3 Well, Emigrant Valley	603380.3217	4124241.087	16	6, 8, 16, 17, 23
FG-48	WELL 3 N817795 E677762 13 FLAT	583818.79	4094559.97	12	4, 12, 17, 23
FG-50	MARBLE TEST N903,93-61 E674,855-99	582846.44	4120530.62	1	14
FG-51	13 LAKE N795500 E687000	587572.8	4087725.44	2	21, 23
FG-52	TEST HOLE 7 N843100 E684700	585915.77	4102285.64	1	14
FG-54	23 Test Well B	588805.0044	4092915.745	1	8
OV-1	ETH I-4	515847.8	4078907	3	15, 16, 21
OV-2	Bailey Hot Spring, Oasis Valley	524774.0114	4091839.681	10	8, 16, 20, 21
OV-3	11S/47-21ABA - SPRING	524972.35	4091655.38	6	23, 26
OV-4	AMARGOSA HOT SPR 6 MI N OF BEATTY NV	525218.78	4091933.44	3	14, 15
OV-5	BURRO HOT SPRING 11S/47E-16dcd	524972.26	4091686.19	14	14
OV-6	II-1	515551.9	4078229	2	14, 15
OV-7	11S/47-16BDC	524178.78	4092485.06	1	14
OV-8	II-2	517359.7	4078202	2	14, 15
OV-9	11S/47E-33bac SPRING	524166.08	4088263.48	5	14
OV-10	Amargosa Springs	524190.63	4088325.18	2	14, 15

unique identifier	site	northing	easting	#avg/mrg	Sources
OV-11	WELL SWSWNE 21-11S-47E NYE CO	524701.99	4091099.93	4	11, 23
OV-12	SPRING 11S/47E-21acc (WELL)	525196.53	4091101.38	1	14
OV-14	SPRING and well NWNWSE 21-11S-47E NYE CO	524727.35	4090884.3	9	6, 15, 16, 23, 26
OV-15	11S/46-26BBB UPPER INDIAN SPRING	517360.61	4089879.98	1	14
OV-16	UPPER INDIAN SPRINGS NWNWSW 26-11S-46E	517337.07	4089294.46	3	14
OV-17	Revert Spring (Beatty Spring), Oasis Valle	522837.5916	4085578.983	13	8, 15, 16, 20, 23, 26
OV-19	11S/47-18ACD CRYSTAL SPRINGS	521656.59	4092663.13	1	14
OV-20	11S/47-10CAA	526250.9	4093970.32	1	14
OV-22	SPRING NWSESW 3-11S-47E NYE CO	525950.13	4095325.23	5	15, 23, 26
OV-23	CRYSTAL SPRING NWSWNE 18-11S-47E NYE CO	521507.31	4093032.52	3	14
OV-24	SPRING SESENW 10-11S-47E NYE CO	526077.31	4094154.67	4	14, 15
OV-25	Spring, Oasis Valley 10S/47E-33aab	525027.584	4098064.945	5	11, 16, 20, 23, 26
OV-26	Beatty Well No. 1, Water and Sanitation Distr	521378	4085334	4	
OV-27	10S/47-33AAB	525052.38	4098034.2	1	14
OV-29	11S/47E-28dac SPRING	525227.03	4089160.18	6	15, 16, 23
OV-30	12S/47-6CDD	521279.49	4085297.61	6	16, 23, 26
OV-31	11S/47-27CBA	525573.47	4089099.59	5	14, 15
OV-32	11S/46-26BCC LOWER INDIAN SPRING	517361.74	4089325.33	1	14
OV-35	Spring, Oasis Valley 11S/47E-04cad	524466.3703	4095628.956	6	15, 16, 23, 26
OV-36	Goss Spring, 11S/47E-10bcc, Oasis Valley	525434.3625	4094245.157	3	8, 16, 26
OV-37	12S/47E-07dbd	521529.66	4084219.76	6	6, 15, 23, 26
OV-38	10S/47-30DCC	521493.7	4098394.19	7	11, 15, 23, 26
OV-39	PEACOCK R.SPRING 10S/47E-31aab	521815.59	4098117.68	6	15, 16, 23, 26
OV-41	12S/47E-19adc	521834.13	4081293.22	4	15, 16, 21, 23, 26
OV-42	SPRING NWSWSW 10-11S-47E NYE CO	525386.87	4093597.91	7	15, 23, 26, 28
PM-1	UE19i N910098 E593107 PAHUTE MESA	557942.13	4122571.59	2	14
PM-3	U-20f PAHUTE MESA	545365.05	4124897.91	7	14
PM-5	UE20d N909200 E554300 PAHUTE MESA	546093.66	4122282.46	13	14
PM-6	UE19fs N900905 E587084 PAHUTE MESA	556112.99	4119785.62	1	14
PM-8	S08 E48 13CADA2 PM- 3	539002.93	4121291.22	1	14
PM-9	ER-20-5 #1, NTS Area 20	546356.6814	4119263.881	4	8, 16
PM-10	UE20h N918015 E567747 PAHUTE MESA	550192.02	4124956.22	3	14
PM-11	U20a-2 N907395 E571439 PAHUTE MESA	551344.53	4121758.23	9	3, 4, 23
PM-12	ER-20-5 #3 Well, NTS, Area 20 (7/96)	546356.8514	4119233.065	4	8, 16
PM-16	Cedar Creek Pass Well, Cactus Flat	545567.7871	4177628.614	3	8, 16
PM-17	ER-20-6 #3	551333.4091	4123576.358	2	8, 16
PM-21	10S/47E-14bab SPRING	527556.48	4102941.54	6	11, 15, 23, 26
PM-22	Water Well 8 (23 HTH #8)	563111.7515	4113271.153	10	3, 4, 8, 16, 20, 23
PM-23	Roller Coaster Well (Sandia Well #8)	523232.3227	4174700.151	2	8, 16
PM-27	ER-20-6 #2	551333.0321	4123637.99	2	8, 16
PM-29	TEST WELL 1 N876855 E629310	569013.04	4112485.37	6	14
PM-30	UE-17a (Eleana)	573659.5436	4102971.177	6	8
PM-32	Sandia Well #6, Cactus Flat	522040	4181696	5	8, 16, 20
PM-35	ER-20-6 #1	551357.4757	4123668.956	2	8, 16

unique identifier	site	northing	easting	#avg/mrg	Sources
PM-37	LONG RANGE 1 N877000 E631000 NTS	569505.84	4112551.06	2	14
PM-39	TUNNEL U12n.03 N892739 E638485	571783.64	4117346.97	2	14
PM-40	UE-16d (Eleana)	574181.6261	4102575.114	2	8, 16
PV-1	Little Ash Spring, Pahranagat Valley	659927.1667	4147635.298	3	8, 16
PV-2	Crystal Springs, Pahranagat Valley	656124.0902	4155147.653	3	8, 16
PV-5	Oreana Spring, Seaman Range	662519.6031	4198098.609	2	8, 16
SP-1	S16 E53 05ADAD1 Army 1 WW	586123.34	4049805.45	15	4, 6, 17, 18, 21, 23, 25
SP-2	AMARGOSA TRACER HOLE NO. 2	569150.8	4043582	5	14, 15
SP-3	S16 E51 27BAA AMARGOSA TRACER WELL 2	569200.57	4043582.1	54	6, 18, 21, 23
SP-4	Johnnie Gold Pan Well	583374.4887	4030795.968	2	16, 19
SP-5	16S-52E-15add	579794.66	4046231.4	1	14
SP-7	Army #1 Water Well, 16S/53E-05adb	586123.3365	4049805.449	3	8, 16
SP-8	AMARGOSA AL OBSERV HOLE N650572 E629255	569225.69	4043551.49	1	14
SP-9	AMARGOSA DESERT 17S/52-8c1	575892.11	4037691.18	3	14
SP-10	TEST WELL 10 N671051 E739075 AURORA SITE	602673.84	4049894.73	5	14
SP-11	PAHRUMP COMMUNITY CHURCH	590938.44	4007699.06	3	14
SP-12	TEST WELL 10	602771.76	4050019.17	1	14
SP-13	S20/53-3CDA	589360.27	4010610.13	1	14
SP-14	WELL (#89?) 3-20S-53E, N OF PAHRUMP	589406.4	4010980.38	1	14
SP-15	230 S17 E52 08CDB 1	576207.7	4038587.59	3	14
SP-16	INDIAN SPRINGS NWNW 14-16S-56E CLARK CO	619139.59	4047210.05	4	23
SP-17	WILCOX WELL SWNE 34-19S-53E NYE CO	589586.74	4012861.94	2	14
SP-18	23 TEST WELL 4, 3 MI W OF CACTUS SPR	608857.58	4048306.59	1	14
SP-19	66-79, INDIAN SPRING	619164.02	4047241.21	3	6, 17, 19, 21
SP-20	162 S20 E53 14 1 WELL NEAR PAHRUMP SPRING	591367.78	4007241.33	2	16, 18, 21
SP-21	White Rock Spring, Spring Mtns.	636825.2105	4004137.769	2	16, 18, 21
SP-23	RIESS OR 6TH ARMY 6A N665641 E690214	587780.02	4048188.94	1	14
SP-26	Indian Springs Prison Well #1	629465.0959	4041780.518	2	16, 18
SP-27	Old Dry Well, Three Lakes Valley	636931.3896	4043221.255	2	16, 18
SP-28	WHITE'S WELL N640480 E643110	573454.57	4040474.22	2	14, 15
SP-29	AMARGOSA DESERT 17S/51-1a1	573731.62	4040076	1	14
SP-30	WELL NW 9-19S-53E 8 M N OF PAHRUMP	587348.73	4019495.18	1	14
SP-31	WELL (FIELD #54) NW 9-19S-53E	587422.92	4019557.56	1	14
SP-32	WELL (FIELD #84) NE 21-19S-53E	588426.46	4016517.04	1	14
SP-33	S19/53-21AAA	588574.25	4016703.43	1	14
SP-34	Six Mile Spring	582613.9	4011252	4	6, 8, 15, 23
SP-37	INDIAN SPR SEWAGE CO #1, N660000 E795000	619820.63	4046510.64	2	14
SP-39	INDIAN SPRINGS - 1 S16 E56 16BBA	619163.17	4047302.84	5	19
SP-40	GRAPEVINE SPRING S19 E58 16BB	635556.99	4018172.26	5	16, 18, 19, 21
SP-41	CACTUS SPRING 16S/55.5E-11a	613778.77	4048370.27	6	23
SP-42	66-77, 16S/55-1/2-11ad	614077.02	4048374.22	2	14
SP-44	WELL NW 36-19S-52E NYE CO	582646.56	4013070.59	1	14
SP-45	S19/52-36BDD	582874.96	4012672.17	1	14
SP-46	161 S16 E56 16BBA 2 INDIAN SPRINGS - 3	619188.02	4047303.18	5	18, 19, 21, 23

unique identifier	site	northing	easting	#avg/mrg	Sources
SP-47	23 TW #7 S19/51E-36b PAHRUMP VALLEY	572891	4012799	2	14, 15
SP-49	S17 E51 23 1	571433.5	4035188	8	5, 6, 15, 21, 23
SP-51	20S/52E-12aba	583349.2	4010058	2	14, 15
YM-2	UE-25 p#1 (0-1200 m) and (1300-1800m)	551508.7	4075663	6	13
YM-3	DH AM101 SWSWNE 27-15S-49E	549552.92	4052721.48	4	6, 13, 21, 23
YM-4	S15 E50 25BD 1	552533.39	4052770.01	1	14
YM-5	UE-25c 1 HTH, 3 HTH, #2	550954.6	4075933	23	1, 2, 13, 15, 16, 18, 21
YM-6	UE-25 c#3	550919.8	4075886	29	13
YM-7	UE-25 c#2	550944	4075867	4	13
YM-8	USW H-6	546188.07	4077816.08	14	1, 2, 13, 15, 16, 18, 21
YM-9	UE-25 b#1 (853-914 m	549954.5	4078422	2	13
YM-10	S12 E50 31BDBC1 UE-25b 1 HTH	549949.06	4078422.79	43	1, 5, 10, 18, 21
YM-11	UE-25 b#1 (0-1220 m)	549954.5	4078422	2	13
YM-12	USW H-5	547665.5	4078838	8	1, 13, 18
YM-13	USW G-4 well, 13 Mtn.	548932.663	4078601.774	6	1, 13, 15, 16, 18
YM-14	USW VH-1 well, Crater Flat	539975.5189	4071714.29	20	1, 13, 16, 21
YM-15	USW VH-1 AMARGOSA WELL #55 CRATER FLAT	539975.52	4071714.29	4	1, 5, 18, 21
YM-16	UE-25 J-11	563816	4071049	13	13
YM-17	J-11 N738968 E611764 JACKASS FLATS	563798.58	4071057.92	12	14
YM-18	USW H-4 well, 13 Mtn.	549187.773	4077309.026	3	1, 15, 16, 18, 27
YM-19	USW H-4	549195	4077322	2	13
YM-20	USW H-1 (572-687 m) and (687-1829m)	548721.8	4079944	4	13
YM-21	USW G-2	548138.6	4082554	24	13, 15
YM-22	USW H-1 13 MTN	548726.97	4079925.63	6	1, 5, 16, 18
YM-23	AMARGOSA DESERT 13S/51-30d1	564462.22	4071802.47	1	14
YM-24	USW VH-2	537737.6	4073222	10	13, 15
YM-25	J-13 well, Area 25, Nevada Test Sit	554016.8747	4073517.231	48	4, 5, 8, 13, 15, 16, 18, 20, 23
YM-26	TW-5	562605	4054686	5	13, 15
YM-27	15S/49E-22dc	549697.31	4053523.47	8	5, 13, 15, 16, 18, 21, 23, 28
YM-28	UE-18r N868100 E564700 PAHUTE MESA	549345.04	4109789.43	27	3, 5, 8, 16, 20, 23
YM-29	LATHROP WELLS NEV	550086.25	4054973.97	4	13, 14, 15
YM-30	AMARGOSA DESERT 15S/49-14a1	551544.69	4056091.9	1	14
YM-31	Airport Well	553289	4055086	1	13
YM-32	NDOT well	554132.4	4055245	6	13
YM-33	JF-3	554498.3	4067974	12	13, 15
YM-35	UE-25 J-12	554435.8	4068767	59	1, 4, 6, 8, 12, 13, 16, 18, 20, 21, 23
YM-36	AMARGOSA DESERT 14S/50-6a1	554739.32	4069053.7	1	14
YM-37	15S/50E-18cdc	553934.3	4055151	3	13, 14, 15
YM-38	11S/48E-1dd	539420.55	4095161.51	1	14
YM-41	WELL NW 19-15S-50E NYE CO	553862.5	4054719.52	6	13, 14
YM-42	S11 E50 10AACB1 UE-29a 1(OR 2) HTH	555753.3	4088350.54	16	1, 13, 15, 16, 18, 20, 21, 24

References for Water Samples

1 Benson, L.V., Robison, J.H., Blankennagel, R.K., and Ogard, A.E., 1983, Chemical composition of groundwater and the location of permeable zones in the Yucca Mountain area, Nevada: U.S. Geological Survey Open-File Report 83-854, 19 p.

2 Benson, L.V., and McKinley, P.W., 1985, Chemical composition of ground water in the Yucca Mountain area, Nevada-An update: U.S. Geological Survey Open-File Report 85-484, 10 p.

3 Blankenagel, R.K., and Weir, J.E., Jr., 1973, Geohydrology of the eastern part of Pahute Mesa, Nevada Test Site: U.S. Geological Survey Professional Paper 712-B, p. B1-B35. (HQS.880517.1733)

4 Claassen, H.C., 1973, Water quality and physical characteristics of Nevada Test Site water-supply wells: U.S, Geological Survey USGS-474-158, 145 p.

5 Claassen, H.C., 1983, Sources and mechanisms of recharge for ground water in the west-central Amargosa Desert, Nevada-A geochemical interpretation: U.S. Geological Survey Professional Paper 712-F, p. F1-F61.

6 Claassen, H.C, U.S. Geological Survey, unpublished data

7 Dudley, W.W., and Larson, J.D., 1976, Effect of irrigation pumping on Desert Pupfish habitats in Ash Meadows, Nye County, Nevada: U.S. Geological Survey Professional Paper 927, 26 p.

8 Farnham, I. and McCord, J., 2006, Geochem06.mdb and A user's guide to the comprehensive water quality database for groundwater in the vicinity of the Nevada Test Site, Underground Test Area Project, Stoller-Navarro Joint Venture.

9 Hardman, George, and Miller, M.R., 1934, The quality of the waters of southeastern Nevada, drainage basins and water resources: The University of Nevada Agricultural Experiment Station, Bulletin No. 136, University of Nevada, Reno, Nevada, 62 p.

10 Lahoud, R.G., Lobmeyer, D.H., and Whitfield, M.S., Jr., 1984, Geohydrology of volcanic tuff penetrated by test well UE-25b#1, Yucca Mountain, Nye County, Nevada: U.S. Geological Survey Water-Resources Investigations Report 84-4253, 44 p.

11 Malmberg, G.T. and Eakin, T.E., 1962, Ground-water appraisal of Sarcobatus Flat and Oasis Valley, Nye and Esmerelda Counties, Nevada: Nevada Department of Conservation and Natural Resources, Ground-water Resources-Reconnaissance Series Report 10, 39 p.

12 Moore, J.E., 1961, Records of wells, test holes, and springs in the Nevada Test Site and surrounding area: U.S. Geological Trace-Elements Investigations Report 781, 22 p.

13 Oliver, T. and Root, T. 1997, Hydrochemical Database for the Yucca Mountain Area, Nye County, Nevada. U.S. Geological Survey. Memo to the Technical Project Officer, pp. 1-9 with figures and Excel database file. Denver, Colorado: U.S. Geological Survey. MOL.19980302.0367.

14 Perfect, D.L., Faunt, C.C., Steinkampf, W.C., and Turner, K.A., 1995, Hydrochemical data base for the Death Valley Region, California and Nevada: U.S. Geological Survey Open-File Report 94-305, 10 p.

15 Root, T.L., 2000, Using ground water chemistry to delineate ground water flow paths near Franklin Lake Playa, Inyo County, California: University of Wisconsin-Madison, Master of Science Thesis, 122 p.

16 Rose, T.P., Kenneally, J.M., Smith, D.K., Davisson, M.L., Hudson, G.B., and Rego, J.H, 1997, Chemical and isotopic data for groundwater in southern Nevada, UCRL-ID-128000, Lawrence Livermore National Laboratory

17 Schoff, S.L., and Moore, J.E., 1964, Chemistry and movement of ground water, Nevada Test Site: U.S. Geological Survey Trace-Elements Investigations Report 838, 75 p.

18 Thomas, J. (unpublished written communication to Perfect, 1989)

19 Thomas, J.M., Lyles, B.F., and Carpenter, L.A., 1991, Chemical and isotopic data for water from wells, springs, and streams in carbonate-rock terrane of southern and eastern Nevada and southeastern California, 1985-88: U.S. Geological Survey Open-File Report 89-422, 24 p.

20 Thomas, J.M., Benedict, F.C, Jr., Rose, T.P., Hershey, R.L., Paces, J.B., Peterman, Z.E., Farnham, I.M., Johannesson, K.H., Singh, A.K., Stetzenbach, K.J., Hudson, G.B., Kenneally, J.M., Eaton, G.F., and Smith, D.K., 2002, Geochemical and isotopic interpretations of groundwater flow in the Oasis Valley Flow System, southern Nevada, U.S. Department of Energy, Pub. No. 45190, 113p.

21 U.S. Geological Survey, National Water Information System (NWIS-1)

22 U.S. Geological Survey, National Water Data Storage and Retrieval System (WATSTORE)

23 U.S. Geological Survey unpublished data

24 Waddell, R.K., 1984, Hydrologic and drill-hole data for test wells UE-29a#1 and UE-29a#2, Fortymile Canyon, Nevada Test Site: U.S. Geological Survey Open-File Report 84-142, 25 p.

25 Walker, G.E., and Eakin, T.E., 1963, Geology and ground water of Amargosa Desert, Nevada-California: Nevada Department of Conservation and Natural Resources, Ground-Water Resources-Reconnaissance Series Report 14, 45 p.

26 White, A.F., 1979, Geochemistry of ground water associated with tuffaceous rocks, Oasis Valley, Nevada: U.S. Geological Survey Professional Paper 712-E, p. E1-E25.

27 Whitfield, M.S., Eshom, E.P., Thordarson, William, and Schaefer, D.H., 1985, Geohydrology of test well USW H-4, Yucca Mountain, Nye County, Nevada: U.S. Geological Survey Water-Resources Investigations Report 85-4030, 33 p.

28 Whitfield, U.S. Geological Survey, unpublished data

Appendix B

Water Samples Collected for this Study:
Sulfur and Strontium Isotopes

Appendix B

Samples collected for this thesis.

spring	analysis	date collected	northing	easting	Sr, ppm	87Sr/86Sr	stdev	34S	stdev
Horseshutem Spring, NV	δ34S		589698	4033355	0.207	0.71918	0.00001	7.9	0.14
Kwichup Spring, Spring Mountains, NV	δ34S, Sr, 87/86Sr	21-Feb-05	586205	4036586				20.5	0.14
Diebert Spring, Spring Mountains, NV	δ34S, Sr, 87/86Sr	21-Feb-05	586450	4036958	3.326	0.73686	0.00001	21.2	0.14
Crystal Spring, Spring Mountains, NV	δ34S, Sr, 87/86Sr	21-Feb-05	592007	4031653	0.266	0.72097	0.00001	9	0.14
Grapevine Springs, Spring Mountains, NV	δ34S, Sr, 87/86Sr	21-Feb-05	587242	4034932	0.614	0.73314	0.00001	10.7	0.07
Cactus Sring hose	δ34S, Sr, 87/86Sr	21-Feb-05	613778	4048370	0.261	0.70993	0.00001	6	0.14
Cactus Spring	δ34S	23-Feb-05	613778	4048370				3.9	0.14
Fisher Ranch, Indian Springs, NV	δ34S, Sr, 87/86Sr	21-Feb-05	619014	4047239	0.240	0.71018	0.00001	3.7	0.14
Specie Spring, Oasis Valley	δ34S	19-Feb-05	530403	4080149				6.5	0.14
Beatty, Oasis Vallley	δ34S	19-Feb-05	522837	4085578	5.746	0.73682	0.00001	15.6	0.14
Ute Spring, Oasis Valley	δ34S	19-Feb-05	525079	4088913				19.4	0.14
Crystal Spring, Oasis Valley	δ34S	19-Feb-05	521507	4093032				10.5	0.07
Lower Indian Spring, Oasis Valley	δ34S	19-Feb-05	518550	4088526				6.8	0.07
Sarcobatus Flat, Oasis Valley	δ34S	19-Feb-05	522278	4081941				17.9	0.07
Crystal Spring, Pahranagat Valley, NV	δ34S, Sr, 87/86Sr	23-Feb-05	656120	4155143	0.230	0.71080	0.00001	1.9	0.07
Ash Spring, Pahranagat Valley, NV	δ34S	23-Feb-05	659924	4147634				3.1	0.07
Hiko Spring, Pahranagat Valley, NV	δ34S	23-Feb-05	657633	4162541				2.2	0.07
Rogers Spring, Ash Meadows NV	δ34S	13-Mar-05	560717	4036954				16.3	0.07
Longstreet Spring, Ash Meadows NV	δ34S	13-Mar-05	560476	4035843				16.2	0.07
Point of Rocks Spring, Ash Meadows NV	δ34S	13-Mar-05	565186	4028544				16.5	0.07

Appendix C

Cluster Analysis Trees
Stiff Diagrams
Piper Plot

Amargosa Desert with 7 clusters

Cluster AD1

cluster analysis observation	unique identifier (App. A)
OB31	AD-33
OB33	AD-35
OB5	AD-5
OB6	AD-6
OB32	AD-34
OB12	AD-12
OB19	AD-20
OB11	AD-11
OB13	AD-13
OB25	AD-27
OB26	AD-28
OB8	AD-8
OB10	AD-10
OB28	AD-30
OB27	AD-29
OB41	AD-43
OB7	AD-7
OB43	AD-45
OB52	AD-56
OB15	AD-16
OB40	AD-42
OB24	AD-26
OB42	AD-44
OB44	AD-46
OB16	AD-17
OB39	AD-41

Cluster AD2

cluster analysis observation	unique identifier (App. A)
OB45	AD-47
OB46	AD-48
OB22	AD-24
OB23	AD-25
OB37	AD-39
OB38	AD-40
OB3	AD-3
OB4	AD-4
OB21	AD-23
OB2	AD-2
OB49	AD-52
OB18	AD-19
OB1	AD-1
OB14	AD-14
OB29	AD-31
OB20	AD-21
OB9	AD-9
OB34	AD-36
OB30	AD-32

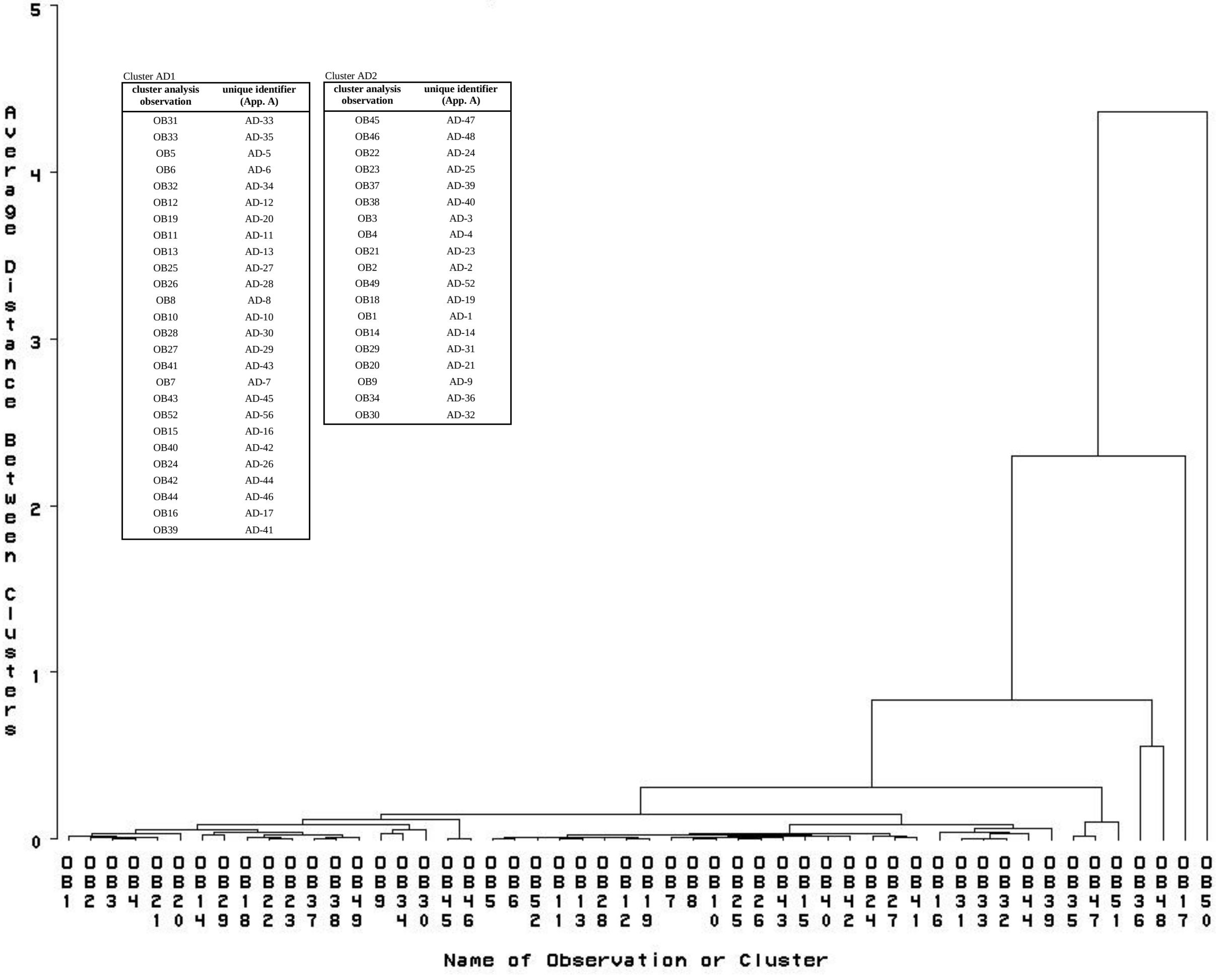

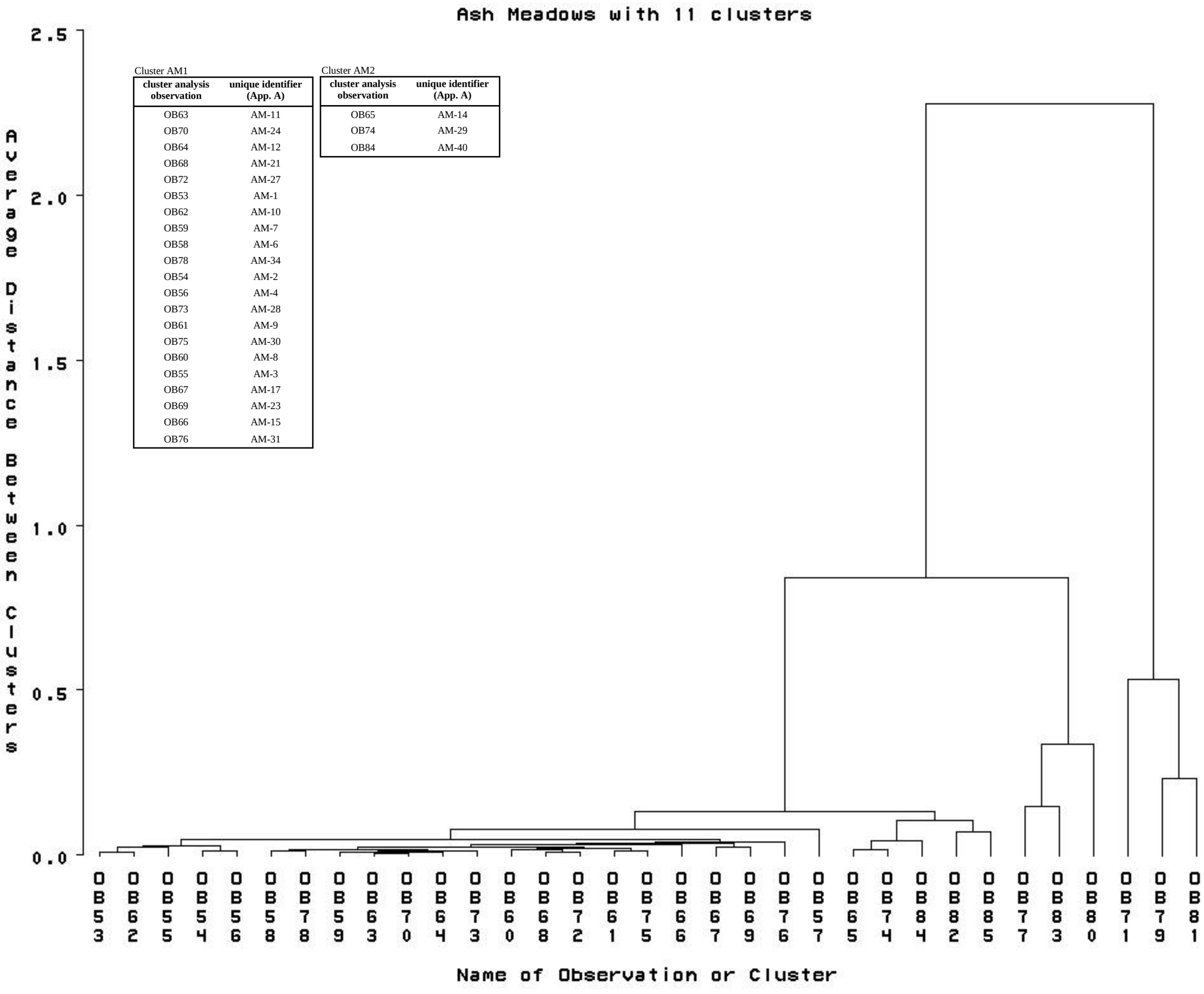

Cluster AM1

cluster analysis observation	unique identifier (App. A)
OB63	AM-11
OB70	AM-24
OB64	AM-12
OB68	AM-21
OB72	AM-27
OB53	AM-1
OB62	AM-10
OB59	AM-7
OB58	AM-6
OB78	AM-34
OB54	AM-2
OB56	AM-4
OB73	AM-28
OB61	AM-9
OB75	AM-30
OB60	AM-8
OB55	AM-3
OB67	AM-17
OB69	AM-23
OB66	AM-15
OB76	AM-31

Cluster AM2

cluster analysis observation	unique identifier (App. A)
OB65	AM-14
OB74	AM-29
OB84	AM-40

Oasis Valley with 6 clusters

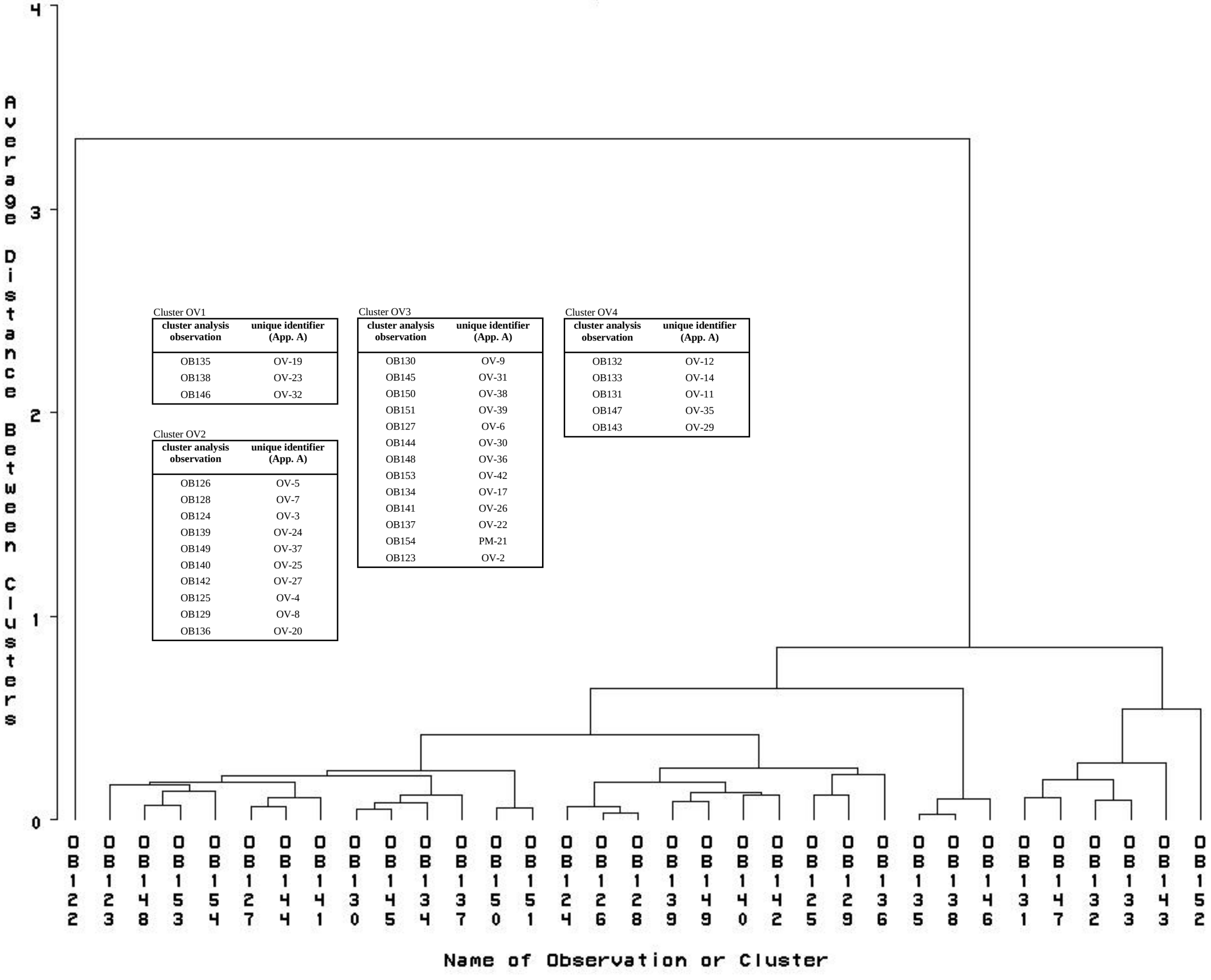

Cluster OV1

cluster analysis observation	unique identifier (App. A)
OB135	OV-19
OB138	OV-23
OB146	OV-32

Cluster OV2

cluster analysis observation	unique identifier (App. A)
OB126	OV-5
OB128	OV-7
OB124	OV-3
OB139	OV-24
OB149	OV-37
OB140	OV-25
OB142	OV-27
OB125	OV-4
OB129	OV-8
OB136	OV-20

Cluster OV3

cluster analysis observation	unique identifier (App. A)
OB130	OV-9
OB145	OV-31
OB150	OV-38
OB151	OV-39
OB127	OV-6
OB144	OV-30
OB148	OV-36
OB153	OV-42
OB134	OV-17
OB141	OV-26
OB137	OV-22
OB154	PM-21
OB123	OV-2

Cluster OV4

cluster analysis observation	unique identifier (App. A)
OB132	OV-12
OB133	OV-14
OB131	OV-11
OB147	OV-35
OB143	OV-29

Yucca Mountain with 10 clusters

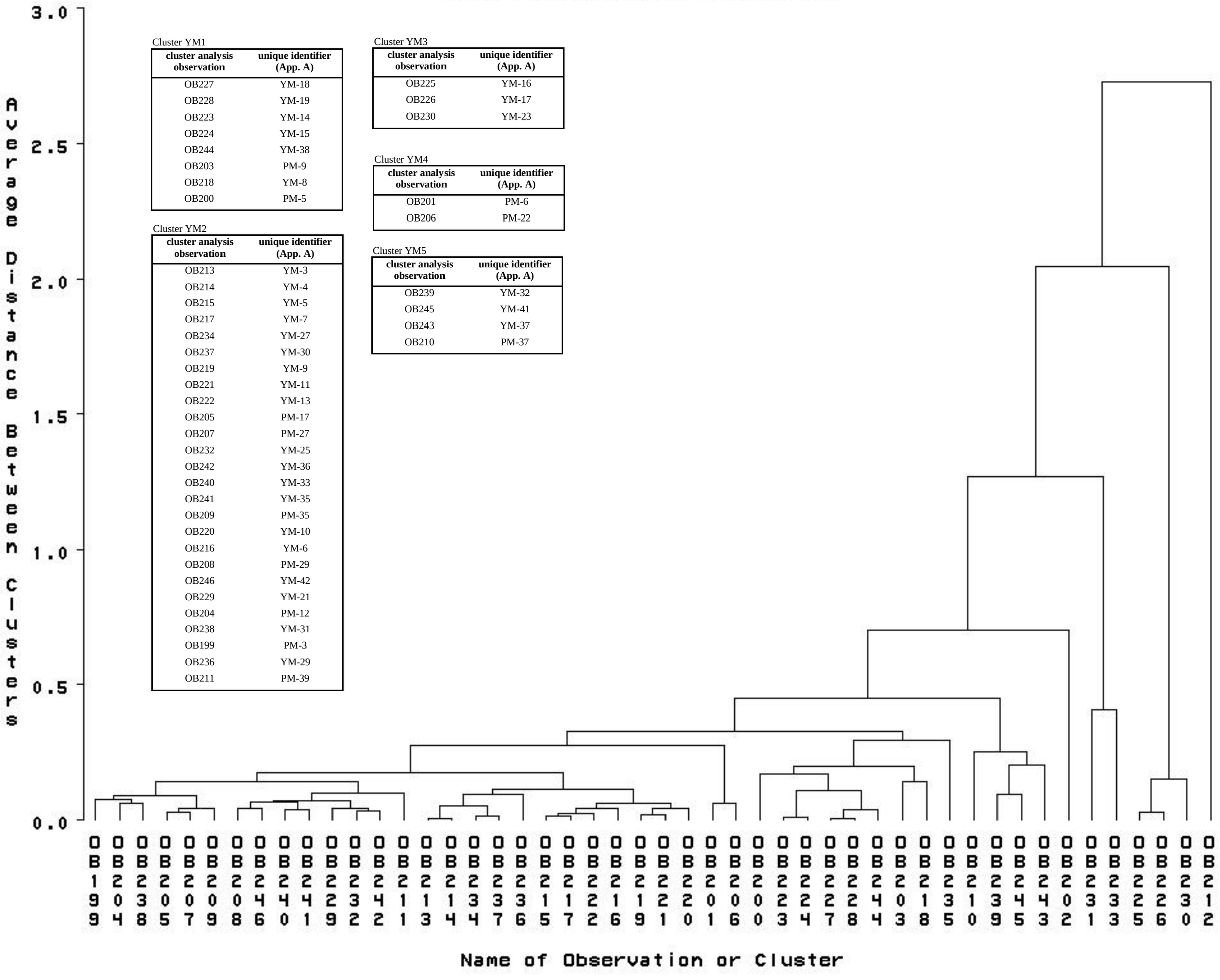

Cluster YM1

cluster analysis observation	unique identifier (App. A)
OB227	YM-18
OB228	YM-19
OB223	YM-14
OB224	YM-15
OB244	YM-38
OB203	PM-9
OB218	YM-8
OB200	PM-5

Cluster YM2

cluster analysis observation	unique identifier (App. A)
OB213	YM-3
OB214	YM-4
OB215	YM-5
OB217	YM-7
OB234	YM-27
OB237	YM-30
OB219	YM-9
OB221	YM-11
OB222	YM-13
OB205	PM-17
OB207	PM-27
OB232	YM-25
OB242	YM-36
OB240	YM-33
OB241	YM-35
OB209	PM-35
OB220	YM-10
OB216	YM-6
OB208	PM-29
OB246	YM-42
OB229	YM-21
OB204	PM-12
OB238	YM-31
OB199	PM-3
OB236	YM-29
OB211	PM-39

Cluster YM3

cluster analysis observation	unique identifier (App. A)
OB225	YM-16
OB226	YM-17
OB230	YM-23

Cluster YM4

cluster analysis observation	unique identifier (App. A)
OB201	PM-6
OB206	PM-22

Cluster YM5

cluster analysis observation	unique identifier (App. A)
OB239	YM-32
OB245	YM-41
OB243	YM-37
OB210	PM-37

Frenchman Groom with 4 clusters

Cluster FG1

cluster analysis observation	unique identifier (App. A)
OB102	FG-25
OB114	FG-46
OB107	FG-35
OB112	FG-44
OB105	FG-32
OB113	FG-45
OB99	FG-18
OB115	FG-48
OB90	FG-6
OB103	FG-26
OB101	FG-23
OB109	FG-39
OB104	FG-30
OB119	FG-54
OB106	FG-33
OB108	FG-38
OB117	FG-51
OB92	FG-9

Cluster FG2

cluster analysis observation	unique identifier (App. A)
OB110	FG-42
OB118	FG-52
OB97	FG-16
OB111	FG-43
OB98	FG-17
OB93	FG-11
OB120	PM-30
OB91	FG-8
OB116	FG-50
OB86	FG-2
OB94	FG-13
OB100	FG-19
OB121	PM-40
OB89	FG-5

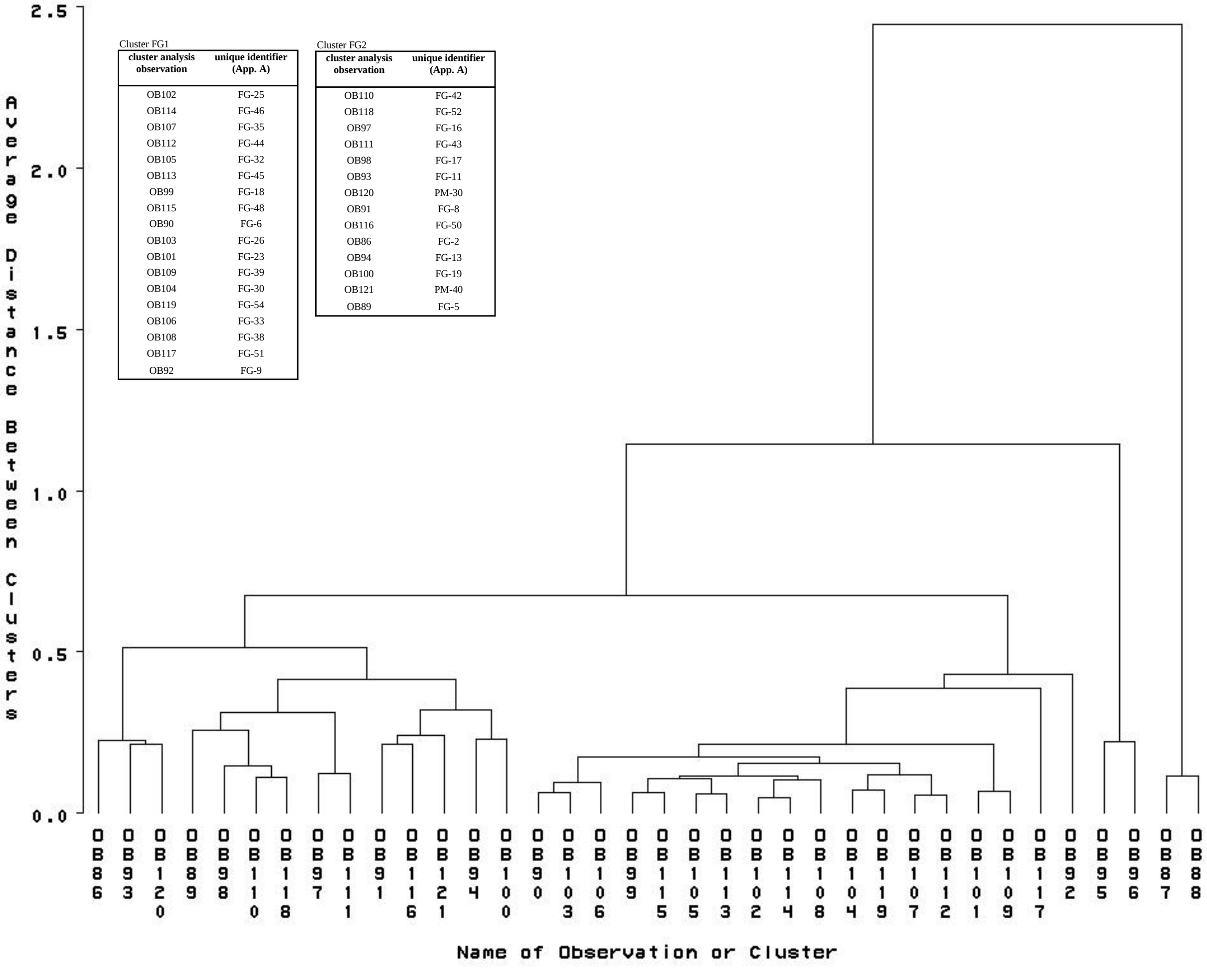

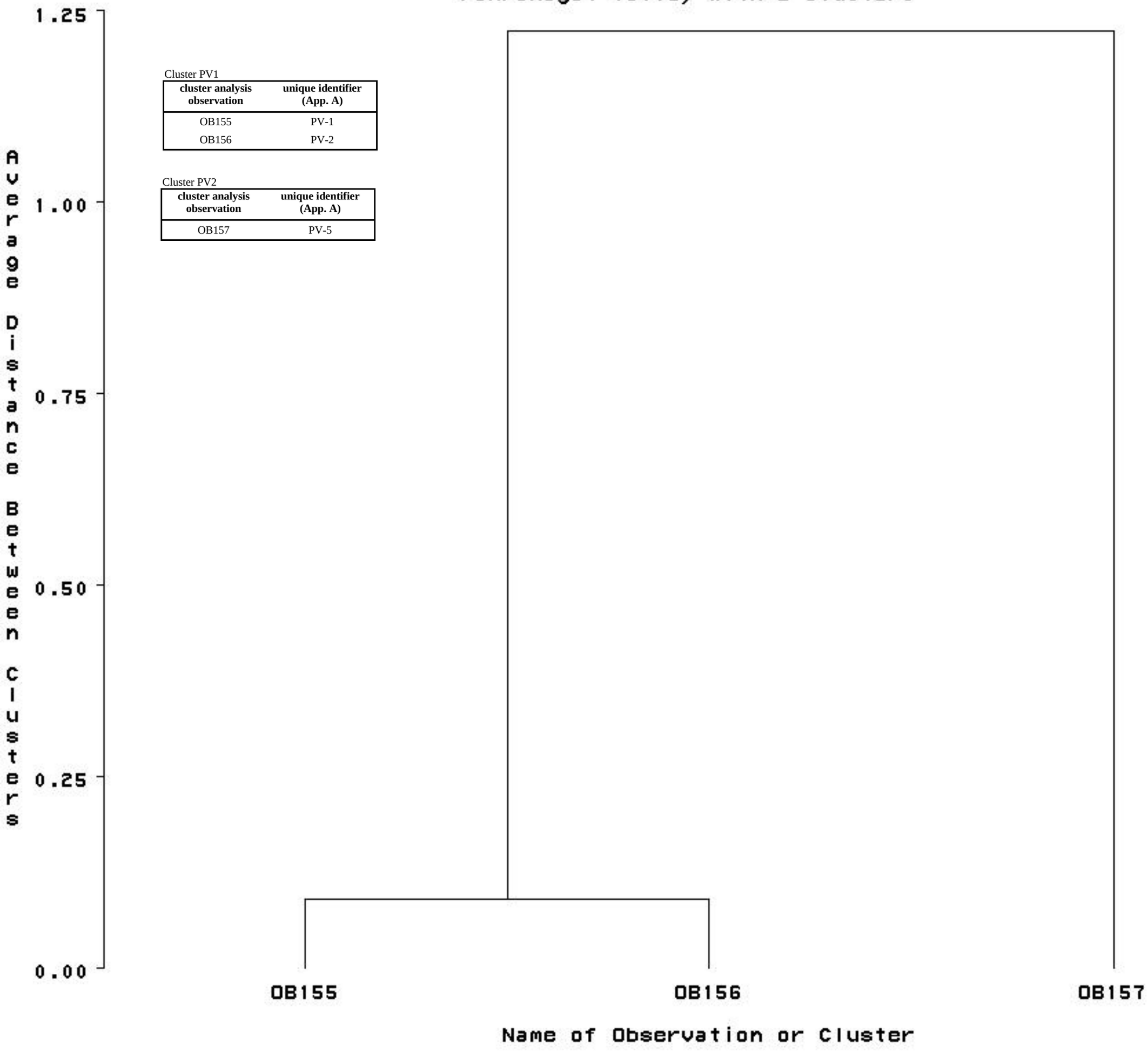

Cluster PV1

cluster analysis observation	unique identifier (App. A)
OB155	PV-1
OB156	PV-2

Cluster PV2

cluster analysis observation	unique identifier (App. A)
OB157	PV-5

Spring Mountains with 9 clusters

Cluster SP1

cluster analysis observation	unique identifier (App. A)
OB169	SP-13
OB170	SP-14
OB185	SP-32
OB186	SP-33
OB193	SP-44
OB194	SP-45
OB191	SP-41
OB192	SP-42
OB175	SP-19
OB195	SP-46
OB166	SP-10
OB168	SP-12
OB172	SP-16
OB189	SP-39
OB179	SP-26
OB176	SP-20
OB188	SP-37
OB174	SP-18
OB167	SP-11
OB180	SP-27
OB198	SP-51
OB173	SP-17
OB161	SP-4
OB163	SP-7

Cluster SP2

cluster analysis observation	unique identifier (App. A)
OB181	SP-28
OB182	SP-29
OB183	SP-30
OB184	SP-31
OB159	SP-2
OB160	SP-3
OB197	SP-49
OB190	SP-40
OB158	SP-1

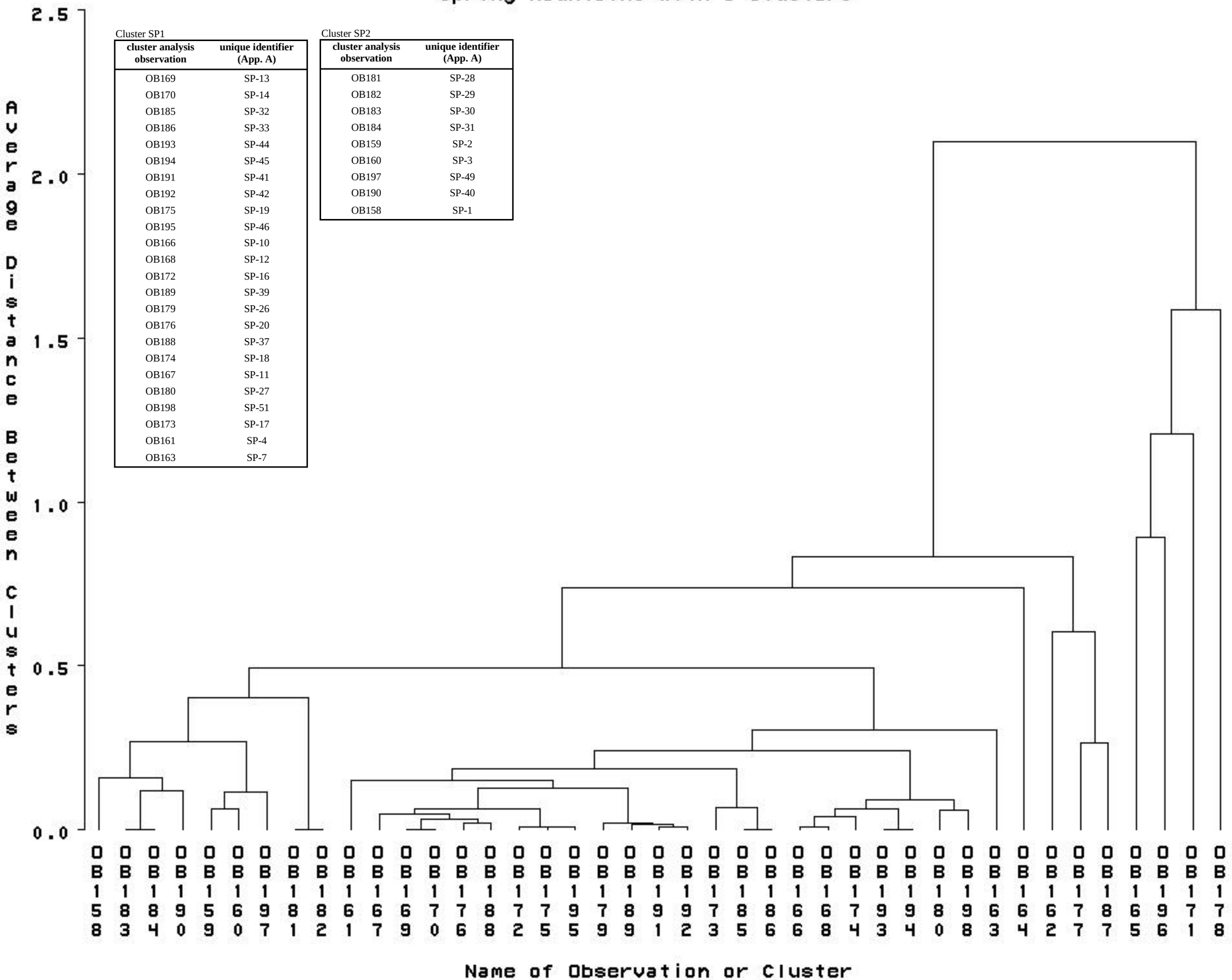

All Data with 30 clusters

Average Distance Between Clusters

10
8
6
4
2
0

Name of Observation or Cluster

Stiff Diagram

Flow Paths to Ash Meadows: Cluster output

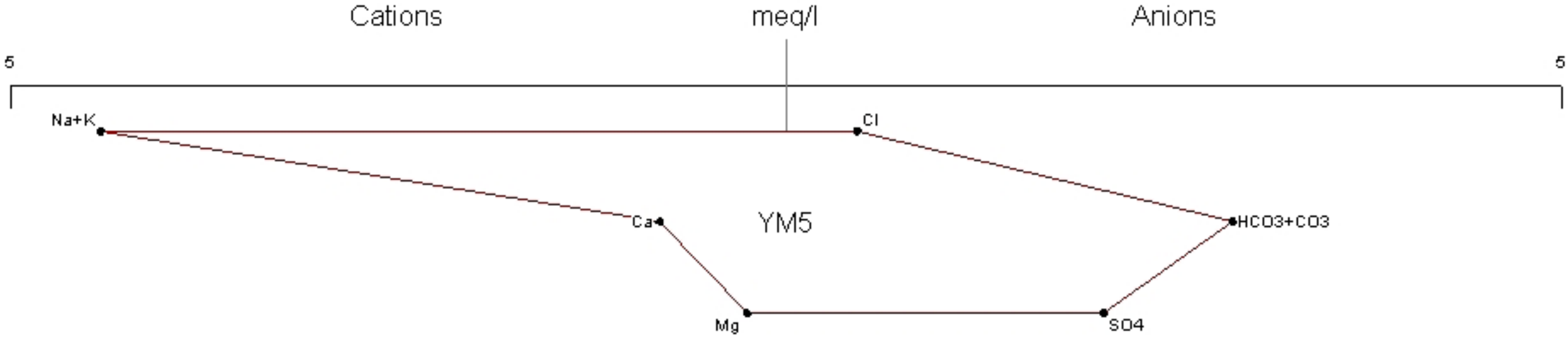

Stiff Diagram

Flow Paths to Ash Meadows: Cluster output

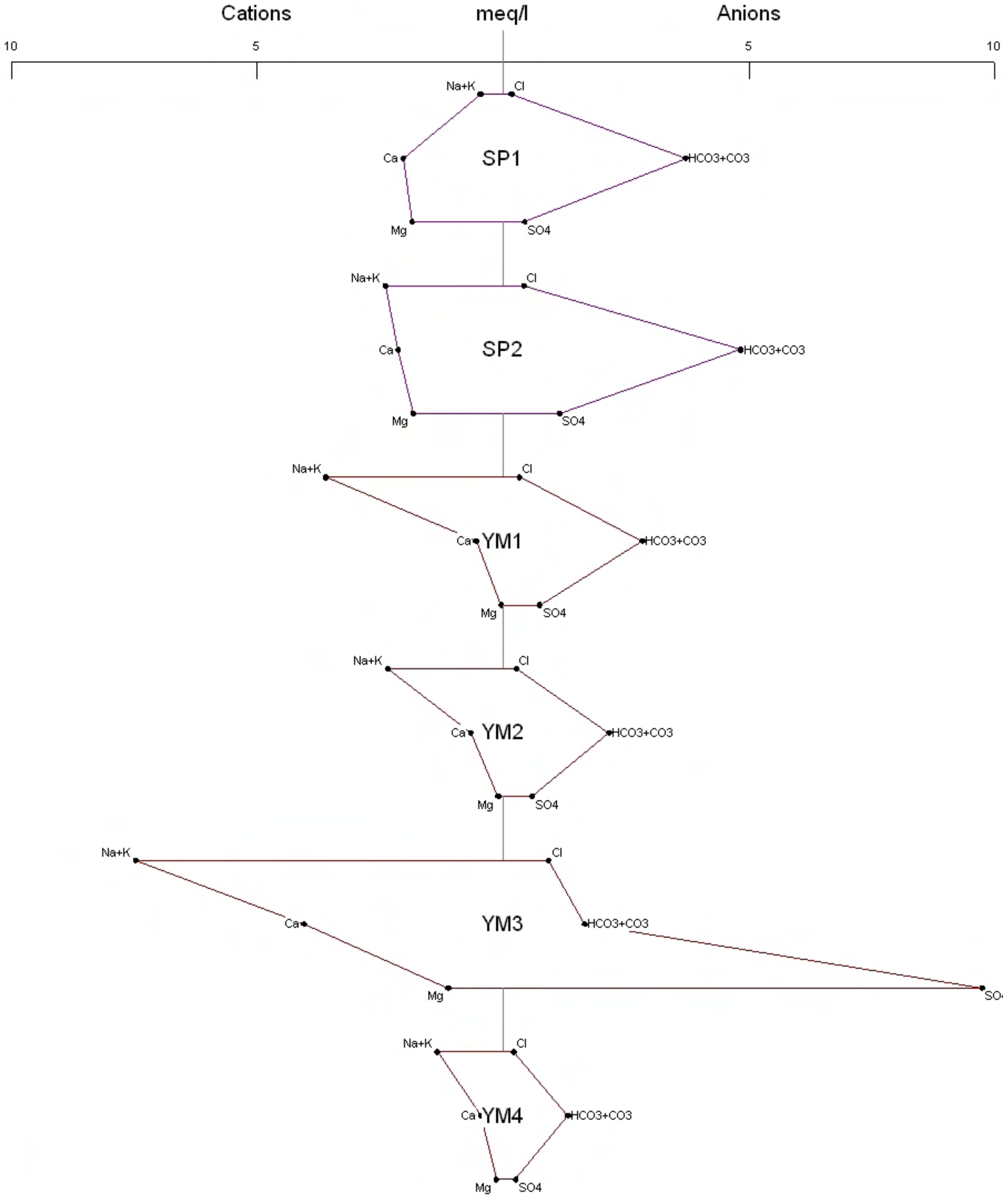

Stiff Diagram

Flow Paths to Ash Meadows: Cluster output

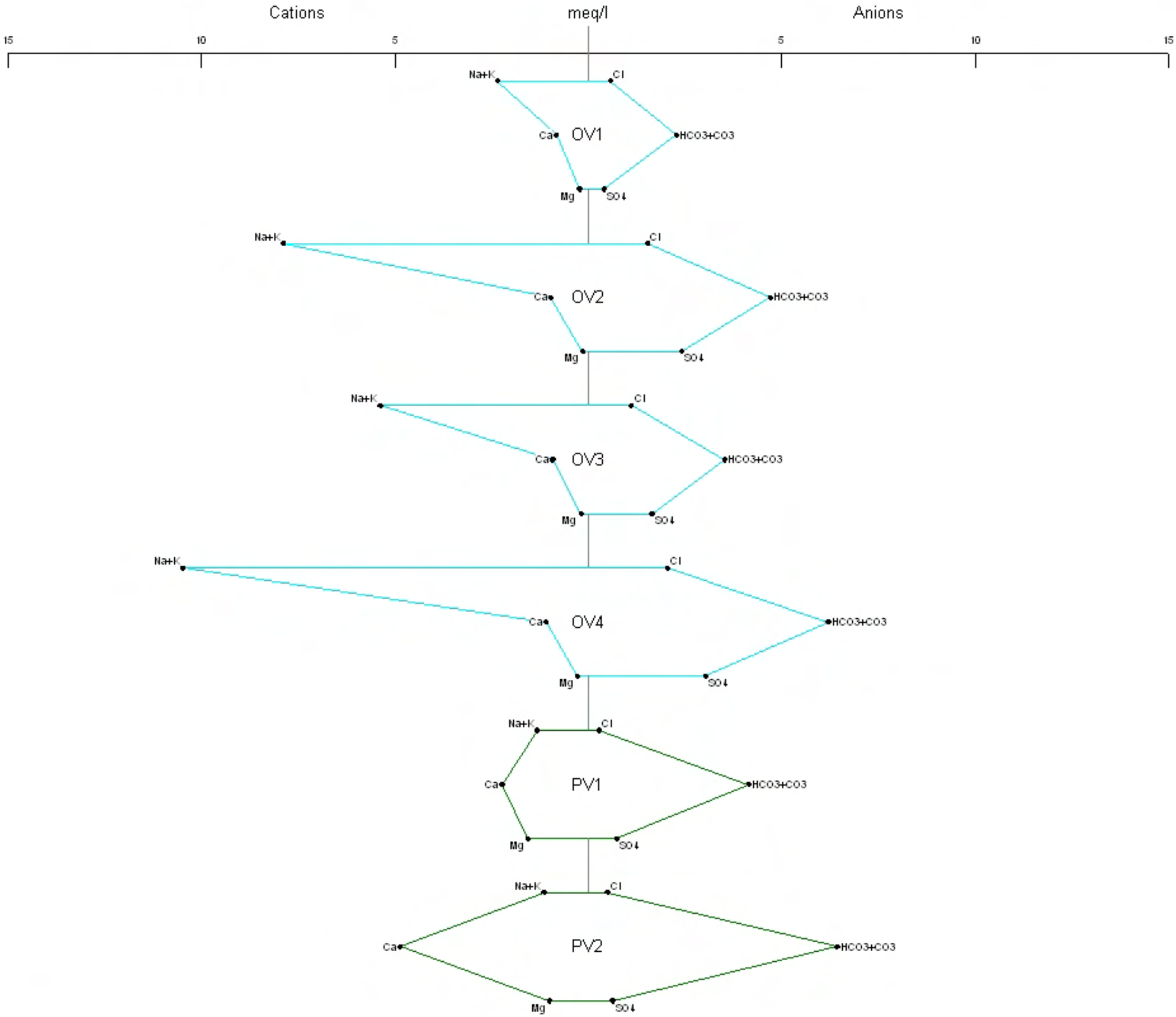

Stiff Diagram

Flow Paths to Ash Meadows: Cluster output

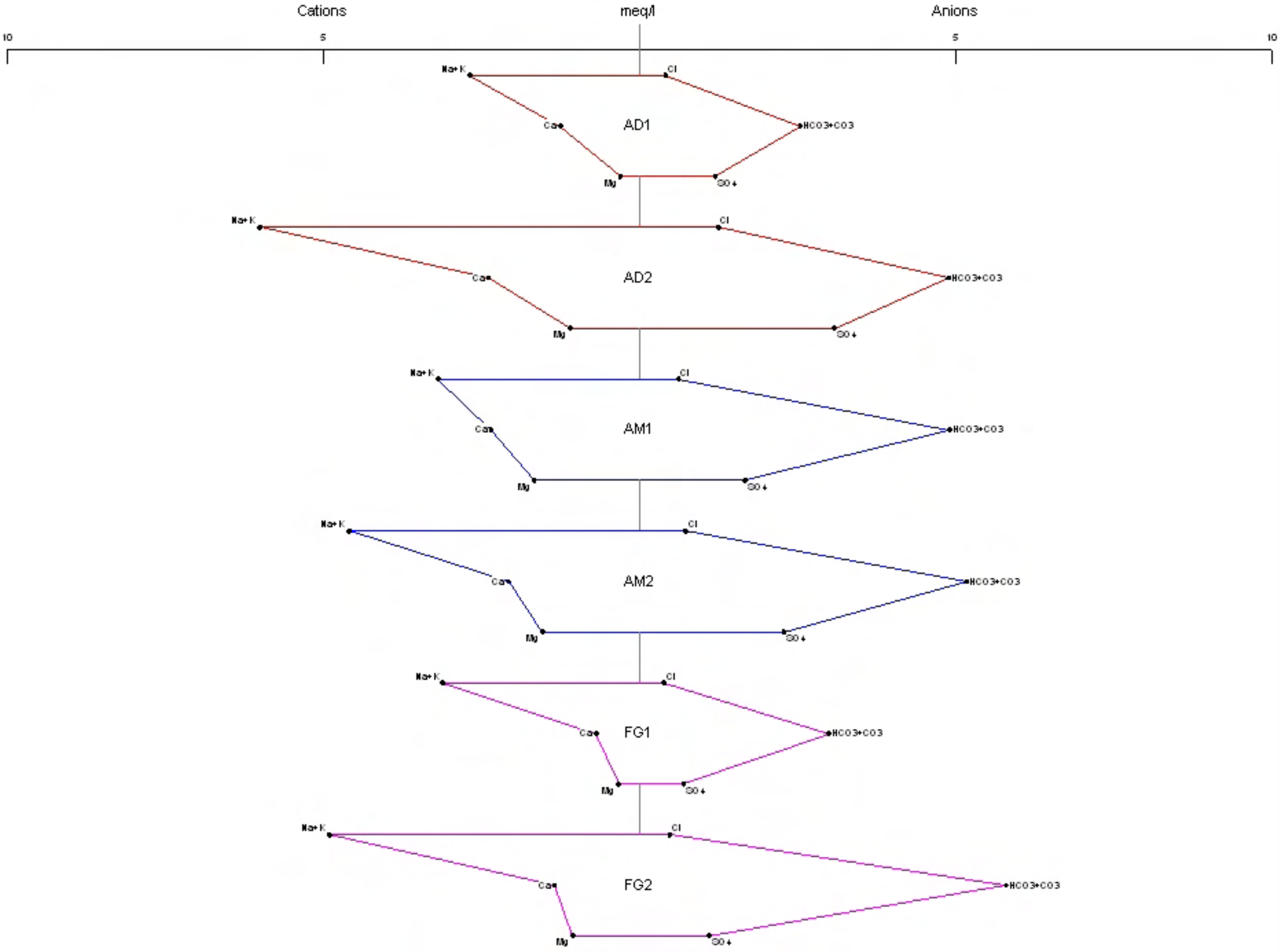

Piper Diagram

Potential Flow Paths to Ash Meadows: Cluster input

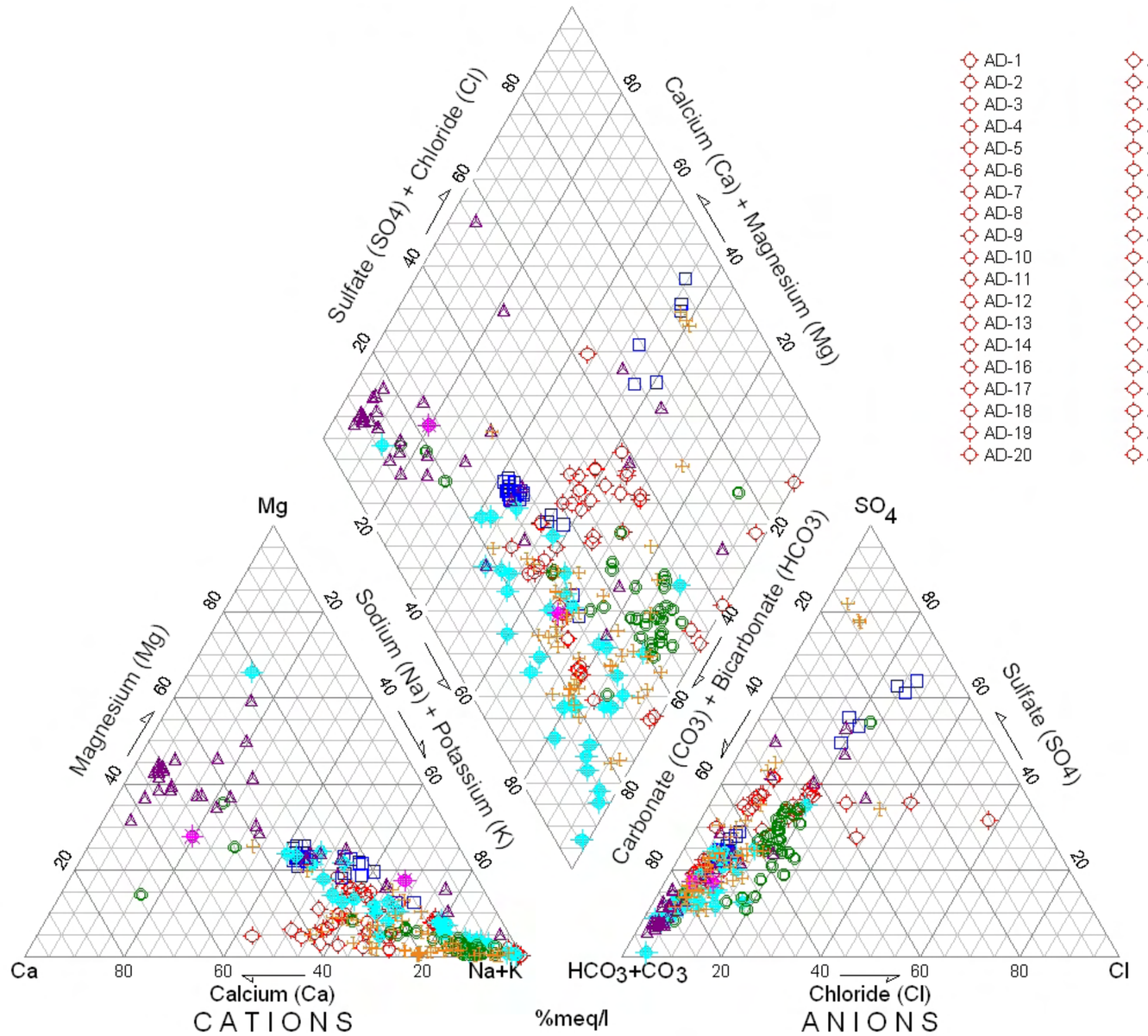

AD-1 AD-2 AD-3 AD-4 AD-5 AD-6 AD-7 AD-8 AD-9 AD-10 AD-11 AD-12 AD-13 AD-14 AD-16 AD-17 AD-18 AD-19 AD-20
AD-21 AD-23 AD-24 AD-25 AD-26 AD-27 AD-28 AD-29 AD-30 AD-31 AD-32 AD-33 AD-34 AD-35 AD-36 AD-37 AD-38 AD-39 AD-40
AD-41 AD-42 AD-43 AD-44 AD-45 AD-46 AD-47 AD-48 AD-50 AD-51 AD-52 AD-54 AD-55 AD-56 AM-1 AM-2 AM-3 AM-4 AM-5
AM-6 AM-7 AM-8 AM-9 AM-10 AM-11 AM-12 AM-14 AM-15 AM-17 AM-21 AM-23 AM-24 AM-26 AM-27 AM-28 AM-29 AM-30 AM-31
AM-33 AM-34 AM-35 AM-36 AM-37 AM-38 AM-39 AM-40 AM-41 FG-2 FG-3 FG-4 FG-5 FG-6 FG-8 FG-9 FG-11 FG-13 FG-14
FG-15 FG-16 FG-17 FG-18 FG-19 FG-23 FG-25 FG-26 FG-30 FG-32 FG-33 FG-35 FG-38 FG-39 FG-42 FG-43 FG-44 FG-45 FG-46
FG-48 FG-50 FG-51 FG-52 FG-54 PM-30 PM-40 OV-1 OV-2 OV-3 OV-4 OV-5 OV-6 OV-7 OV-8 OV-9 OV-11 OV-12 OV-14
OV-17 OV-19 OV-20 OV-22 OV-23 OV-24 OV-25 OV-26 OV-27 OV-29 OV-30 OV-31 OV-32 OV-35 OV-36 OV-37 OV-38 OV-39 OV-41
OV-42 PM-21 PV-1 PV-2 PV-5 SP-1 SP-2 SP-3 SP-4 SP-5 SP-7 SP-8 SP-9 SP-10 SP-11 SP-12 SP-13 SP-14 SP-15
SP-16 SP-17 SP-18 SP-19 SP-20 SP-21 SP-23 SP-26 SP-27 SP-28 SP-29 SP-30 SP-31 SP-32 SP-33 SP-34 SP-37 SP-39 SP-40
SP-41 SP-42 SP-44 SP-45 SP-46 SP-47 SP-49 SP-51 PM-3 PM-5 PM-6 PM-8 PM-9 PM-12 PM-17 PM-22 PM-27 PM-29 PM-35
PM-37 PM-39 YM-2 YM-3 YM-4 YM-5 YM-6 YM-7 YM-8 YM-9 YM-10 YM-11 YM-13 YM-14 YM-15 YM-16 YM-17 YM-18 YM-19
YM-21 YM-23 YM-24 YM-25 YM-26 YM-27 YM-28 YM-29 YM-30 YM-31 YM-32 YM-33 YM-35 YM-36 YM-37 YM-38 YM-41 YM-42

Appendix D

Mean Cluster Samples for NETPATH Modeling

cluster	temp	pH	diss O2	HCO3	TIC	CO3	Ca	Mg	Na	K	Cl	SO4	F	SiO2	Si	B	Ba	Li	Sr	Fe	Mn	NO3	PO4	13C	14C (pmc)	delta D	18O	Sr87/86	Al	cations	anions	charge balance
AD1	**24.33**	**7.80**		**155.05**	**2.44**	**0.04**	**25.15**	**3.73**	**57.13**	**7.91**	**14.56**	**57.40**	**1.43**	**67.48**		**14.40**		**0.12**	**0.31**		**0.00**	**2.64**	**0.37**	**-6.05**	**22.85**	**-102.72**	**-13.14**		**0.038**	**4.25**	**4.23**	**0.29**
AD2	25.28	7.61		298.05	4.07	0.01	47.90	13.33	131.17	11.74	44.07	147.79	3.07	54.48		0.52		0.08	0.19		0.00	1.64	0.16	-5.27	21.82	-101.29	-12.82		0.021	9.49	9.34	0.79
AM1	**31.55**	**7.64**	**2.34**	**297.46**	**312.00**	**0.71**	**47.11**	**20.33**	**68.44**	**8.19**	**21.70**	**79.99**	**1.63**	**22.74**	**11.94**	**0.30**	**0.06**	**0.09**	**0.89**	**0.02**	**0.00**	**0.50**	**0.01**	**-5.77**	**7.89**	**-103.62**	**-13.78**	**0.71272**	**0.121**	**7.21**	**7.24**	**-0.24**
AM2	27.45	7.57	3.20	313.86	320.00	0.77	41.58	18.70	100.30	9.10	25.64	109.60	1.25	30.67	13.51	0.55	0.05	0.13	0.93	0.02	0.00	0.58	0.06	-3.63	3.02	-100.92	-13.45	0.71709	0.160	8.21	8.22	-0.09
FG1	**26.75**	**8.15**	**3.53**	**173.11**	**157.38**	**4.74**	**13.76**	**4.08**	**66.93**	**7.86**	**13.61**	**33.45**	**1.19**	**58.94**	**24.53**	**0.25**	**0.02**	**0.24**	**0.09**	**0.19**	**0.06**	**4.01**	**0.28**	**-7.24**	**17.20**	**-106.86**	**-13.78**	**0.71152**	**0.054**	**4.13**	**4.09**	**0.68**
FG2	32.07	7.89	2.17	331.99	270.47	10.60	27.05	12.85	108.14	7.90	16.88	52.61	1.43	33.63	18.63	0.32	0.08	0.08	0.19	0.59	0.02	2.44	0.05	-7.73	4.14	-102.57	-13.74	0.71095	0.108	7.31	7.34	-0.23
OV1	**22.62**	**7.80**		**138.33**		**0.00**	**16.68**	**2.77**	**52.38**	**2.89**	**19.94**	**19.13**	**0.48**	**46.05**		**0.31**		**0.07**	**0.05**		**0.01**	**18.00**	**0.00**							**3.41**	**3.25**	**2.28**
OV2	29.53	7.91		282.45		2.00	19.54	1.81	177.51	6.29	54.43	115.54	5.03	53.91		0.29		0.21	0.15		0.00	1.33	0.01	-6.88	100.00	-108.00	-14.00		0.252	9.01	8.87	0.78
OV3	**25.31**	**7.96**	**3.75**	**213.82**	**191.00**	**0.37**	**18.42**	**2.35**	**119.85**	**6.28**	**39.34**	**78.66**	**2.85**	**56.16**	**26.72**	**0.29**	**0.01**	**0.13**	**0.27**	**0.02**	**0.01**	**1.12**	**0.00**	**-5.69**	**40.76**	**-106.03**	**-14.09**	**0.71050**	**0.039**	**6.49**	**6.41**	**0.56**
OV4	26.82	8.00		367.80		5.08	21.93	3.45	235.78	8.56	72.23	145.45	5.77	56.14		0.36		0.25	0.20		0.01	0.10	0.00	-5.75		-108.67	-14.03		0.011	11.85	11.53	1.41
PV1	**32.50**	**7.53**	**1.88**	**252.50**	**252.50**		**44.73**	**18.99**	**26.81**	**6.06**	**9.55**	**34.85**	**0.59**	**28.14**	**13.15**	**0.06**	**0.12**	**0.01**	**0.37**	**0.02**	**0.01**			**-5.33**	**7.11**	**-107.50**	**-14.17**	**0.71251**	**0.060**	**5.12**	**5.16**	**-0.49**
PV2	20.00	7.85		392.00	392.00		97.52	12.19	25.50	1.38	17.50	30.00	0.22	59.06	27.60	0.06	0.02	0.01	0.46	0.02	0.01			-8.95	96.68	-85.00	-10.10		0.060	7.01	7.55	-3.71
SP1	**24.16**	**7.78**	**3.75**	**226.28**	**400.00**	**0.00**	**40.75**	**22.56**	**9.61**	**1.80**	**5.81**	**20.70**	**0.26**	**18.23**	**9.70**	**0.19**	**0.08**	**0.01**	**0.24**	**0.33**	**0.00**	**1.85**	**0.13**	**-8.37**	**12.37**	**-97.29**	**-13.11**	**0.71196**	**0.060**	**4.35**	**4.32**	**0.38**
SP2	25.16	7.63		294.39		0.09	42.88	22.25	50.70	7.41	14.90	54.93	0.84	21.08		0.18		0.07	0.94		0.00	1.25	0.11	-7.37	24.40	-96.88	-12.40		0.200	6.37	6.44	-0.51
YM1	**34.68**	**7.82**		**170.26**	**94.64**	**1.07**	**11.12**	**0.51**	**81.70**	**2.05**	**11.71**	**35.59**	**4.54**	**45.78**	**24.35**	**0.20**	**0.00**	**0.09**	**0.05**	**0.22**	**0.02**	**0.66**	**0.04**	**-6.86**	**12.11**	**-107.21**	**-14.20**	**0.71072**	**1.649**	**4.20**	**4.11**	**1.12**
YM2	31.81	7.90	5.74	128.21	67.76	1.44	13.24	1.27	52.11	3.42	9.36	27.95	1.87	45.51	26.47	0.11	0.01	0.10	0.05	0.31	0.03	3.42	0.43	-8.49	23.50	-102.63	-13.69	0.71040	0.651	3.12	3.07	0.88
YM3	**34.40**	**7.81**		**100.80**		**0.00**	**81.21**	**13.62**	**162.49**	**15.82**	**32.70**	**467.53**	**1.07**	**55.71**		**1.16**			**0.03**		**0.00**	**7.12**	**0.00**					**0.70935**		**12.65**	**12.36**	**1.13**
YM4	31.95	7.61	6.00	80.31	30.00	0.00	9.23	1.74	29.11	2.97	7.41	12.05	2.18	47.43	20.80	0.05	0.00	0.03	0.02	0.02	0.03	2.35	0.03	-10.50	24.88	-104.00	-13.10	0.71027	0.060	1.95	1.89	1.44
YM5	**24.14**	**8.02**		**170.63**		**2.38**	**16.33**	**3.09**	**99.21**	**3.91**	**16.17**	**98.13**	**1.48**	**35.92**		**0.13**		**0.08**	**0.02**		**0.00**	**6.63**	**0.12**					**0.71113**		**5.48**	**5.45**	**0.28**

Appendix E

Normalization of Mean Samples Relative to Ash Meadows Water

cluster	HCO3	CO3	Ca	Mg	Na	K	Cl	SO4	F	SiO2	Si	B	Ba	Li	Sr	Fe	Mn	NO3	PO4	Al
AD1	155.05	0.04	25.15	3.73	57.13	7.91	14.56	57.40	1.43	67.48		14.40		0.12	0.31		0.00	2.64	0.37	0.038
AD2	298.05	0.01	47.90	13.33	131.17	11.74	44.07	147.79	3.07	54.48		0.52		0.08	0.19		0.00	1.64	0.16	0.021
AM1	297.46	0.71	47.11	20.33	68.44	8.19	21.70	79.99	1.63	22.74	11.94	0.30	0.06	0.09	0.89	0.02	0.00	0.50	0.01	0.121
AM2	313.86	0.77	41.58	18.70	100.30	9.10	25.64	109.60	1.25	30.08	13.51	0.55	0.05	0.13	0.93	0.02	0.00	0.58	0.06	0.160
FG1	173.11	4.74	13.76	4.08	66.93	7.86	13.61	33.45	1.19	53.20	24.53	0.25	0.02	0.24	0.09	0.19	0.06	4.01	0.28	0.054
FG2	331.99	10.60	27.05	12.85	108.14	7.90	16.88	52.61	1.43	33.59	18.63	0.32	0.08	0.08	0.19	0.59	0.02	2.44	0.05	0.108
OV1	138.33	0.00	16.68	2.77	52.38	2.89	19.94	19.13	0.48	46.05		0.31		0.07	0.05		0.01	18.00	0.00	
OV2	282.45	2.00	19.54	1.81	177.51	6.29	54.43	115.54	5.03	53.91		0.29		0.21	0.15		0.00	1.33	0.01	0.252
OV3	213.82	0.37	18.42	2.35	119.85	6.28	39.34	78.66	2.85	56.16	26.72	0.29	0.01	0.13	0.27	0.02	0.01	1.12	0.00	0.039
OV4	367.80	5.08	21.93	3.45	235.78	8.56	72.23	145.45	5.77	56.14		0.36		0.25	0.20		0.01	0.10	0.00	0.011
PV1	252.50		44.73	18.99	26.81	6.06	9.55	34.85	0.59	28.14	13.15	0.06	0.12	0.01	0.37	0.02	0.01			0.060
PV2	392.00		97.52	12.19	25.50	1.38	17.50	30.00	0.22	59.06	27.60	0.06	0.02	0.01	0.46	0.02	0.01			0.060
SP1	226.28	0.00	40.75	22.56	9.61	1.80	5.81	20.70	0.26	18.33	9.70	0.19	0.08	0.01	0.24	0.33	0.00	1.85	0.13	0.060
SP2	294.39	0.09	42.88	22.25	50.70	7.41	14.90	54.93	0.84	21.08		0.18		0.07	0.94		0.00	1.25	0.11	0.200
YM1	170.26	1.07	11.12	0.51	81.70	2.05	11.71	35.59	4.54	46.57	24.35	0.20	0.00	0.09	0.05	0.22	0.02	0.66	0.04	1.649
YM2	128.21	1.44	13.24	1.27	52.11	3.42	9.36	27.95	1.87	47.14	26.47	0.11	0.01	0.10	0.05	0.31	0.03	3.42	0.43	0.651
YM3	100.80	0.00	81.21	13.62	162.49	15.82	32.70	467.53	1.07	55.71		1.16			0.03		0.00	7.12	0.00	
YM4	80.31	0.00	9.23	1.74	29.11	2.97	7.41	12.05	2.18	47.43	20.80	0.05	0.00	0.03	0.02	0.02	0.03	2.35	0.03	0.060
YM5	170.63	2.38	16.33	3.09	99.21	3.91	16.17	98.13	1.48	35.92		0.13		0.08	0.02		0.00	6.63	0.12	

NORMALIZED

cluster	HCO3	CO3	Ca	Mg	Na	K	Cl	SO4	F	SiO2	Si	B	Ba	Li	Sr	Fe	Mn	NO3	PO4	Al
AD1	0.52	0.06	0.53	0.18	0.83	0.97	0.67	0.72	0.87	2.97	0.00	48.41	0.00	1.32	0.35	0.00	-0.69	5.25	31.42	0.31
AD2	1.00	0.02	1.02	0.66	1.92	1.43	2.03	1.85	1.88	2.40	0.00	1.76	0.00	0.95	0.22	0.00	0.44	3.26	13.68	0.17
AM1	***1.00***	***1.00***	***1.00***	***1.00***	***1.00***	***1.00***	***1.00***	***1.00***	***1.00***	***1.00***	***1.00***	***1.00***	***1.00***	***1.00***	***1.00***	***1.00***	***1.00***	***1.00***	***1.00***	***1.00***
AM2	1.06	1.09	0.88	0.92	1.47	1.11	1.18	1.37	0.77	1.32	1.13	1.85	0.72	1.49	1.05	1.00	-0.84	1.16	4.73	1.32
FG1	0.58	6.73	0.29	0.20	0.98	0.96	0.63	0.42	0.73	2.34	2.05	0.85	0.31	2.70	0.11	9.56	-15.70	7.97	24.05	0.45
FG2	1.12	15.04	0.57	0.63	1.58	0.96	0.78	0.66	0.87	1.48	1.56	1.08	1.33	0.88	0.21	29.40	-4.30	4.86	4.32	0.89
OV1	0.47	0.00	0.35	0.14	0.77	0.35	0.92	0.24	0.30	2.02	0.00	1.03	0.00	0.73	0.05	0.00	-1.42	35.82	0.00	0.00
OV2	0.95	2.84	0.41	0.09	2.59	0.77	2.51	1.44	3.08	2.37	0.00	0.98	0.00	2.40	0.17	0.00	-0.59	2.65	0.72	2.08
OV3	0.72	0.52	0.39	0.12	1.75	0.77	1.81	0.98	1.74	2.47	2.24	0.98	0.13	1.42	0.30	1.00	-2.69	2.24	0.26	0.32
OV4	1.24	7.21	0.47	0.17	3.45	1.05	3.33	1.82	3.53	2.47	0.00	1.23	0.00	2.79	0.23	0.00	-2.11	0.20	0.00	0.09
PV1	0.85	0.00	0.95	0.93	0.39	0.74	0.44	0.44	0.36	1.24	1.10	0.20	1.89	0.11	0.42	1.00	-2.70	0.00	0.00	0.50
PV2	1.32	0.00	2.07	0.60	0.37	0.17	0.81	0.38	0.13	2.60	2.31	0.20	0.31	0.11	0.52	1.00	-2.70	0.00	0.00	0.50
SP1	0.76	0.00	0.86	1.11	0.14	0.22	0.27	0.26	0.16	0.81	0.81	0.64	1.20	0.16	0.27	16.50	-0.04	3.68	11.14	0.50
SP2	0.99	0.13	0.91	1.09	0.74	0.91	0.69	0.69	0.51	0.93	0.00	0.61	0.00	0.75	1.06	0.00	-0.47	2.50	9.10	1.65
YM1	0.57	1.51	0.24	0.03	1.19	0.25	0.54	0.44	2.78	2.05	2.04	0.68	0.06	1.07	0.06	10.80	-6.65	1.32	3.04	13.62
YM2	0.43	2.05	0.28	0.06	0.76	0.42	0.43	0.35	1.14	2.07	2.22	0.36	0.11	1.17	0.05	15.46	-7.70	6.81	37.01	5.38
YM3	0.34	0.00	1.72	0.67	2.37	1.93	1.51	5.84	0.65	2.45	0.00	3.91	0.00	0.00	0.03	0.00	0.00	14.16	0.00	0.00
YM4	0.27	0.00	0.20	0.09	0.43	0.36	0.34	0.15	1.33	2.09	1.74	0.15	0.02	0.38	0.02	1.00	-7.51	4.68	2.36	0.50
YM5	0.57	3.37	0.35	0.15	1.45	0.48	0.74	1.23	0.91	1.58	0.00	0.42	0.00	0.90	0.03	0.00	0.34	13.20	10.60	0.00

Amargosa Desert
Normalized relative to Ash Meadows

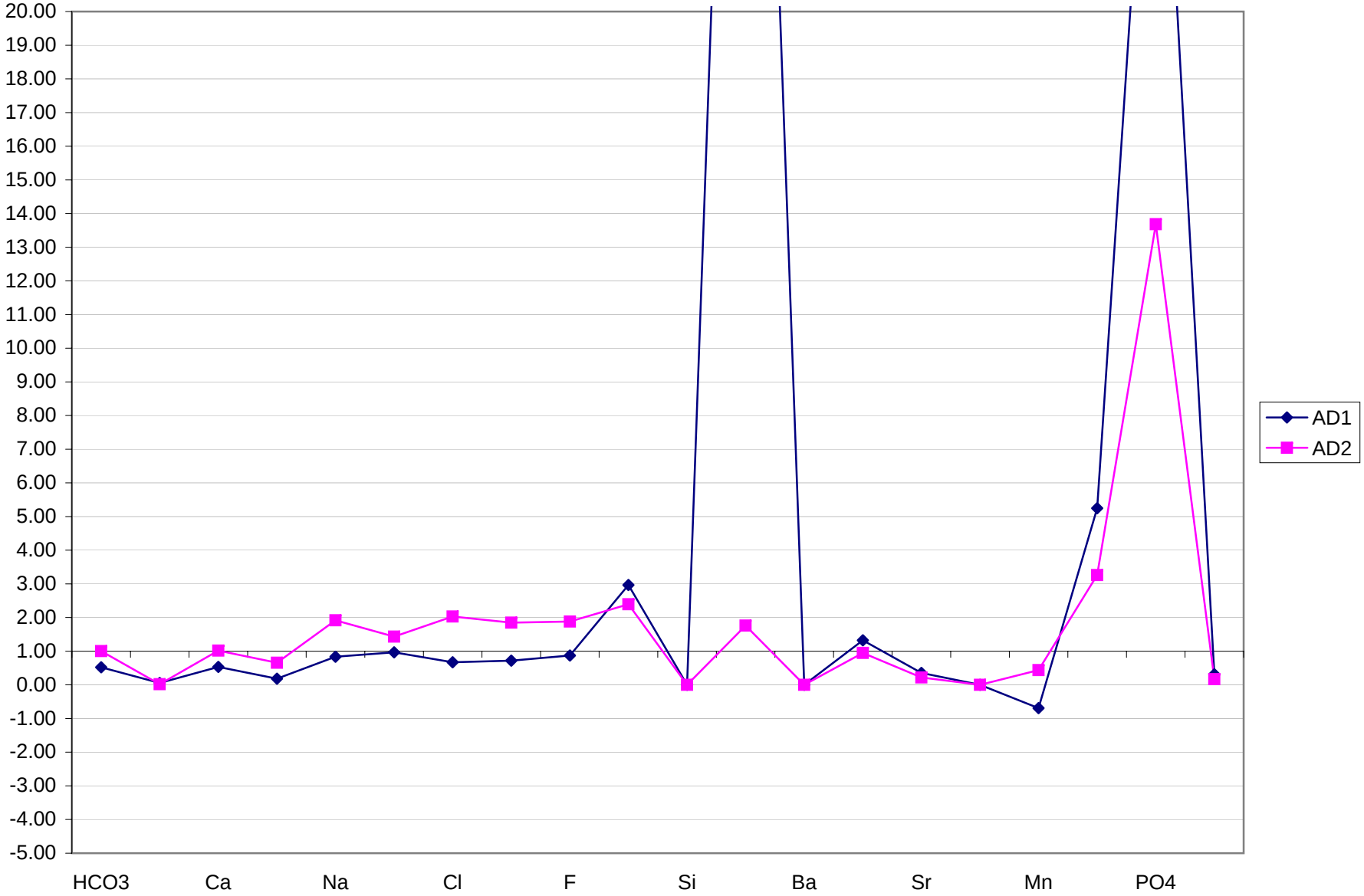

Oasis Valley
Normalized relative to Ash Meadows

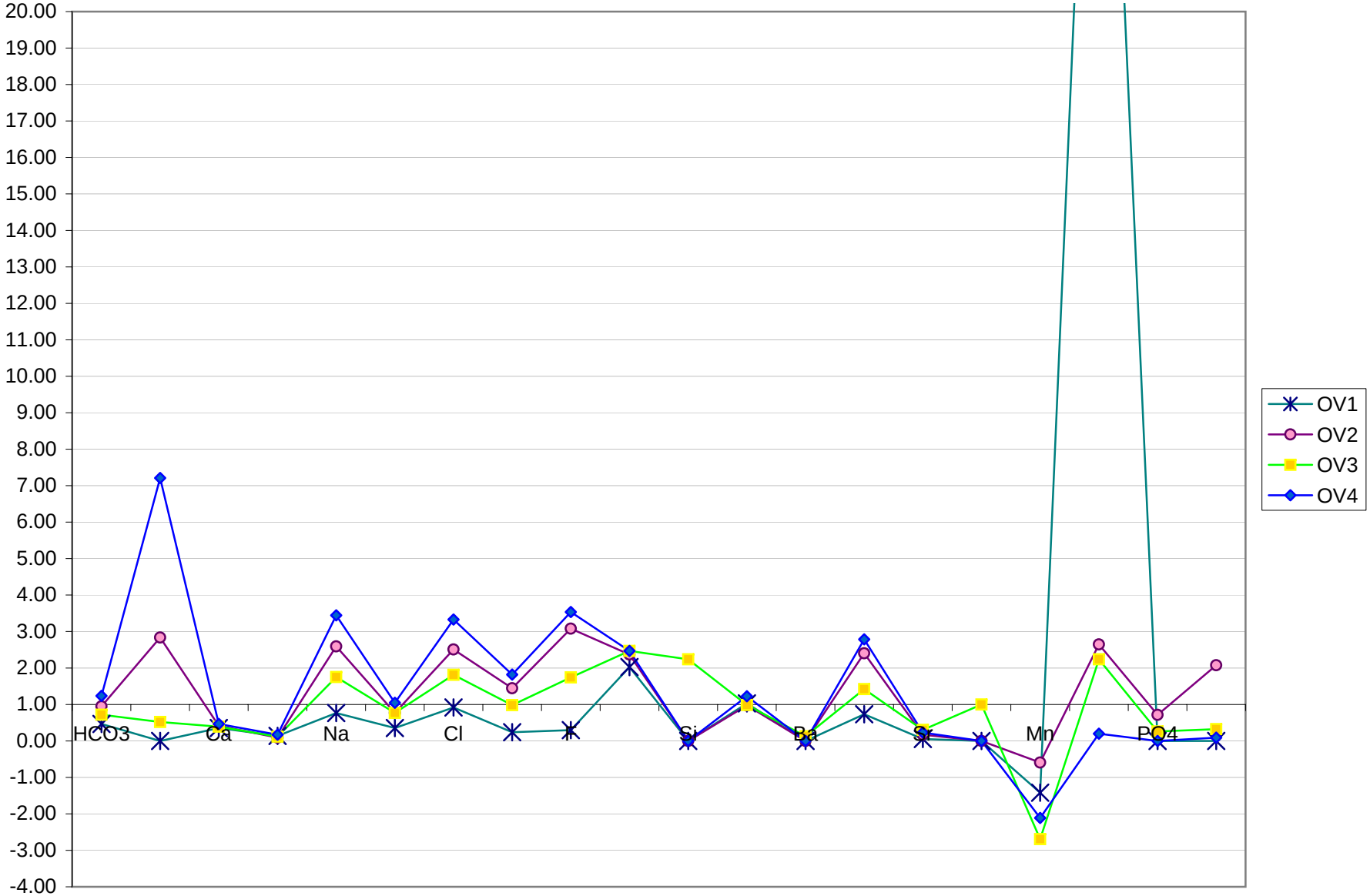

Yucca Mountain
Normalized relative to Ash Meadows

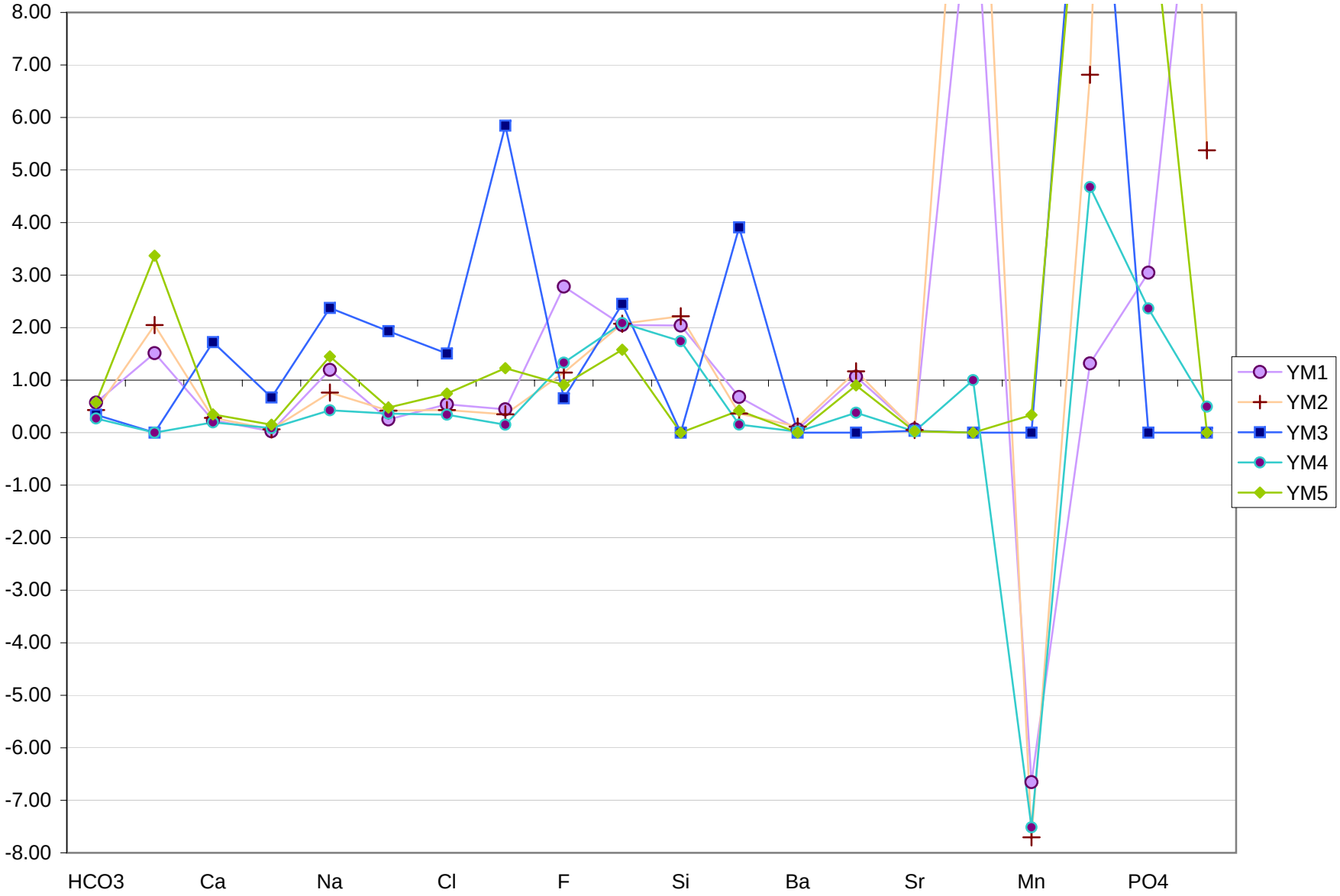

Frenchman Groom
Normalized relative to Ash Meadows

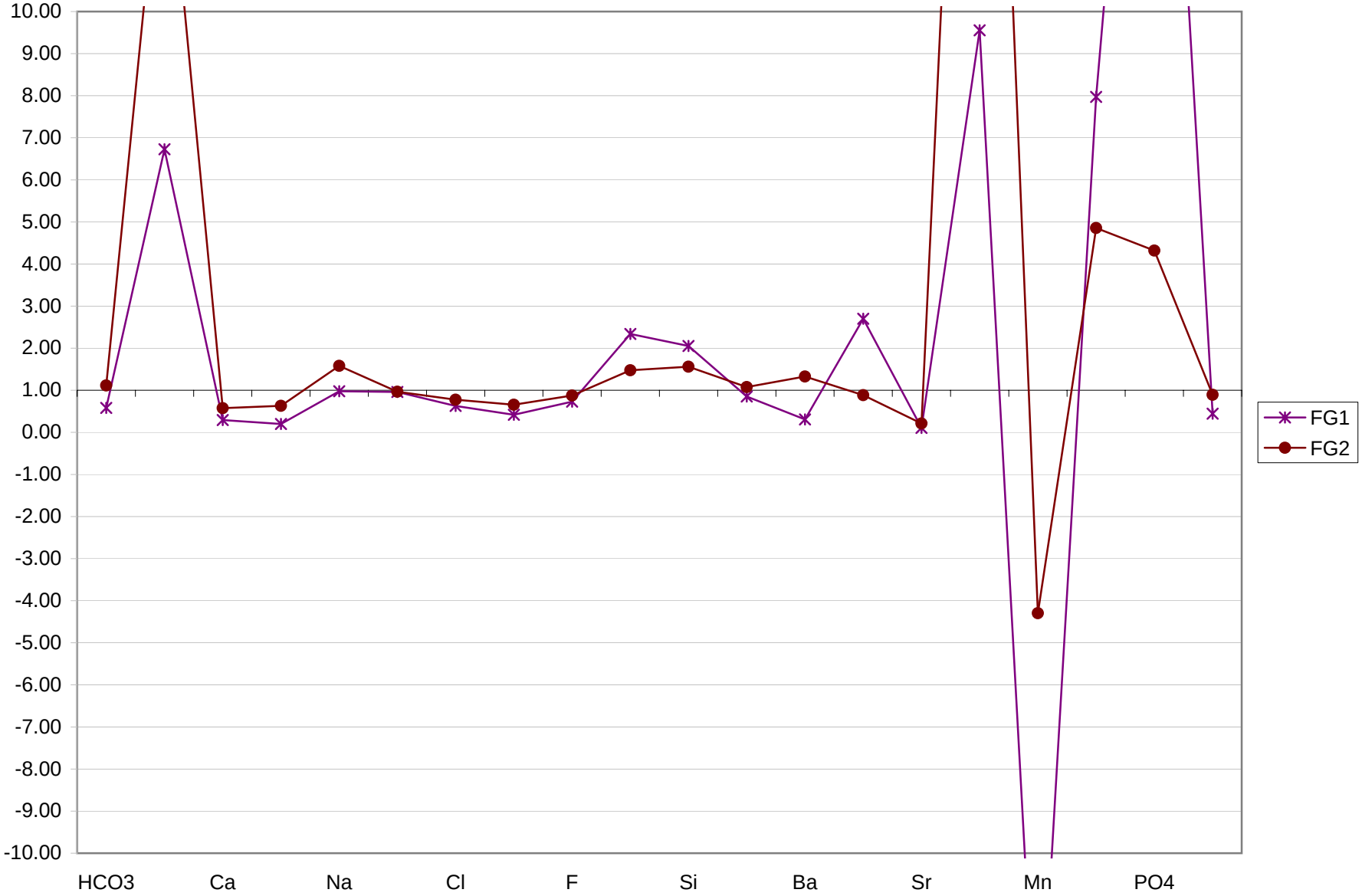

Spring Mountain
Normalized relative to Ash Meadows

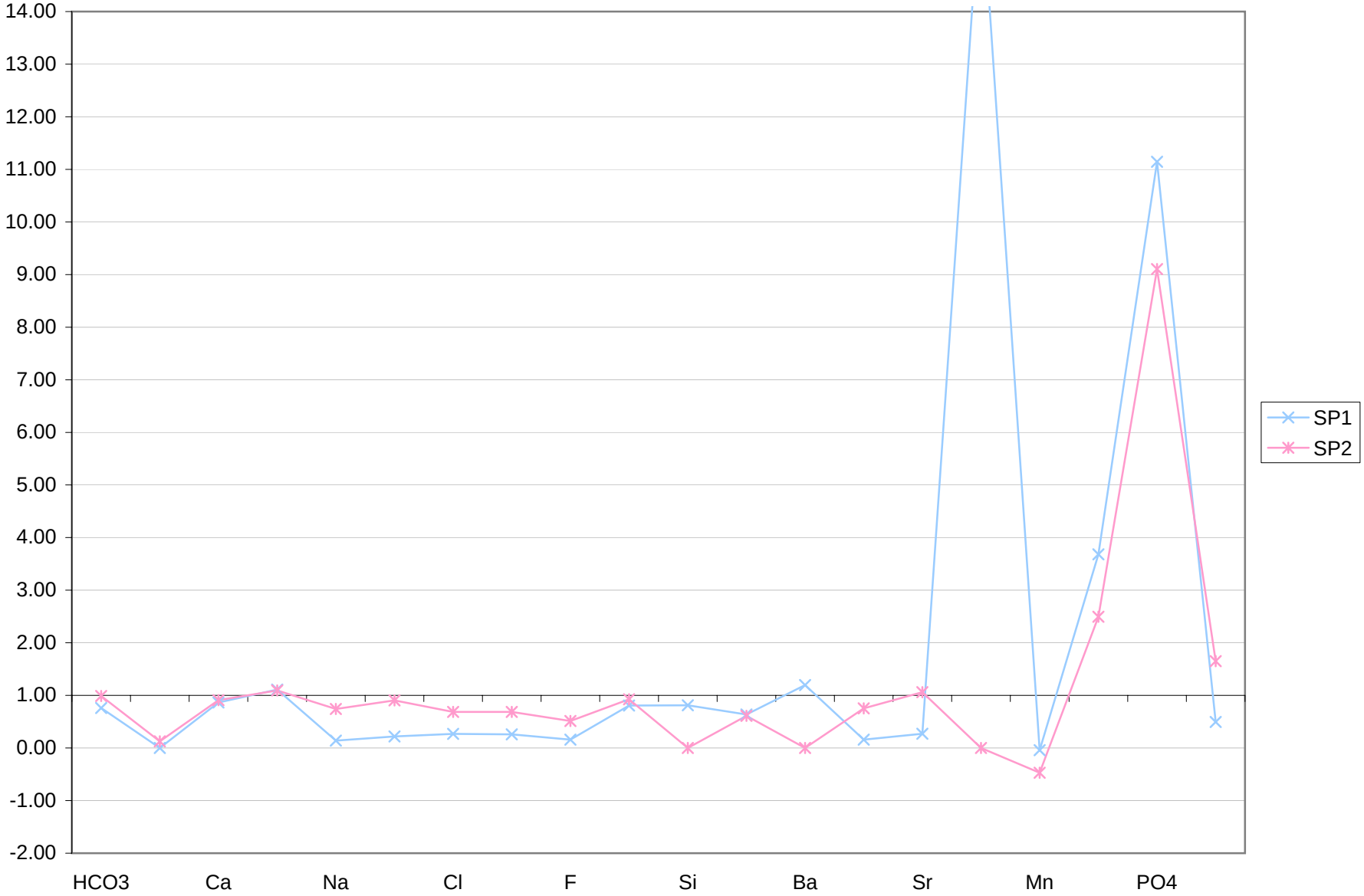

Pahranagat Valley
Normalized relative to Ash Meadows

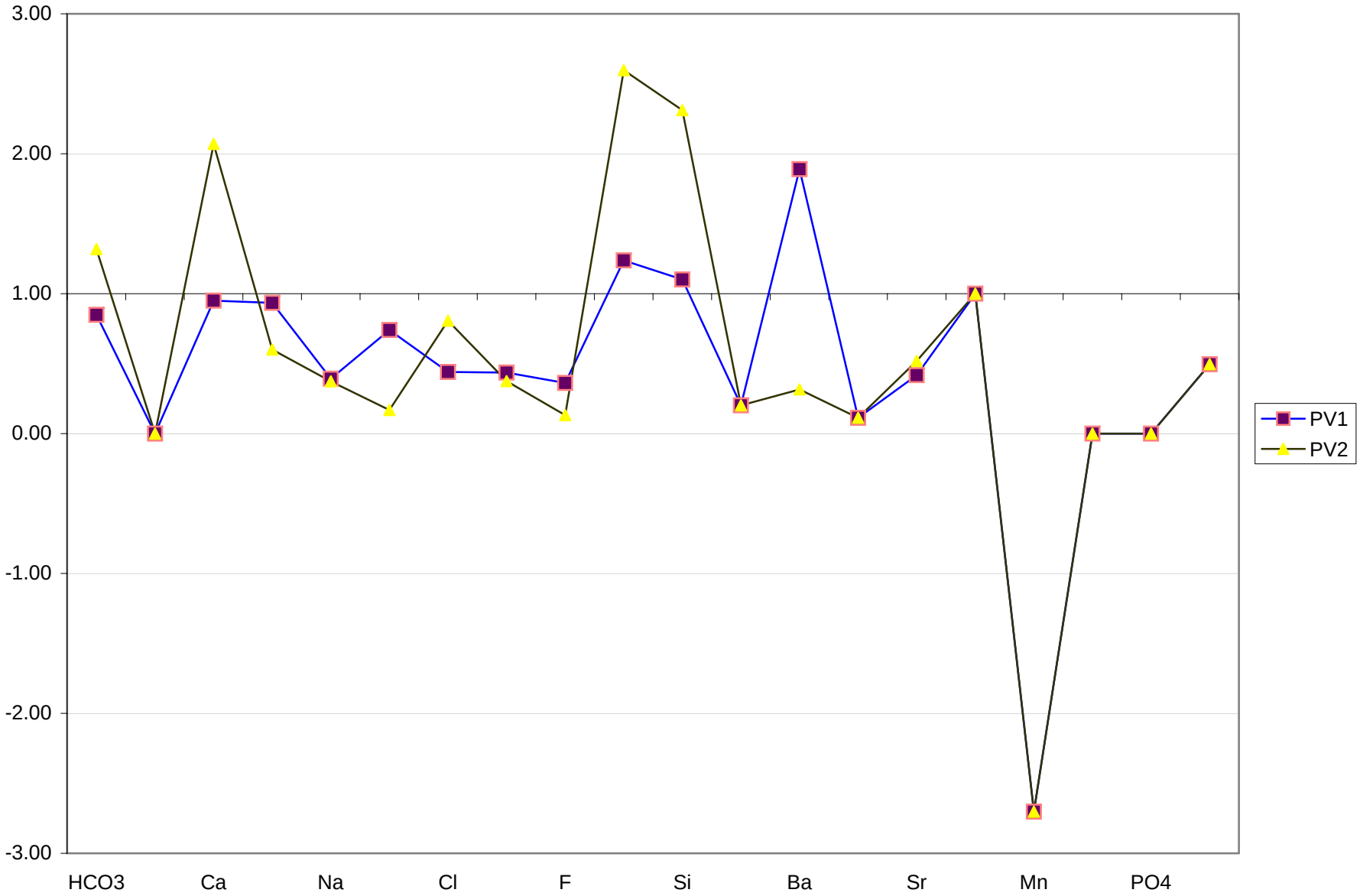

Appendix F

WATEQ Saturation Indices

WATEQ saturation indices

			Log AP/K for Minerals											
Sample	Temp deg	pH	Magnesite	Dolomite (	Calcite	Anhydrite	Gypsum	Aragonite	Albite	Kmica	Illite	Kaolinite	Fluorite	Montmoril
AD1	24.33	7.8	-1.1496	-1.2018	-0.0789	-2.4094	-2.1869	-0.2231	0.6572	9.5456	3.883	4.6908	-1.0905	4.4015
AD2	25.28	7.61	-0.5685	-0.3131	0.2225	-1.8746	-1.6559	0.0789	0.395	8.8254	3.2433	4.2235	-0.2809	3.7039
AM1	31.55	7.64	-0.1779	0.2568	0.3659	-2.0889	-1.8987	0.2268	-0.6476	8.7618	2.7792	4.1972	-0.8821	3.1591
AM2	27.45	7.57	-0.3654	-0.1238	0.1953	-2.0367	-1.827	0.0533	0.2555	10.3239	4.1125	5.2982	-1.1339	4.5839
FG1	26.75	8.15	-0.6194	-0.4534	0.1239	-2.8765	-2.6638	-0.0186	0.402	8.5853	3.1269	3.7925	-1.5312	3.2753
FG2	32.07	7.89	-0.0351	0.494	0.4578	-2.4764	-2.289	0.319	-0.0262	8.5276	2.8329	3.8785	-1.2244	3.0516
OV1	22.62	7.8	-1.3201	-1.5895	-0.2846	-3.0147	-2.7859	-0.4301					-2.1538	
OV2	29.53	7.91	-1.0488	-0.8068	0.1839	-2.3031	-2.103	0.0433	1.3234	10.4986	4.4134	5.2739	-0.2606	4.94
OV3	25.31	7.96	-1.0579	-0.9556	0.0692	-2.4515	-2.2328	-0.0743	0.6726	8.7326	3.1671	4.1027	-0.6806	3.6293
OV4	26.82	8	-0.6528	-0.2395	0.3708	-2.2203	-2.0081	0.2283	0.2969	6.843	1.7238	2.7193	-0.1039	2.0277
PV1	32.5	7.53	-0.3232	-0.0329	0.2168	-2.4134	-2.2282	0.0783					-1.7507	
PV2	20	7.85	-0.3298	0.5191	0.8527	-2.2496	-2.0125	0.7053					-2.149	
SP1	24.16	7.78	-0.2174	0.0864	0.2782	-2.6927	-2.4695	0.1338	-1.6093	7.8603	2.2113	4.0119	-2.3907	2.8817
SP2	25.16	7.63	-0.2738	0.0004	0.242	-2.2934	-2.0741	0.0984	-0.2544	10.3363	4.0151	5.3464	-1.4044	4.4658
YM1	34.68	7.82	-1.7111	-1.8421	-0.2145	-2.8862	-2.7129	-0.3515	1.3245	11.6922	5.142	6.3926	-0.5373	6.083
YM2	31.81	7.9	-1.3857	-1.5068	-0.1911	-2.9033	-2.7144	-0.3301	0.92	11.0192	4.7488	5.7685	-1.1767	5.4146
YM3	34.4	7.81	-0.7711	-0.4972	0.1915	-1.236	-1.0612	0.0543					-1.1799	
YM4	31.95	7.61	-1.6979	-2.4246	-0.7975	-3.3627	-3.1745	-0.9364	-0.3506	8.4414	2.7341	4.2786	-1.1541	3.5704
YM5	24.14	8.02	-0.9908	-0.9888	-0.0235	-2.4011	-2.1779	-0.1678					-1.2831	

Amargosa Desert
WATEQ Saturaion Indices

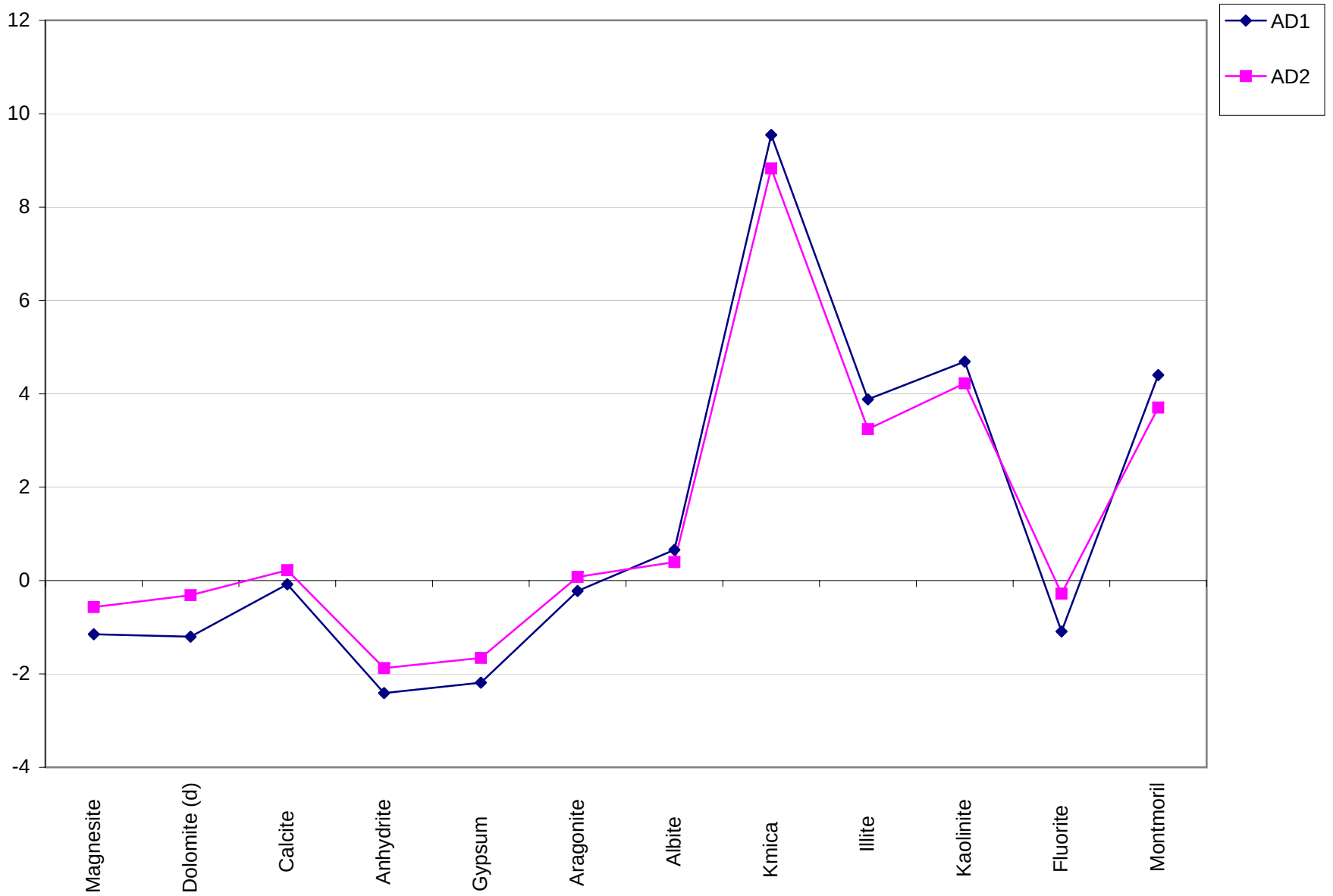

Oasis Valley
WATEQ Saturaion Indices

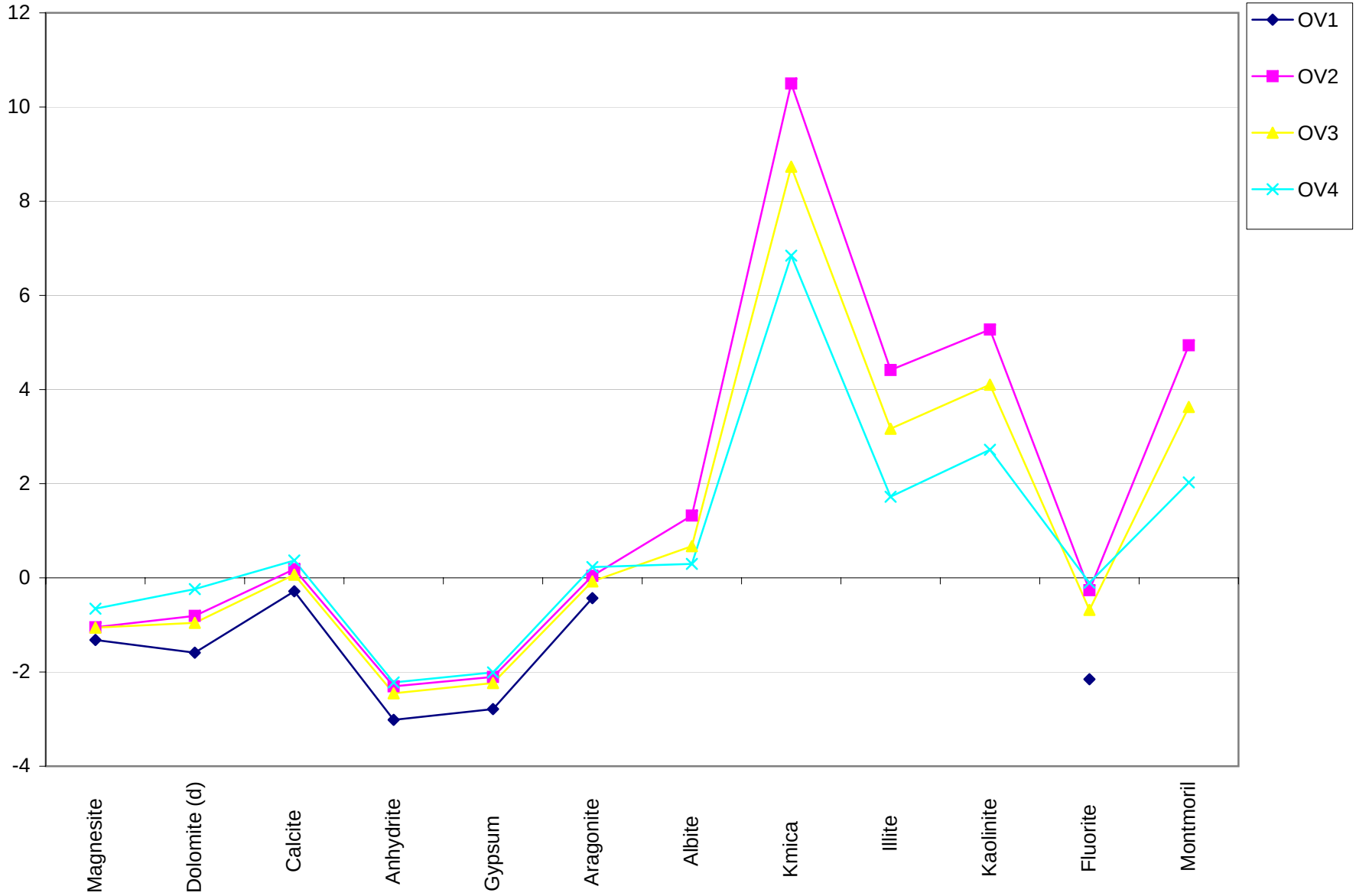

Frenchman Groom
WATEQ Saturaion Indices

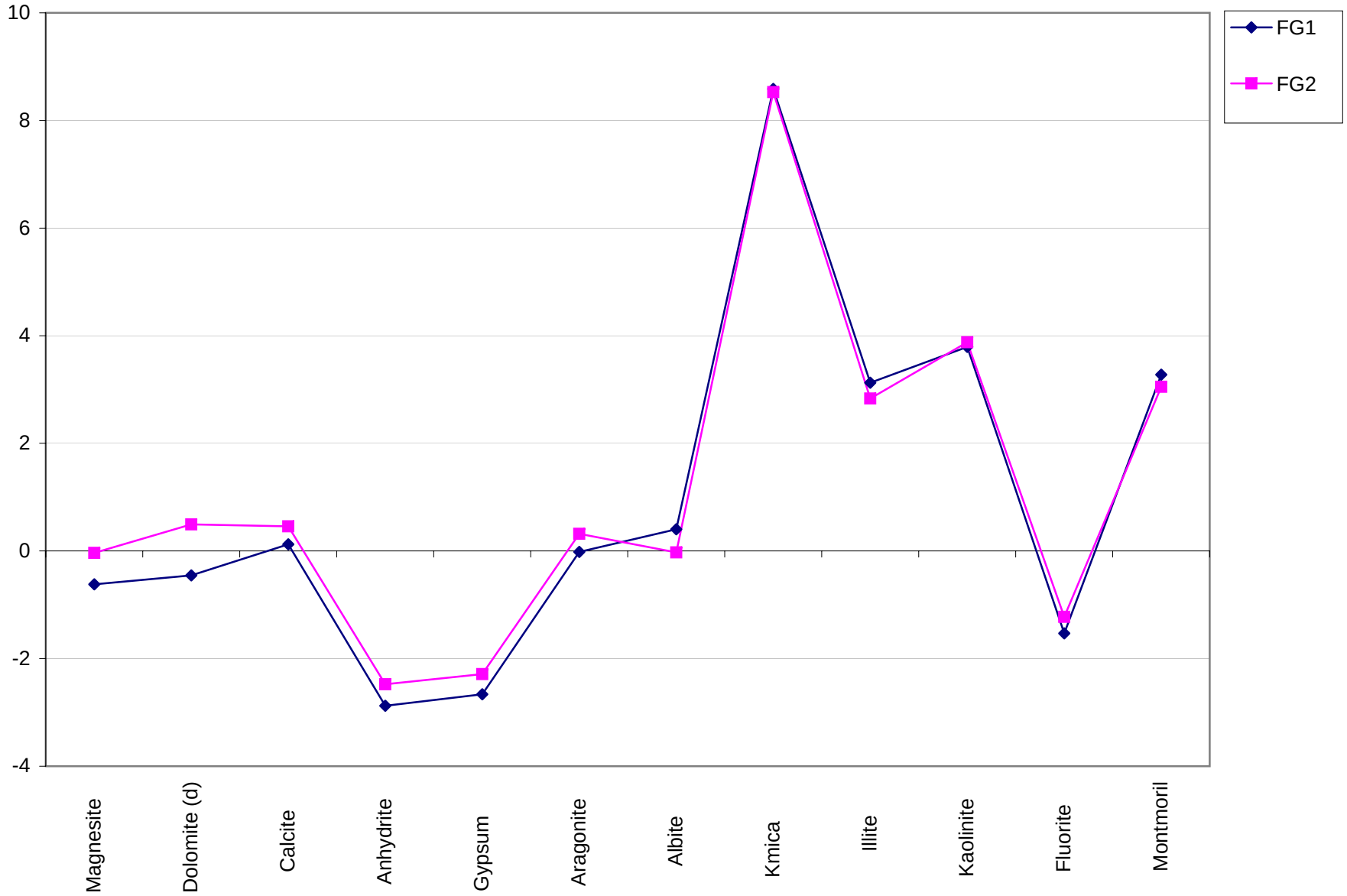

Yucca Mountain
WATEQ Saturaion Indices

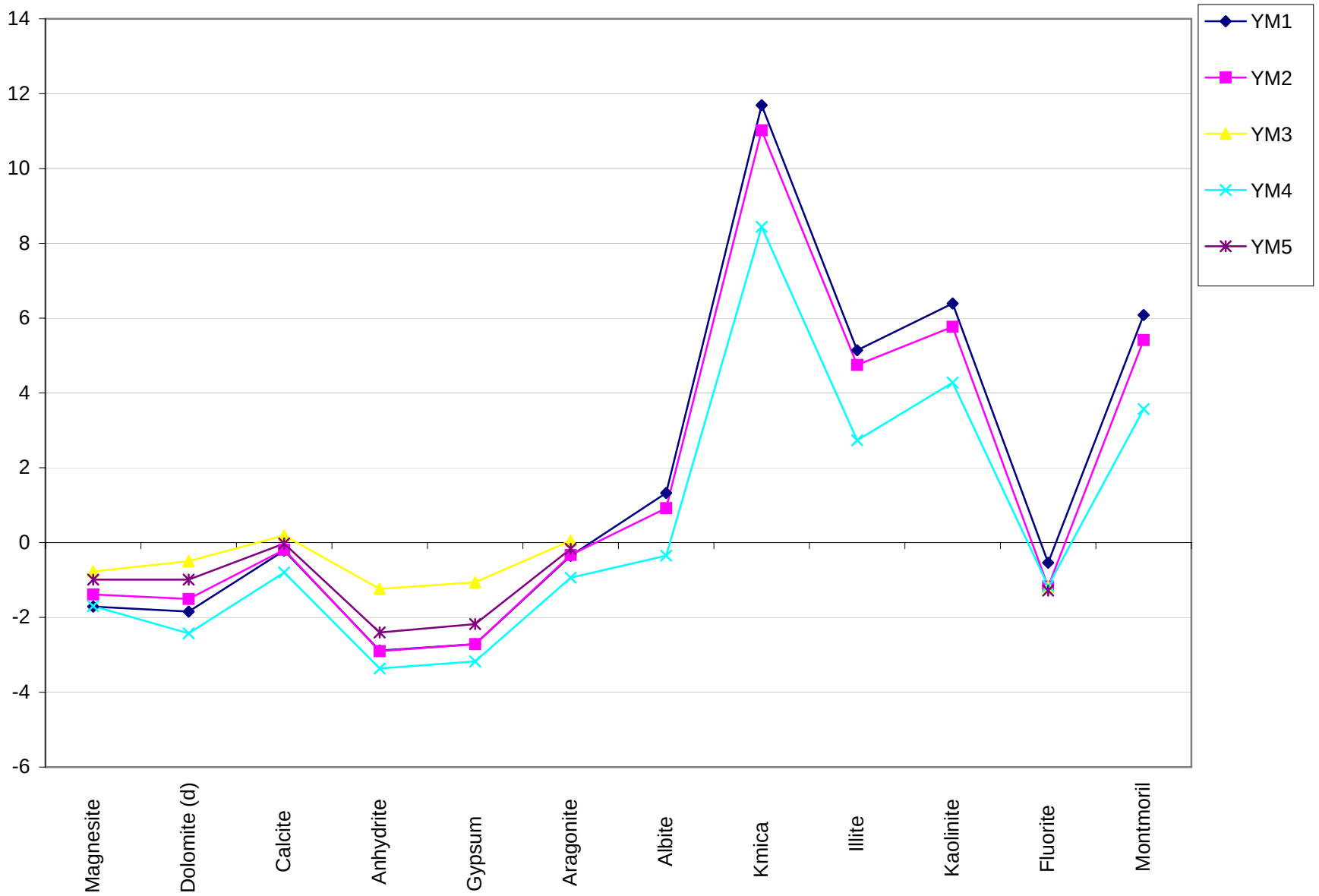

Pahranagat Valley
WATEQ Saturaion Indices

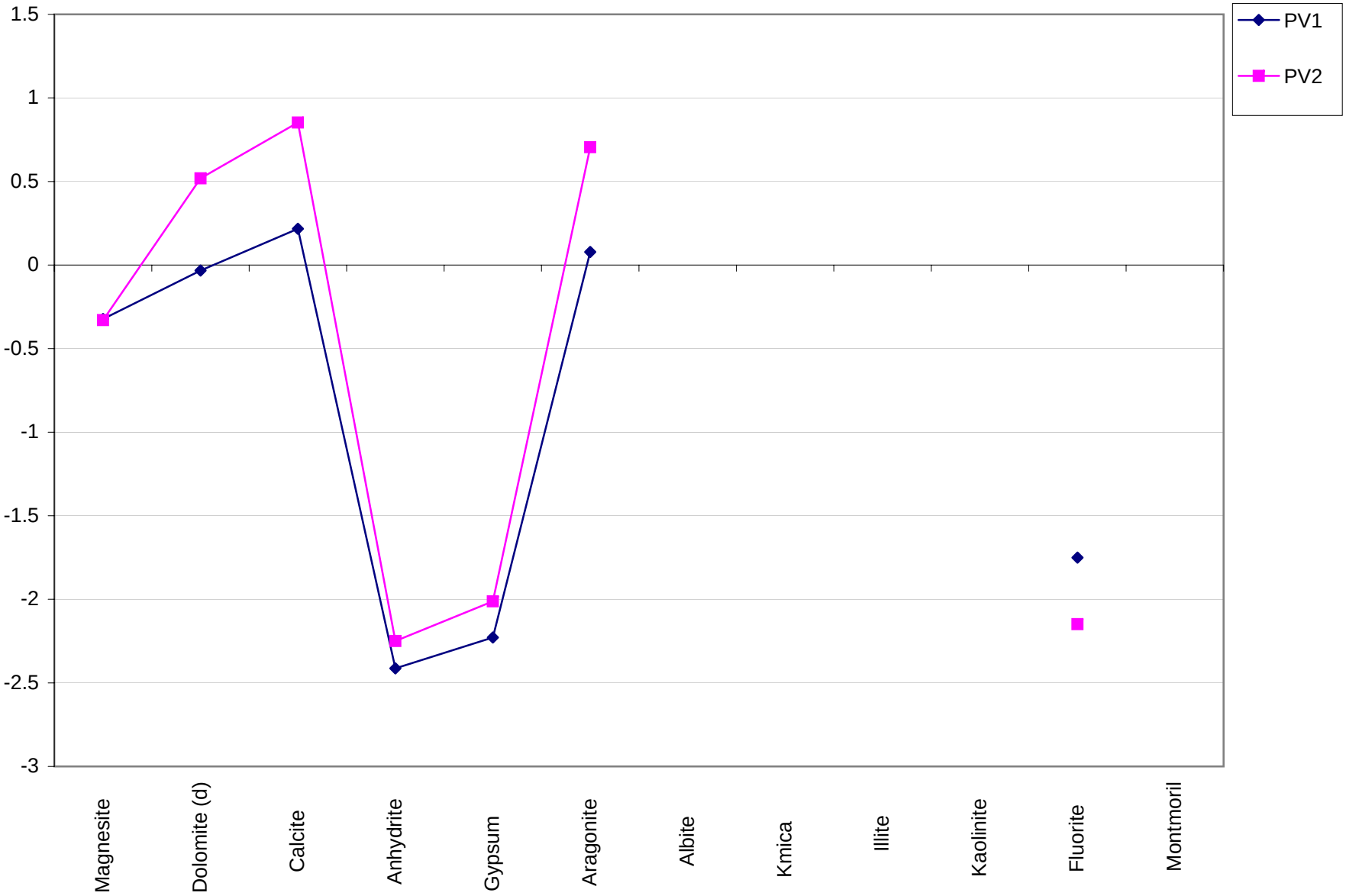

Spring Mountains
WATEQ Saturaion Indices

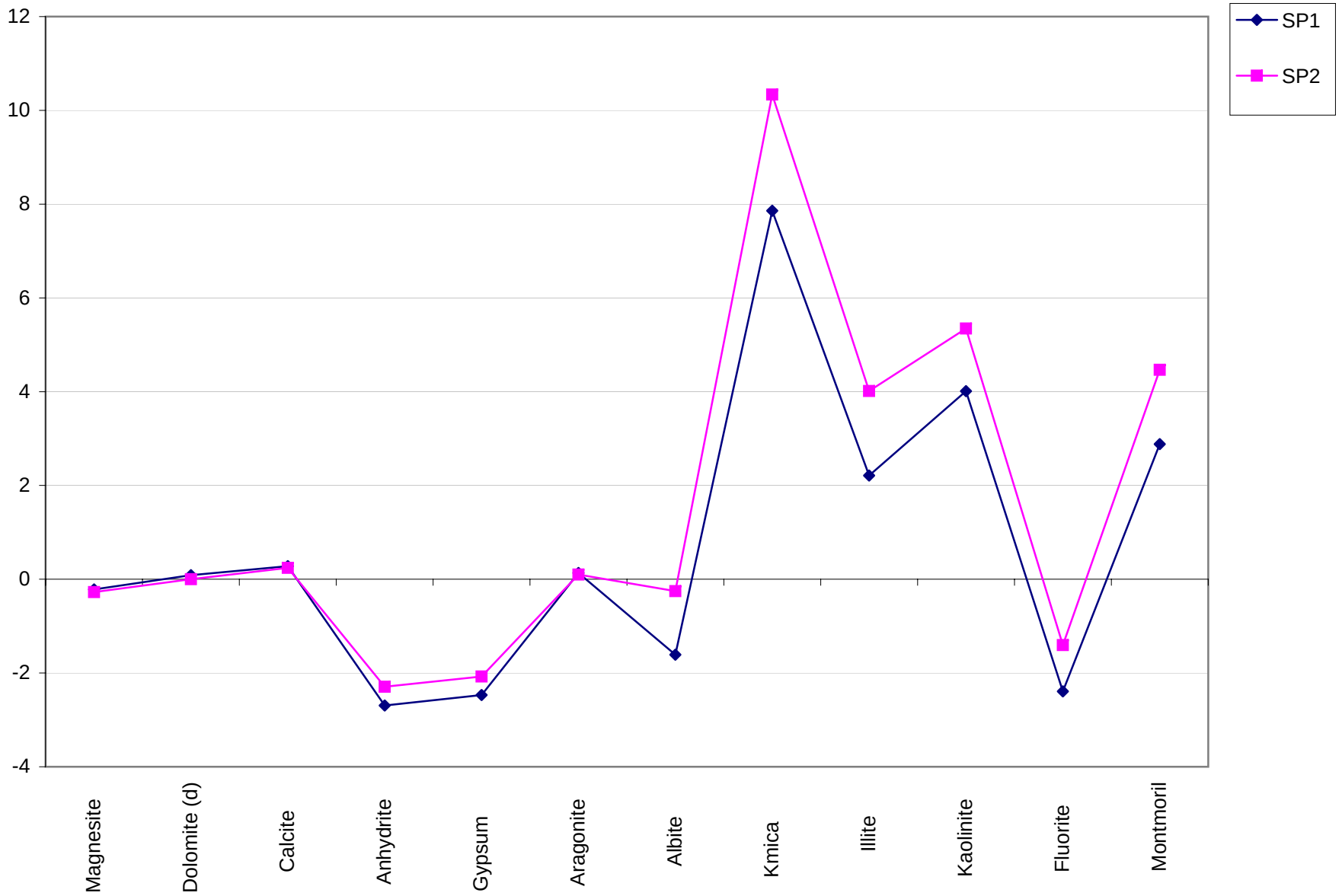

Appendix G

Water-Rock Interactions Modeled in NETPATH

Appendix G
Water-Rock Interactions Modeled in NETPATH

Oasis Valley

Rocks[1]	*Minerals (Phases)*	*Elements (Constraints)*
Quartzite	Quartz	C
Dolomite	Kaolinite	Ca
Limestone	K-spar	Al (when available)
Lava flows (rhyolite,	Mica (k-mica)	Mg
intermediate, basalt)	Calcite	Na
Tuffs (comendite, calk-alk,	Dolomite	K
peralkaline, metaluminous)	Plagioclase	Si
Pluton (intermediate	Pyroxene (Diopside)	Fe (when available)
composition)	Biotite	
Sandstone	CO_2	
Siltstone	Ca-Na exchange	
Shale	Illite	
Conglomerate		

Amargosa Desert

Rocks	*Minerals (Phases)*	*Elements (Constraints)*
Quartzite	Quartz	C
Limestone	Kaolinite	Ca
Dolomite	K-mica	Al
Sandstone	Illite	Mg
Siltstone	Calcite	K
Shale	Dolomite	Si
Conglomerate	CO_2	
	Ca-Na Exchange	

[1] Surface geology taken from Workman et al., 2001a. Subsurface geology taken from Sweetkind et al., 2001.

Yucca Mountain

Rocks	*Minerals (Phases)*	*Elements (Constraints)*
Quartzite	Quartz	C
Dolomite	Kaolinite	Ca
Limestone	K-spar	Al (when available)
Lava flows (rhyolite,	Mica (k-mica)	Mg
intermediate, basalt)	Calcite	Na
Tuffs (comendite, calk-alk,	Dolomite	K
peralkaline, metaluminous)	Plagioclase	Si
Sandstone	Pyroxene (Diopside)	Fe (when available)
Siltstone	Biotite	
Shale	CO_2	
Conglomerate	Ca-Na exchange	
	Illite	

Frenchman Groom

Rocks	*Minerals (Phases)*	*Elements (Constraints)*
Quartzite	Quartz	C
Dolomite	Kaolinite	S
Limestone	K-spar	Ca
Lava flows (rhyolite,	Mica (k-mica)	Al (when available)
intermediate, basalt)	Calcite	Mg
Tuffs (comendite, calk-alk,	Dolomite	Na
peralkaline, metaluminous)	Plagioclase	K
Sandstone	Pyroxene (Diopside)	Cl
Siltstone	CO_2	Si
Shale	Ca-Na exchange	
Conglomerate	Illite	
Playa/Salt pan deposits	Gypsum	
	Halite	

Spring Mountains

Rocks	*Minerals (Phases)*	*Elements (Constraints)*
Quartzite	Quartz	C
Dolomite	Kaolinite	S
Sandstone	K-spar	Ca
Siltstone	Mica (k-mica)	Al
Shale	Calcite	Mg
Conglomerate	Dolomite	Na
Playa/Salt pan deposits	CO_2	K
	Ca-Na exchange	Cl
	Illite	Si
	Gypsum	
	Halite	

Pahranagat Valley

Rocks	*Minerals (Phases)*	*Elements (Constraints)*
Quartzite	Quartz	C
Dolomite	Kaolinite	Ca
Limestone	K-spar	Al
Lava flows (basalt)	Mica (k-mica)	Mg
Tuffs (silicic, peralkaline)	Calcite	Na
Sandstone	Dolomite	K
Siltstone	Plagioclase	Fe
Shale	Pyroxene (Diopside)	
	Biotite	Note: Si data unavailable for these samples
	CO_2	
	Ca-Na exchange	
	Illite	

Appendix H

NETPATH Model Constraints and Phases

NETPATH Model Constraints and Phases

					Constraints															
Model #	IW#	Initial Well	FW#	Final Well	C-1	S-2	Ca-3	Al-4	Mg-5	Na-6	K-7	Cl-8	Si-10	Fe-16	Redox-20	δ13C-21	biotite #10	calcite #12	CO2(g) #17	diopside #20	dolomite #21	Exchange #22
230	1	AD1	3	AM1	x		x	x	x		x		x		x	x	~	dissolve	diss/prec	~	dissolve	diss/prec
231	2	AD2	3	AM1	x		x	x	x		x		x		x	x	~	precipitate	diss/prec	~	dissolve	diss/prec
232	5	FG1	3	AM1	x	x	x	x	x	x	x	x	x		x	x	~	precipitate	diss/prec	diss/prec	dissolve	diss/prec
233	6	FG2	3	AM1	x	x	x	x	x	x	x	x	x		x	x	~	precipitate	diss/prec	diss/prec	precipitate	diss/prec
234	7	OV1	3	AM1	x		x	x	x	x	x		x	x	x	x	diss/prec	dissolve	diss/prec	diss/prec	dissolve	diss/prec
235	8	OV2	3	AM1	x		x	x	x	x	x		x	x	x	x	diss/prec	precipitate	diss/prec	diss/prec	dissolve	diss/prec
236	9	OV3	3	AM1	x		x	x	x	x	x		x	x	x	x	diss/prec	diss/prec	diss/prec	diss/prec	dissolve	diss/prec
237	10	OV4	3	AM1	x		x	x	x	x	x		x	x	x	x	diss/prec	precipitate	diss/prec	diss/prec	dissolve	diss/prec
238	11	PV1	3	AM1	x		x	x	x	x	x		x	x	x	x	diss/prec	precipitate	diss/prec	diss/prec	dissolve	diss/prec
239	12	PV2	3	AM1	x		x	x	x	x	x		x	x	x	x	diss/prec	precipitate	diss/prec	diss/prec	precipitate	diss/prec
240	13	SP1	3	AM1	x	x	x	x	x	x	x	x	x		x	x	~	precipitate	diss/prec	~	diss/prec	diss/prec
241	14	SP2	3	AM1	x	x	x	x	x	x	x	x	x		x	x	~	precipitate	diss/prec	~	diss/prec	diss/prec
242	15	YM1	3	AM1	x		x	x	x	x	x		x	x	x	x	diss/prec	diss/prec	diss/prec	diss/prec	dissolve	diss/prec
243	16	YM2	3	AM1	x		x	x	x	x	x		x	x	x	x	diss/prec	diss/prec	diss/prec	diss/prec	dissolve	diss/prec
244	17	YM3	3	AM1	x		x	x	x	x	x		x	x	x	x	diss/prec	diss/prec	diss/prec	diss/prec	dissolve	diss/prec
245	18	YM4	3	AM1	x		x	x	x	x	x		x	x	x	x	diss/prec	dissolve	diss/prec	diss/prec	dissolve	diss/prec
246	19	YM5	3	AM1	x		x	x	x	x	x		x	x	x	x		diss/prec	diss/prec	diss/prec	dissolve	diss/prec

NETPATH Model Constraints and Phases

					Phases							
Model #	IW#	Initial Well	FW#	Final Well	gypsum #30	illite #36	k-spar #37	K-mica #38	kaolinite #40	NaCl #61	plagioclase #68	SiO2 #78
230	1	AD1	3	AM1	~	precipitate	~	precipitate	precipitate	~	~	precipitate
231	2	AD2	3	AM1	~	precipitate	~	precipitate	precipitate	~	~	precipitate
232	5	FG1	3	AM1	dissolve	precipitate	diss/prec	precipitate	precipitate	diss/prec	diss/prec	precipitate
233	6	FG2	3	AM1	dissolve	precipitate	diss/prec	precipitate	precipitate	diss/prec	diss/prec	precipitate
234	7	OV1	3	AM1	~	~	diss/prec	~	~	~	diss/prec	precipitate
235	8	OV2	3	AM1	~	precipitate	diss/prec	precipitate	precipitate	~	diss/prec	precipitate
236	9	OV3	3	AM1	~	precipitate	diss/prec	precipitate	precipitate	~	diss/prec	precipitate
237	10	OV4	3	AM1	~	precipitate	diss/prec	precipitate	precipitate	~	diss/prec	precipitate
238	11	PV1	3	AM1	~	~	~	~	~	~	diss/prec	precipitate
239	12	PV2	3	AM1	~	~	~	~	~	~	diss/prec	precipitate
240	13	SP1	3	AM1	dissolve	precipitate	diss/prec	precipitate	precipitate	diss/prec	~	dissolve
241	14	SP2	3	AM1	dissolve	precipitate	diss/prec	precipitate	precipitate	diss/prec	~	dissolve
242	15	YM1	3	AM1	~	precipitate	diss/prec	precipitate	precipitate	~	diss/prec	precipitate
243	16	YM2	3	AM1	~	~	diss/prec	~	~	~	diss/prec	precipitate
244	17	YM3	3	AM1	~	precipitate	diss/prec	precipitate	precipitate	~	diss/prec	precipitate
245	18	YM4	3	AM1	~	precipitate	diss/prec	precipitate	precipitate	~	diss/prec	precipitate
246	19	YM5	3	AM1	~	precipitate	diss/prec	precipitate	precipitate	~	diss/prec	precipitate